University of Zabol

Agriculture, Environment & Society

Biannual, Volume 4, Issue 2, December 2024

Agriculture, Environment & Society (AES)

Volume 4, Issue 2, December 2024

Publisher: University of Zabol

Editorial Office: ***Faculty of Agriculture, University of Zabol, Zabol, Iran, P.O. Box 538-98615***

Tel: +98-54-31232102

Website: http://aes.uoz.ac.ir

Email: aes@uoz.ac.ir, aes.uoz.journal@gmail.com

Aims and Scopes

Agricultural, Environment and Society is an international journal that deals with interactions between agricultural systems and the life-supporting environment on which human wellbeing ultimately depends. The journal publishes original article, short communications and review article. The journal's focus should capture the current needs of the agricultural systems with the goal of advancing the well-being of the people. The papers in the journal should address the critical issues that will move agricultural systems forward and improve the living conditions of the people. In this regard, the three critical systems that we need to understand to accomplish this end are environment, agriculture and society. The role of Journal is to provide a forum to agricultural scientists to deliberate on important issues of agricultural research, education and extension and present views of the scientific community as policy inputs to planners, decision/opinion makers at various levels.

Agricultural, Environment and Society honors scientists at various levels, and encourages cutting edge research in a variety of agricultural disciplines. The journal's mission is to publish papers on new and emerging disciplines and concepts in order to provide future directions for agricultural research across the world. It is a unique journal that promotes inter-disciplinary research by encompassing all fields of crop sciences, animal sciences, fishery sciences, forestry sciences, agricultural machinery and natural resources management sciences, to stimulate interest in inter-disciplinary research.

The following should be included in all manuscripts submitted to *Agricultural, Environment and Society:*

- ***Generally, should focus on the critical issues that will move agricultural systems forward and improve the living conditions of people.***
- ***Substantial natural science material (particularly farm- or landscape-level, sometimes coupled with social sciences), and***
- ***A thorough examination and discussion of the interconnections between agricultural system components and other systems.***

Agriculture, Environment & Society (AES)

Volume 4, Issue 2, December 2024

Contents

Agriculture, Environment & Society

Journal homepage: www.aes.uoz.ac.ir

The Effect of crop rotation on energy indices and greenhouse gas emissions in wheat (*Triticum aestivum* L.) and chickpea (*Cicer arietinum*) dryland agroecosystems in Kermanshah region, Iran

Farzaneh Angazi [a], Farzad Mondani [*b], Mokhtar Ghobadi [b], Mohammad Yousefi [c]

[a] M.Sc. student of Crop Ecology, Department of Plant Production and Genetics, Razi University, Kermanshah, Iran
[b] Department of Plant Production and Genetics, Razi University, Kermanshah, Iran
[c] Ph.D. Graduated of Crop Ecology, Department of Plant Production and Genetics, Razi University, Kermanshah, Iran

ARTICLE INFO

Article history:
Received: 4 October 2024
Accepted: 15 November 2024
Available online: 1 December 2024

Keywords:
Energy productivity
Energy use efficiency
Global warming potential
Monoculture

ABSTRACT

The application of appropriate agricultural practices leads to savings in fuel consumption, energy, and a reduction in greenhouse gas emissions. Therefore, this research was conducted to compare wheat-chickpea crop rotation with wheat monoculture in terms of energy indices and amount of greenhouse gas emissions in dryland agroecosystems during 2021. The amounts of inputs consumed and all agricultural operations in the studied agroecosystems from planting to harvesting were calculated through questionnaires and energy analysis. Data analysis included three components: energy inputs, energy outputs, and global warming potential due to greenhouse gas emissions. The results indicated that total energy input for wheat-chickpea rotation and wheat monoculture was 13550.5 and 15106.8 Mj ha^{-1}, respectively. The total energy output for wheat-chickpea rotation and wheat monoculture were 45802.5 and 41860.3 Mj ha^{-1}, respectively. Energy use efficiency for wheat-chickpea rotation and wheat monoculture were 3.4 and 2.8, respectively. In wheat monoculture system, CO_2 emission was about 184.9% higher than wheat-chickpea rotation, which were related to use of fossil fuel (59.2%), nitrogen fertilizer (30.8%), and phosphate fertilizer (7.4%). Nitrogen oxide emissions in wheat monoculture were higher than wheat-chickpea rotation. The global warming potential in wheat monoculture and wheat-chickpea rotation systems were 709.3 and 627.9 kg eq Co_2 h^{-1}, respectively. Overall, the results showed that wheat monoculture has lower energy efficiency and higher global warming potential compared to wheat-chickpea rotation. Therefore, to prevent further emission of greenhouse gases and combat climate change, wheat-chickpea crop rotation is recommended instead of wheat monoculture in dryland agroecosystems.

Highlights

- Wheat-chickpea rotation cuts energy input by 11% (13550.5 vs. 15106.8 MJ ha^{-1}) vs. monoculture.
- Energy efficiency rises 18% in rotation (3.4) over monoculture (2.8) in Kermanshah.
- CO2 emissions 184.9% higher in monoculture due to fossil fuel and nitrogen use.
- Rotation boosts energy output 9% (45802.5 vs. 41860.3 MJ ha^{-1}) vs. monoculture.
- GWP lower in rotation (627.9 kg CO_2 eq ha^{-1}) than monoculture (709.3 kg CO_2 eq ha^{-1}).

1. Introduction

The inappropriate and excessive use of fossil resources by humanity to meet energy needs for ensuring well-being and increasing food supply has led to numerous problems, including the future generations facing fossil fuel shortages, rising energy carrier prices, and climate change phenomena due to greenhouse gas emissions (such as carbon dioxide, methane, and nitrogen oxides). Among the

* Corresponding author.
E-mail address: f.mondani@razi.ac.ir
https://doi.org/10.22034/jelsa.2025.492300.1091

most significant outcomes of increased fossil energy consumption are environmental pollution and climate change (Feyzbakhsh and Alizadeh, 2018) .

In the essential sectors of human life, agricultural systems act as both energy producers and consumers; thus, a close relationship exists between agriculture and energy consumption (Singh et al., 2004). Today, most developed countries and even developing nations are striving to optimize energy use in agricultural systems by examining energy inputs at various stages of agricultural product production and calculating energy indices (Nasirian et al., 2006). By optimizing the use of energy inputs in agriculture, environmental problems can be minimized, preventing the destruction of Earth's ecological resources and reinforcing sustainable agricultural practices as an appropriate system for agricultural product production (Kizilaslan, 2009). In addition to fossil fuels, the excessive and unprincipled use of chemical inputs such as nitrogen fertilizers in agriculture has caused numerous environmental problems (Soltani et al., 2010), to the extent that this sector contributes nearly 40% of nitrogen oxides emissions (Energy the Balance Sheet, 2008). Another study has reported that nitrogen fertilizer consumption has led to the emission of 10 to 40% of nitrogen oxides (Linzmeier et al., 2001).

As previously mentioned, the increase in agricultural production has resulted in widespread use of agricultural inputs such as chemical fertilizers, pesticides, and agricultural machinery (Brentrup et al., 2004a, 2004b), leading to a severe dependency of the agricultural sector on energy consumption in recent decades (Sefeedpari et al., 2014). High energy consumption has numerous negative effects on the public health of human societies and the environment, emphasizing the importance of examining energy consumption patterns for efficient use in the agricultural sector (Rafiee et al., 2010). Therefore, one of the significant needs for sustainable development in agriculture is studying the effective use of energy and greenhouse gas emissions in agricultural ecosystems (Mohammadi et al., 2011).

Crop rotation is one of the sustainable agricultural strategies that leads to reduced energy consumption in the process of producing agricultural products. Integrating leguminous plants such as chickpea into crop rotation with other crops results in savings in nitrogen fertilizer use (Nemecek et al., 2008), thereby enhancing energy consumption efficiency. In another study, implementing suitable crop rotations was identified as one of the factors reducing fertilizer consumption and consequently lowering energy consumption and greenhouse gas emissions caused by chemical fertilizers, particularly nitrogen, in wheat production in New Zealand (Safa and Samarasinghe, 2012). A study examining the long-term effects of crop rotation and tillage on greenhouse gas emissions in the United States reported that using a corn-soybean rotation led to a reduction in nitrogen oxide emissions by approximately 35% (Behnke et al., 2018). Another research that measured the effects of irrigation, tillage, crop rotation, and nitrogen fertilizer on greenhouse gas emissions in North Dakota indicated that a no tillage chickpea-barley rotation could reduce greenhouse gas emissions (Sainju et al., 2012).

Kermanshah is considered one of the most important provinces for agricultural production in Iran. The province's favorable climatic diversity has led to the cultivation of various agricultural products. The area of Kermanshah's agricultural ecosystems is approximately 840000 ha, of which 74 and 26% are dedicated to dryland and irrigated agroecosystems, respectively (MJA, 2022). One of common crops in the dryland agroecosystems is wheat which usually cultivated either as a monoculture or in rotation with chickpeas. Therefore, wheat and chickpeas are regarded as the most critical agricultural products in Kermanshah province. The objective of this research was 1) to measure energy inputs and energy outputs 2) to calculate the amount of greenhouse gas emissions due to consumption of energy inputs such as nitrogen, phosphorus, potassium, herbicides, insecticides, and fungicides and 3) to evaluate global warming potential in wheat monoculture agroecosystem compared to wheat-chickpea rotation dryland agroecosystem in Kermanshah region.

2. Materials and Methods

This research was conducted in the Kermanshah region (34◦19′N, 47◦50′E, altitude 1400 m) during 2021 (Figure 1). In terms of climate conditions, this region is classified as a semi-arid region based on the Dumartin climate classification (Bagherabadi, 2022), where wheat and chickpeas are cultivated in its dryland agroecosystems, either as a monoculture or in rotation with each other.

Wheat is sown in mid-October to mid-November and it is harvested in early July. Chickpeas are usually sown in mid-March and it is harvested in June. The statistical population included all dryland farmers who cultivated wheat and chickpeas as a monoculture or in rotation with each other. To determine the sample size, Cochran's formula was used (Snedecor and Cochran, 1989):

$$n = \frac{N(s\times t)^2}{(N-1)d^2+(s\times t)^2} \quad (1)$$

In this equation, s represents the estimate of the population standard deviation, t= 1.96 (at a 95% confidence level), d is the desired precision level set at 0.05, N is the population size (number), and n is the sample size (number). In 2021, approximately 87000 ha of wheat and 36000 ha of chickpeas were cultivated in the dryland agroecosystems of Kermanshah region (MJA, 2022). The number of farmers who cultivated dryland wheat and dryland chickpeas were 17049 and 7790, respectively, and based on the results of Cochran's equation (Eq. 1), 600 farmers (350 and 250 for wheat and chickpeas, respectively) were selected as a sample from the total target statistical population. After determining the number of farmers, information related to all agricultural operations in the wheat and chickpea production process, such as the use of agricultural machinery, preparation of seedbeds, consumption of chemical inputs, fossil fuels, weed control, plant protection , harvesting and transportation of the

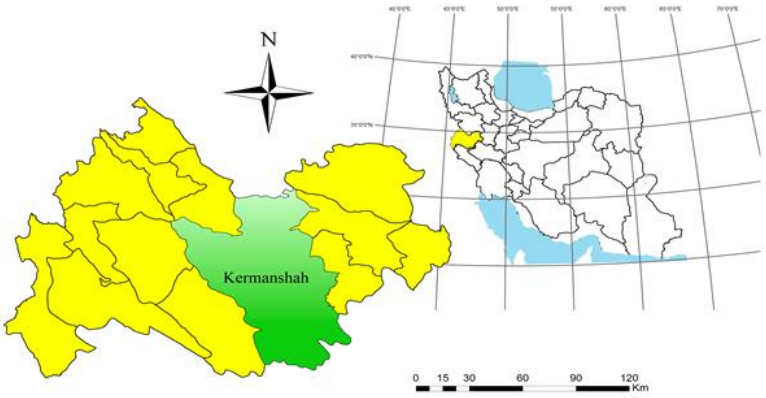

Figure1. Geographical location of the study area (Kermanshah region)

product, was collected in the form of a questionnaire and through face-to-face interviews with farmers and agricultural experts.

2.1. Energy Input (Consumption)

At this stage, the consumption values of each input from planting to harvesting were recorded, and based on the relevant coefficients, the amount of energy input was calculated (Table 1). The total energy input was computed from the sum of energies of labor, machinery, fuel, chemical and animal fertilizers, pesticides, and seeds. To estimate the energy consumption in consumable inputs such as fertilizers, pesticides, and insecticides, the energy per gram of active ingredient was multiplied by the relevant coefficients and their specific weights. Other calculations of consumed energy for inputs and outputs used in production and agricultural operations for each method were carried out using coefficients obtained from various sources.

2.2. Energy Analysis

The data collected through the completion of questionnaires, after classification and processing according to Table 1, was converted into energy equivalents, and all input and output were converted into energy units**.**

Table 1. Equivalents of input and output energies consumed in wheat monoculture and wheat-chickpea rotation ecosystems

Input and output	Unit (hectare)	Energy equivalent	References
	Input		
Human labor	hr	1.96	Ozkan et al., 2004
Seed	kg	14.7	
Machinery	kg	62.7	Hatirili et al., 2005
	Chemical fertilizers		
Nitrogen	kg	66.14	Yilmaz et al., 2005; Esengun et al., 2007
Phosphor	kg	12.44	Yilmaz et al., 2005; Esengun et al., 2007
Potassium	kg	11.15	Yilmaz et al., 2005; Esengun et al., 2007
Diesel fuel	L	51.33	Erdal et al., 2007; Esengun et al., 2007
Herbicides	kg	101.2	Ghiyasi et al., 2008; Yaldiz et al., 1993
Pesticides	kg	199.0	Hensel et al., 1992
Fungicide	kg	181.9	Mohammadi et al., 2008
	Output		
Seed	kg	14.7	Ozkan et al, 2004; Mandal et al.,2002
Straw	kg	12.5	Ozkan et al., 2004; Yousefi et al., 2014

After calculating the energy inputs and energy outputs in the dryland wheat and chickpea agroecosystems, the energy use efficiency (EUE), energy productivity (EP) in kg Mj^{-1}, and net energy (NEY) in Mj ha^{-1} were obtained through equations 2 to 4 (Rezvantalab et al., 2018).

$$EUE=EO/EI \quad (2)$$

$$EP=GY/EI \quad (3)$$

$$NEY=EO-EI \quad (4)$$

In these equations, EO is the total energy outputs (Mj ha^{-1}), EI is the total energy inputs (Mj ha^{-1}), and GY is the grain yield (t ha^{-1}). Subsequently, based on the types of agricultural activities and input resources utilized in the wheat and chickpea dryland agroecosystems, the shares of renewable and non-renewable energies from the total energy consumption were calculated. According to the types of inputs, labor and seed energies were categorized as renewable, while fossil fuels, chemical fertilizers, herbicides, pesticides, fungicides, and machinery categorized as non-renewable energies**.**

2.3. Global Warming Potential (GWP)

The GWP refers to the total amount of greenhouse gases produced, expressed in terms of carbon dioxide equivalents (IPCC, 1996). To calculate the GWP, the emissions of greenhouse gases such as carbon dioxide, nitrous oxide, and methane resulting from energy

consumption in the production of inputs and various agricultural operations were considered. These inputs and operations included nitrogen, phosphorus, and potassium fertilizers, chemical herbicides, fungicides, and insecticides, as well as fossil fuel consumption for agricultural operations, transportation, and the production and maintenance of agricultural equipment**.** Finally, to determine the amount of greenhouse gas emissions, the quantities of energy inputs consumed were multiplied by the equivalents of greenhouse gas production and emissions (Table 2) (Rezvantalab et al., 2018)**.**

Table 2. Amounts of greenhouse gas emissions (in grams) per consumption of chemical inputs and global warming potential

Inputs	CH_4	N_2O	CO_2	References
Diesel fuel (L ha^{-1})	5.2	0.7	3560	Kramer et al., 1999
Nitrogen fertilizers (kg ha^{-1})	3.37	0.03	3100	Snyder et al., 2009
Phosphate fertilizers (kg ha^{-1})	1.8	0.02	1000	Snyder et al., 2009
Potassium fertilizers (kg ha^{-1})	1.0	0.1	700	Snyder et al., 2009
Global warming potential	21.0	310.0	1.0	Tzilivakis et al., 2005

2.4. Statistical Analysis

Various input usage values and comprehensive data were collected and recorded at each stage from planting to harvesting, and their processing was performed using Excel software. Data analysis was performed in three sections: energy inputs (consumed), energy outputs (produced), and the GWP resulting from greenhouse gas emissions in the wheat monoculture and wheat-chickpea rotation dryland agroecosystems**.**

3. Results and Discussion

3.1. Input and Output Energies

The total energy input in the wheat monoculture and wheat-chickpea rotation dryland agroecosystems were 15106.8 and 13550.5 Mj ha^{-1}, respectively (Tables 3 and 4). In the wheat monoculture agroecosystem, the highest share of energy consumption corresponded to fossil fuel (37.6%), nitrogen fertilizers (28.9%), and seeds (18.0%). In the wheat-chickpea rotation agroecosystem, the highest share of energy consumption corresponded to fossil fuel (37.1%), nitrogen fertilizers (26.5%), and seeds (19.8%). Although the percentages of consumed energies in the investigated agroecosystems were relatively similar in terms of input contributions, there were differences in the amounts of inputs consumed (Tables 3 and 4).

Table 3. The amount of energy inputs and outputs in the wheat monoculture dryland agroecosystem

Inputs	Unit	Amount	Energy equivalent	Total energy equivalent	Percentage of total
Human labor	$hr.ha^{-1}$	129.48	1.96	253.78	1.67
Machinery	$hr.ha^{-1}$	15.83	62.7	992.54	6.57
Diesel fuel	$l.ha^{-1}$	110.54	51.33	5674.17	37.56
Nitrogen	kg ha^{-1}	66.08	66.14	4370.53	28.93
Phosphor	kg ha^{-1}	49.27	12.44	612.92	4.05
Potassium	kg ha^{-1}	24.22	11.15	270.05	1.78
Herbicides	L ha^{-1}	0.89	101.2	90.07	0.59
Pesticides	L ha^{-1}	0.47	199.0	93.53	0.61
Fungicide	L ha^{-1}	0.27	120.0	32.40	0.21
Seed	kg ha^{-1}	184.82	14.7	2716.85	17.98
Total energy input	MJ ha^{-1}			15106.85	
Wheat grain	kg ha^{-1}	1648.66	14.7	24235.30	57.89
Wheat straw	kg ha^{-1}	1410.00	12.5	17625.00	42.11
Total energy output	MJ ha^{-1}			41860.30	

Table 4. The amount of energy inputs and outputs in the wheat-chickpea rotation dryland agroecosystem

Inputs	Unit	Amount	Energy equivalent	Total energy equivalent	Percentage of total
Human labor	$hr.ha^{-1}$	112.66	1.96	220.81	1.69
Machinery	$hr.ha^{-1}$	13.91	62.7	872.16	6.43
Diesel fuel	$l.ha^{-1}$	97.99	51.33	5029.62	37.11
Nitrogen	kg ha^{-1}	54.22	66.14	3586.11	26.46
Phosphor	kg ha^{-1}	54.07	12.44	672.63	4.96
Potassium	kg ha^{-1}	24.38	11.15	271.84	2
Herbicides	L ha^{-1}	0.78	101.2	78.94	0.58
Pesticides	L ha^{-1}	0.51	199	101.49	0.74
Fungicide	L ha^{-1}	0.26	120	31.2	0.23
Seed	kg ha^{-1}	182.7	14.7	2685.69	19.81
Total energy input	MJ ha^{-1}			13550.48	
Wheat grain	kg ha^{-1}	1870.92	14.7	27502.52	60.04
Wheat straw	kg ha^{-1}	1464	12.5	18300	39.95
Total energy output	MJ ha^{-1}			45802.52	

In the wheat monoculture agroecosystem, the consumption of fossil fuels and nitrogen fertilizers were 110.5 L ha^{-1} and 66.1 kg ha^{-1}, respectively, while these values for the wheat-chickpea rotation agroecosystem were 0.98 L ha^{-1} and 2.54 kg ha^{-1}. The lower input consumption in the wheat-chickpea rotation agroecosystem, compared to wheat monoculture agroecosystem, may be attributed to improved soil nitrogen content and reduced soil compaction. The presence of leguminous plants in the rotation contributes to improving soil nitrogen content through biological nitrogen fixation, while their deep tap root system enhances root development depth, which may impact soil compaction levels**.** Another study has reported that the application of forage crop rotation with legumes in Western Canada resulted in reduced energy consumption compared to monoculture systems (Hoeppner et al., 2000).

The results of this investigation also showed that the total energy output in the dryland wheat monoculture agroecosystem was 41860.3 Mj ha^{-1}, with grain and straw production accounting for 57.9% and 42.1%, respectively (Table 3). The total energy output in the dryland wheat-chickpea rotation agroecosystem was 45802.5 Mj ha^{-1}, with grain and straw production contributing 60.1% and 39.9%, respectively (Table 4).

Table 5. Energy indicators in wheat monoculture and wheat-chickpea rotation dryland agroecosystems

Energy indicators	Unit	Monoculture	Wheat-chickpea rotation
Total energy input	MJ ha^{-1}	15106.8	13550.48
Total energy output	MJ ha^{-1}	41860.3	45802.52
Energy use efficiency	-	2.77	3.38
Energy productivity	kg MJ^{-1}	0.109	0.138
Net energy	MJ ha^{-1}	26753.4	32252.1
Renewable energy	MJ ha^{-1}	2970.6 (19.7%)	2906.5 (21.4%)
Nonrenewable energy	MJ ha^{-1}	12136.2 (80.3%)	10644.0 (78.6%)

3.2. Energy indicators

The total energy input in the wheat monoculture agroecosystem was about 12% higher than in the wheat-chickpea rotation agroecosystem. The total energy output in the wheat monoculture agroecosystem was approximately 9% lower than that of the wheat-chickpea rotation agroecosystem. The energy use efficiency in the dryland wheat-chickpea rotation agroecosystem was about 18% higher than that of the dryland wheat monoculture agroecosystem (Table 5). The lower consumption of chemical inputs and fossil fuels, combined with higher energy outputs, appears to enhance energy use efficiency in the wheat-chickpea rotation agroecosystem compared to wheat monoculture agroecosystem. Another study reported that increasing the diversity of agricultural products and utilizing crop rotation could be an effective method for enhancing energy use efficiency and reducing environmental pollution (Alluvione et al., 2011). Other researchers, by examining the effects of crop rotation on the energy efficiency of irrigated potato with cereals, canola, and alfalfa over a 14-year period in Canada, emphasized that potato producers should incorporate legumes into their crop rotation systems to maintain yield levels while increasing energy use efficiency (Khakbazan et al., 2019)**.**

For every unit of energy in the wheat-chickpea dryland agroecosystem, 0.13 kg of grain are produced, whereas under monoculture conditions, 0.10 kg of grain are produced. The energy productivity in the wheat-chickpea rotation agroecosystem is approximately 21% higher than that of the wheat monoculture agroecosystem. The lower energy consumption and more optimal use of energy inputs during their conversion to dry matter in the wheat-chickpea rotation compared to monoculture conditions may have led to the improvement in energy productivity. Additionally, in the wheat-chickpea dryland agroecosystem, the net energy is 17% higher than in the wheat monoculture agroecosystem. In the wheat-chickpea rotation agroecosystem, the shares of non-renewable and renewable energies are 78.6% and 21.4%, respectively, while in the wheat monoculture agroecosystem, the shares of these energies are 80.3% and 19.7% of total energy input (Table 5). Renewable energies have an ecological origin that is produced within the agroecosystems, whereas non-renewable energies are imported from outside the agroecosystems. Therefore, the higher the proportion of renewable energies in the management of agricultural systems, the greater the sustainability of those agroecosystems. In another study, it was reported that the proper application of crop rotation resulted in improved energy productivity (Khakbazan et al., 2019). It has also been reported that the use of crop rotation involving forage crops with legumes led to a reduction in the consumption of non-renewable energies due to the biological nitrogen fixation by legumes (Hoeppner et al., 2000).

3.3. Global Warming Potential (GWP)

The GWP in the wheat monoculture and wheat-chickpea rotation agroecosystems were 709.28 and 672.92 kg eq CO_2 h^{-1}, respectively (Table 6). The GWP in wheat monoculture agroecosystem was 11.50% higher compared to the wheat-chickpea rotation agroecosystem. In the wheat monoculture and wheat-chickpea rotation agroecosystems, fossil fuel consumption had the largest share in the emissions of greenhouse gases CO_2, N_2O, and CH_4. The highest and lowest greenhouse gas emissions were attributed to fossil fuel consumption and potassium fertilizers, respectively (Table 6). Results also indicated that nitrogen fertilizer consumption in the wheat monoculture agroecosystem was higher than in the wheat-chickpea rotation agroecosystem.

It seems that in the wheat monoculture agroecosystems, due to the plant's inadequate response to the consumed nitrogen, increasing nitrogen levels may not significantly improve yield and, therefore, nitrogen uptake efficiency is low under. In another study, it was determined that transitioning from traditional rotation (celery-tomato-

lettuce) to modified (clover-tomato-lettuce) reduced nitrogen fertilizer input by up to 25%, nitrous oxide emissions by up to 24%, and the GWP by up to 14% (Min et al., 2016). The presence of legume crops in crop rotation in Mediterranean dryland agroecosystems significantly altered greenhouse gas emissions and carbon sequestration due to low soil organic matter content and fertility (Guardia et al., 2016). Another study reported that lupin-wheat rotation, compared to wheat monoculture, resulted in reduced greenhouse gas emissions (Barton et al., 2013).

Table 6. Greenhouse gases emission (kg ha^{-1}) and global warming potential (kg eq Co_2 h^{-1}) in wheat monoculture and wheat-chickpea rotation agroecosystems

Inputs	Monoculture				Wheat-chickpea rotation			
	CO_2	N_2O	CH_4	GWP	CO_2	N_2O	CH_4	GWP
Diesel fuel	393.53	0.0773	0.5748	429.56	348.83	0.0685	0.5095	380.76
Nitrogen fertilizers	204.84	0.0019	0.2226	210.10	168.08	0.0016	0.1827	172.41
Phosphate fertilizers	49.27	0.0009	0.0886	51.41	54.07	0.0010	0.0973	56.42
Potassium fertilizers	16.954	0.0024	0.0242	18.21	17.066	0.0024	0.0243	18.32
Global warming potential				709.28				627.92

The results of this study also indicated that the application of nitrogen fertilizers led to higher greenhouse gas emissions and GWP compared to other chemical inputs (Table 6). The nitrogen emission coefficient (1.3 kg CO_2 $kg^{-1}{}_N$) is higher compared to phosphorus and potassium (Lal, 2004), which is related to the nitrogen fixation and production process in the factory (Snyder et al., 2009). The production of nitrogen in the factory is a very costly process that directly uses fossil fuels as an energy source. Therefore, any approach that can lead to a reduction in the consumption of synthetic nitrogen in agroecosystems could directly decrease greenhouse gas emissions and GWP during the agricultural product production process. Increasing biodiversity through crop rotation is one of the most important factors in enhancing nitrogen efficiency in agroecosystems (Montemuro et al., 2006). In rotational systems, the productivity of consumed resources, especially accessible nitrogen, increases due to improved plant growth conditions and reduced limiting factors for production, while nitrogen losses are minimized. Choosing a high-efficiency nitrogen rotation system reduces the dependence of agroecosystems on nitrogen fertilizers and thus decreases energy consumption and enhances system sustainability. Since the amount of fertilizer applied per production yield in rotational systems is less than in monoculture agroecosystems, the land use efficiency in a rotational pattern will increase at intermediate and low nitrogen levels (Franszluebbers et al., 1995).

4. Conclusion

To achieve a suitable level of sustainability in agroecosystems, it is essential to consider the balance between energy inputs and energy outputs, as increased energy inputs reduces energy efficiency. The results of this study showed that in the wheat-chickpea rotation agroecosystem compared to the wheat monoculture agroecosystem the total energy input was lower, while in this agroecosystem the total energy output was higher. The energy use efficiency and the energy productivity were higher in the wheat-chickpea rotation agroecosystem compared to the wheat monoculture agroecosystem. The greenhouse gas emissions in the wheat-chickpea rotation agroecosystem compared to wheat monoculture agroecosystem was lower due to reduced consumption of fossil fuels and nitrogen fertilizers. Planting chickpeas before wheat had positive effects, such as soil fertility improvement, reduced need for nitrogen fertilizer, decreased use of agricultural equipment, and ultimately increased wheat grain yield. These results led to lower greenhouse gas emissions and, consequently, a reduced GWP. Therefore, to prevent greenhouse gas emissions in Kermanshah's dryland agroecosystems, it is recommended to further promote the wheat-chickpea crop rotation agroecosystem compared to wheat monoculture agroecosystem.

Acknowledgments

Thanks and appreciation are expressed to the staff of the Agricultural Jihad Organization of Kermanshah province for their support in collecting information for this research.

References

Alluvione, F., Moretti, B., Sacco, D., & Grignani, C. (2011). EUE (energy use efficiency) of cropping systems for a sustainable agriculture. *Energy*, *36*, 4468-4481. **doi: 10.1016/j.energy.2011.03.075**

Bagherabadi, R. (2022). Investigation of climate change on the kermanshah city using the demartoune, ambrothermic and embereger in 1991-2021. *Geography and human Relationships, 4*(4), 173-185. [In Persian]. **doi: doi: 20.1001.1.26453851.1401.4.4.12.4**

Barton, L., Murphy, D. V., & Butterbach-Bahl, K. (2013). Influence of crop rotation and liming on greenhouse gas emissions from a semi-arid soil. *Agriculture, Ecosystems & Environment, 167*, 23-32. **doi: 10.1016/j.agee.2013.01.003**

Behnke, G. D., Zuber, S. M., Pittelkow, C. M., Nafziger, E. D., & Villamil, M. B. (2018). Long-term crop rotation and tillage effects on soil greenhouse gas emissions and crop production in illinois, USA. *Agriculture, Ecosystems and Environment, 261*, 62-70. **doi: 10.1016/j.agee.2018.03.007**

Brentrup, F., Küsters, J., Kuhlmann, H., & Lammel, J. (2004a). Environmental impact assessment of agricultural production systems using the life cycle assessment methodology: I. Theoretical concept of a LCA method tailored to crop production. *European Journal of Agronomy, 20*(3), 247-264. **doi: 10.1016/s1161-0301(03)00024-8**

Brentrup, F., Küsters, J., Lammel, J., Barraclough, P., & Kuhlmann, H. (2004b). Environmental impact assessment of agricultural production systems using the life cycle assessment (LCA) methodology ii. The application to N fertilizer use in winter wheat production systems. *European Journal of Agronomy, 20*(3), 265-279. **doi: 10.1016/s1161-0301(03)00039-x**

Energy the Balance Sheet. 2008. Available at Web site http://www.moe.gov.ir.

Feyzbakhsh, M. T., & Alizadeh, P. (2018). Comparison of silage corn (*Zea mays* L.) and forage sorghum (*Sorghum bicolor L*.) productions in terms of energy consumption and global warming potential in gorgan region. *Journal of Agroecology, 10*(1), 218-233. [In Persian]. **doi: 10.22067/jag.v10i1.56517**

Franszluebbers, A., Hons, F., & Saladino, V. (1995). Sorghum, wheat and soybean production as affected by long-term tillage, crop sequence and N fertilization. *Plant and Soil, 173*, 55-65. **doi: 10.1007/bf00155518**

Guardia, G., Tellez-Rio, A., García-Marco, S., Martin-Lammerding, D., Tenorio, J. L., Ibáñez, M. Á., & Vallejo, A. (2016). Effect of tillage and crop (cereal versus legume) on greenhouse gas emissions and global warming potential in a non-irrigated mediterranean field. *Agriculture, Ecosystems & Environment, 221*, 187-197. **doi: 10.1016/j.agee.2016.01.047**

Hoeppner, J. W., Entz, M. H., McConkey, B. G., Lafond, G. P., & Zentner, R. P. (2000). The role of forage legumes in reducing on-farm non-renewable energy use *Soils and crops workshop*.

Khakbazan, M., Mohr, R. M., Huang, J., Xie, R., Volkmar, K. M., Tomasiewicz, D. J., & Nelson, A. (2019). Effects of crop rotation on energy use efficiency of irrigated potato with cereals, canola, and alfalfa over a 14-year period in Manitoba, Canada. *Soil and Tillage Research, 195*, 104357. **doi: 10.1016/j.still.2019.104357**

Kizilaslan, H. (2009). Input–output energy analysis of cherries production in Tokat province of Turkey. *Applied Energy, 86*, 1354-1358. **doi: 10.1016/j.apenergy.2008.07.009**

Lal, R. (2004). Carbon emission from farm operations. *Environment International, 30*(7), 981-990. **doi: 10.1016/j.envint.2004.03.005**

Linzmeier, W., Gutser, R., & Schmidhalter, U. (2001). Nitrous oxide emission from soil and from a nitrogen 15-labelled fertilizer with the new nitrification inhibitor 3, 4-dimethylpyrazole phosphate (DMPP). *Biology and Fertility of Soils, 34*(2), 103-108. **doi: 10.1007/s003740100383**

Min, J., Lu, K., Sun, H., Xia, L., Zhang, H., & Shi, W. (2016). Global warming potential in an intensive vegetable cropping system as affected by crop rotation and nitrogen rate. *Clean–Soil, Air, Water, 44*(7), 766-774. **doi: 10.1002/clen.201400785**

Ministry of Jihad-e-Agriculture of Iran (MJA). 2022. Agricultural Jihad Organization of Kermanshah Province.

Mohammadi, A., Tabatabaeefar, A., Shahin, S., Rafiee, S., & Keyhani, A. (2008). Energy use and economical analysis of potato production in iran a case study: Ardabil province. *Energy Conversion and Management, 49*, 3566-3570.

Montemuro, F., Maiorana, M., Ferri, D., & Convertini, G. (2006). Nitrogen indicators, uptake and utilization efficiency in a maize and barley rotation cropped at different levels and source of N fertilization. *Field Crops Research, 99*, 114-124. **doi: 10.1016/j.fcr.2006.04.001**

Nasirian, N., Almasi, M., Minaee, S., & Bakhoda, H. (2006). Study of energy flow in sugarcane production in an agro-industry unit in south of Ahvaz *Proceeding 4th national congress of agricultural machines*. Tabriz, Iran, 11-14 March. [In Persian].

Nemecek, T., Richthofen, J. S., Dubois, G., Casta, P., Charles, R., & Pahl, H. (2008). Environmental impacts of introducing grain legumes into European crop rotations. *European Journal of Agronomy, 28*, 380-393. **doi: 10.1016/j.eja.2007.11.004**

Ozkan, B., Akcaoz, H., & Karadeniz, F. (2004). Energy requirement and economic analysis of citrus production in Turkey. *Energy Conversion Management, 45*, 1821-1830. **doi: 10.1016/j.enconman.2003.10.002**

Rafiee, S., Avval, S. H. M., & Mohammadi, A. (2010). Modeling and sensitivity analysis of energy inputs for apple production in Iran. *Energy, 35*(8), 3301-3306. **doi: 10.1016/j.energy.2010.04.015**

Rezvantalab, N., Soltani, A., Zeinali, E., & Foroughinia, A. (2018). Study of energy indicators and greenhouse gas emissions in wheat production in Golestan province. *Journal of Agroecology, 9*(1), 17-38. [In Persian].

Safa, M., & Samarasinghe, S. (2012). Co_2 emissions production in Canterbury, New Zealand. *Environmental Pollution, 171*, 126-132. **doi: 10.1016/j.envpol.2012.07.032**

Sainju, U. M., Stevens, W. B., Caesar-TonThat, T., & Liebig, M. A. (2012). Soil greenhouse gas emissions affected by irrigation, tillage, crop rotation, and nitrogen fertilization. *Journal of environmental quality, 41*(6), 1774-1786. **doi: 10.2134/jeq2012.0176**

Sefeedpari, P., Shokoohi, Z., & Behzadifar, Y. (2014). Energy use and carbon dioxide emission analysis in sugarcane farms: A survey on Haft-Tappeh Sugarcane Agro-Industrial company in Iran. *Journal of Cleaner Production, 83*, 212-219. **doi: 10.1016/j.jclepro.2014.07.048**

Singh, G., Singh, S., & Singh, J. (2004). Optimization of energy inputs for wheat crop in Punjab. *Energy Conversion and Management, 45*(3), 453-465. **doi: 10.1016/s0196-8904(03)00155-9**

Snedecor, G. W., & Cochran, W. G. (1989). *Statistical methods,* 8th Edn: Iowa State University Press.

Snyder, C. S., Bruulsema, T. W., Jensen, T. L., & Fixen, P. E. (2009). Review of greenhouse gas emissions from crop production systems and fertilizer management effects. *Agriculture, Ecosystems and Environment, 133*, 247-266. **doi: 10.1016/j.agee.2009.04.021**

Soltani, A., Rajabi, M. H., Zeinali, E., & Soltani, E. (2010). Evaluation of environmental impact of crop production using LCA: Wheat in Gorgan. *Crop Production, 3*(3), 201-218. **dor: 20.1001.1.2008739.1389.3.3.12.1**

Yaldiz, O., Ozturk, H. H., Zeren, Y., & Bascetincelik, A. 1993. Energy usage in production of field crops in Turkey. In: 5th International Congress on Mechanisation and Energy Use in Agriculture, October., Kusadas, Turkey, pp. 11-14

Agriculture, Environment & Society

Journal homepage: www.aes.uoz.ac.ir

Watershed management by identifying suitable places for water storage, a way to ecological compression (case study: Talandasht district, Kermanshah-Iran)

Ahmad Ghanbari [*a], Sadegh Jalilian [b], Alireza Bagheri [c], Bita Abbasi [d]

[a] Department of Agronomy, Faculty of Agriculture, University of Zabol, Zabol, Iran
[b] Ph.D student, Department of Agronomy, Faculty of Agriculture, University of Zabol, Zabol, Iran
[c] Department of Plant Production and Genetic Engineering, Campus of Agriculture and Natural Resources, Razi University, Kermanshah, Iran
[d] Ph.D student of Agroecology, Department of Plant Production and Genetic Engineering, Razi University, Kermanshah, Iran

ARTICLE INFO

Article history:
Received: 4 June 2024
Accepted: 10 September 2024
Available online: 1 December 2024

Keywords:
Analysis Hierarchical Process (AHP)
Rainwater harvesting
Remote Sensing
Sustainable Management

ABSTRACT

This study aims to determine the optimal locations for rainwater harvesting in the Talandasht region of the province of Kermanshah. As a multivariate analysis, the Analytic Hierarchy Process (AHP) was used to determine the optimal sites. GIS identifies the optimal locations for the Talandasht region based on the biophysical characteristics taken into account. In this study, slopes between five and fifteen percent were given the highest score, while slopes below five and above sixty percent received the lowest score. The soil permeability was measured using soil hydrological groups, with hydrological groups 4 (D) and 1 (A) receiving the highest and lowest scores, respectively. Over 10,000 hectares of Talandasht's total area have a slope greater than five percent, and runoff is flowing in it. If the average annual rainfall is 400 mm, there will be 34285714 cubic meters of precipitation. By determining the optimal storage location, water can be stored and used for additional purposes, including supplemental irrigation and the creation of rainfed gardens. In various regions of the country, rainwater collection has a high executive potential. Conservation and integrated agriculture are excellent opportunities for conserving and storing rainwater in the region and reducing the region's yield gap.

Highlights

- This study determines Kermanshah's Talandasht region's best rainwater harvesting sites.
- Runoff flows in over 10,000 ha of Talandasht's slopes greater than 5%.
- Water can be stored for irrigation and rainfed gardens by finding the best storage location.
- Conservation and integrated agriculture can store rainwater and reduce the region's yield gap.

1. Introduction

Dry areas are areas with an aridity index (average ratio of annual precipitation to potential evapotranspiration) less than 0.65. As the world's largest biome, these regions cover about 45% of the earth's surface (Prăvălie, 2016). They support and feed approximately 38% of the world's human population (Ray-Shyan et al., 2018). Dry areas have difficult conditions for agriculture in terms of climate and soil because the annual water balance is negative, the rainy season is short and variable, the content of soil organic matter is low, and soil erosion and salinity are high (Kassam et al., 2012). However, due to population growth and climate change scenarios, the long-term sustainability of rain-fed agriculture in dry areas is critical to global food security (García-Palaciosa et al., 2019). The yield gap (difference between potential and actual yields) is high in dry areas, especially in dry farming. The water -holding capacity of the soil, a key regulatory system in dry farming, is strongly related to the soil structure (Maestre et al., 2016).

The world today faces many challenges, including poverty, environmental degradation, climate change, and ensuring food security. At the same time, there is a lot of competition for land, water, energy, and other inputs in food production. The entry of humankind into a new historical period called the Anthropocene (climate change

* Corresponding author.
E-mail address: ghanbari@uoz.ac.ir
https://doi.org/10.22034/aes.2023.367206.1046

caused by human activities) has exposed the universe to the biggest drivers of change; Agriculture is one of the main factors that cause these changes. As a result, food insecurity and climate changes in a region can have wide political and economic effects. These challenges require action through a transformation in the food production system. Increasing food production per unit area in a way that creates less pressure on the environment and maintains production capacity in the future can be a suitable response to these factors. Sustainable compression in this framework seeks to increase the achievements of the agricultural sector while keeping the ecological footprint low. Sustainable compaction is the result of two technological and socio-economic approaches. Among these, there are two technological principles: one is the use of agro-environmental processes, such as sustainable or ecological compression, and the other is the use of plant and animal breeding (genetic compression). Therefore, policymakers for food production systems should consider multiple objectives from multifunctional perspectives, including biodiversity, sustainable development, rural economy, etc.

Sustainable compression is a method of production in which crop production is improved without negative environmental effects or cultivating new lands. The FAO also recently defined ecological compaction or sustainable compaction in the organic farming complex as an increase in primary production per unit area without compromising the system's ability to maintain its productive capacity (Ray-Shyan et al., 2018).

Rainwater harvesting, which has gained renewed attention since the 1980s, has been a rational approach to water scarcity for thousands of years (Ray-Shyan et al., 2018). Increasing the efficiency and productivity of water depends on the identification of rainwater collection sites. Every year, about 413 billion cubic meters of water enter the country as a result of precipitation, of which about 283 billion cubic meters reenter the atmosphere through evaporation and transpiration. Only 130 billion cubic meters of it are renewable and are either stored behind dams or used to feed underground water tables. The purpose of implementing rainwater collection projects is actually to use the 283 billion cubic meters of water that are lost every year in the form of evaporation and transpiration. It should be noted that the generalization of this plan on a wide scale can lead to a lack of serious attention to the category of natural nutrition. The underground water tables and aquifers will be destroyed. As a result, it will have adverse effects on the environment.

Moving towards a sustainable compression model requires some operational strategies. The following can be mentioned:

1) Planning and applying on-farm practices in the fields of watersheds, ecosystems, and landscapes, and maximizing productivity by increasing ecological activities and actions

2) Combining ecosystem-based strategies with beneficial practices in which natural capital (soil, biodiversity, water, etc.) and multifunctional ecosystems are used as tools for developing productive and resilient agricultural systems.

3) Development of agricultural practices based on systems thinking in which land, water, food, livestock, and crop management are integrated.

4) Using the cyclical system to manage natural resources (for example, food recycling),

5) Controlling agroecological processes, such as the food cycle, biological nitrogen fixation, metamorphosis, etc.

6) Helping farmers to accept barriers to sustainable compaction and creating motivation for its sustainable adoption by addressing long-term profitable ecological practices.

7) Creating strong organizations consisting of smallholder farmers by taking advantage of the role of women, who are recognized as intermediaries between the markets and the government.

Sustainable intensification can provide more food and better ecosystems and transform agriculture into a major contributor to global sustainability (Foley et al., 2011).

Ameri Ekhtearabadi et al. (2011) conducted a study with the aim of determining suitable water harvesting locations using the Analytical Hierarchy Process (AHP). They used the river, slope, vegetation, land use, and road profiles digitally. After the relative weighting of the layers in the GIS† environment, suitable catchment locations were divided into five areas based on priority. In a similar way to the results of Jalili et al. (2007) in Sarab Niloufer Plain of Kermanshah, it was showed that the parameters of permeability, texture, and thickness of the critical layer had the highest importance. An important parameter for suitable areas for rainwater harvesting is rainfall. In this case, factors such as the number of days when the rainfall exceeds the basin threshold, the minimum and maximum rainfall probability, and the annual average rainfall probability are important. Land use or vegetation is another important parameter that affects surface runoff (Ameri Ekhtearabadi et al., 2011). It has been proven that the density of vegetation will increase infiltration and thus reduce the share of runoff. The type of soil and environmental issues are also important (Jalili et al., 2014).

Identifying potential sites for rainwater harvesting is an important step toward maximizing water and land productivity in arid regions. In addition to identifying the appropriate location, their technical design is also a key factor in the success of rainwater harvesting systems (Al-Adamat et al., 2012). The suitability of rainwater harvesting sites depends on several criteria (Mahmoud and Alazba, 2014), technique, and method (Winnaar et al., 2007). Analysis of the main factors to decide and choosing the best method and location size depends on the target area (Ray-Shyan et al., 2018). One group of studies on biophysical parameters such as rainfall, drainage system, slope, land use, and soil type (Kumar et al., 2008: Kadam et al., 2012) and another group on socio-economic parameters (land ownership, distance to residential areas, streams, roads, agricultural area, population density, and

†. Geographic information system

associated cost) (Bulcock and Jewitt., 2013: Hobbs et al., 2008: Kahinda et al., 2008; Krois and Schulte., 2014). The most common biophysical criteria used in arid and semi-arid regions to identify suitable sites for rainwater harvesting (as a percentage of all reviewed studies) are slope (83%), land use/cover (75%), soil type (75%), and rainfall (56%). Distance to settlements (25%), distance to streams (15%), distance to roads (15%), and cost (8%) were also the most important socio-economic criteria, which are discussed in another category.To identify suitable sites using biophysical criteria, tools, and methods such as GIS and remote sensing (Bamne et al., 2014), hydrological modeling with GIS and remote sensing (Mahmoud and Alazba., 2014), the multi-criteria analysis combined with modeling Hydrological, GIS and remote sensing (Khan and Khattak, 2012) and multi-criteria analysis with Shamiri GIS (Shamiri and Ziadat, 2012) have been used. All methods and tools used in research studies related to site selection for rainwater harvesting have limitations. However, the GIS/remote sensing tool is the first practical tool to identify suitable locations. While to achieve more accurate results and multi-criteria areas, the integration of multi-purpose analysis methods and tools and GIS-based hydrological modeling is highly recommended. A study was conducted in the western part of Iraq in Anbar province. The catchment area of this region is 13370 square kilometers, and it has a dry climate with dry summers and cool winters. The average annual temperature is 21°C, July is the hottest, and January is the coldest month of the year. The average annual rainfall is very low (75 to 150 mm). About 49% of the rain falls in winter, 36% in spring, and 15% in fall. The average annual potential evaporation is 3200 mm (Adham et al., 2016). This watershed is dry most of the year, but during the rainy season, severe flooding occurs in a short time. Therefore, dams are one of the methods of storing rainwater in the rainy season for use in the dry season and are effective structures for the proper use of water in Iraq. This study focuses on choosing a suitable place for rainwater harvesting in the Talandasht region of Kermanshah. In this area, most of the people are engaged in agriculture and animal husbandry. In this article, the results of the design, management, and implementation of a rainwater harvesting pilot project in Kermanshah with the aim of supplemental irrigation of rain-fed crops and garden development have been examined. In fact, the study of a vast watershed with limited data to choose a location can be complicated considering all factors, but using GIS and remote sensing is easy in the location selection process.

2. Materials and methods

2.1. Study area

Talandasht study area, with an area of about 12,685 hectares, is located at the geographical position of 46°52' to 47°3' east longitude and 24°1' to 24°6' north latitude. Talandasht district is located in the northwest of Hasanabad Plain (Islamabad West) and the south of Mahidasht in Kermanshah county. Talandasht district has nine villages, including Akhundi, Talandasht, Taghtaq, Taviran Olia, Taviran Sofla, Anjirak, Toh Ruileh Olia, Toruileh Sofla, and Tawalegah. Figure 1 shows the geographical location of the Talandasht watershed in the political divisions of the province. The maximum height above sea level is 2100 meters, and the minimum height at the outlet of the basin is 1600 meters. Fan alluviums of connected form, cut plateaus and alluvial plains form the physiographic ranges of this region (Jalili et al., 2007).

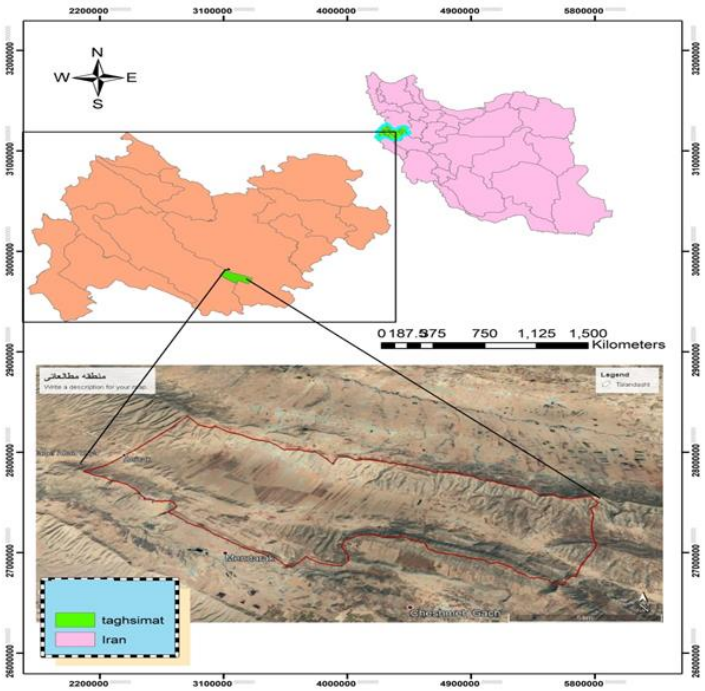

Figure 1. Geographical location of the study basin

Table 1. Monthly of climatic data of Mahidasht station from(1986-1996)

Climatic data	Month											
	Sep	Oct	Nov	Dec	Jan	Feb	Mar	Apr	May	Jun	Jul	Aug
Absolute minimum air temperature (℃)	-2	-9.5	-12.5	-25	-24	-24	-9	-4	0	0	3	4
Absolute maximum air temperature (℃)	38	35	28	12	20	26	32	32	39	43	42	40
Average maximum air temperature (℃)	0.4	20	12	7.8	7.7	11.8	16.8	20.9	30.3	26.5	32.2	24.6
Average air temperature (℃)	2.65	10.5	1.8	1.3	1.2	4.4	9.2	12.8	19.1	19.5	22.8	18
Average minimum air temperature (℃)	4.9	1	-1.5	-5.1	-5.2	-2.9	1.7	5.1	7.9	12.5	13.4	11.4
Potential evapotranspiration (mm)	0.2	45	27.9	24.8	23.6	65.1	90	120.9	152	64.3	151.9	123
ET_0 Talandasht	0.5	42	27.2	0.3	0.2	0.9	78	108.5	142	0.2	0.8	123
Rainfall (mm)	0.1	55.2	69.2	66.8	62	95.6	62.9	22.9	1.2	0.2	0.4	0.7

2.2. Climatic characteristics of the study area

The average annual rainfall is about 450 mm, the annual evaporation from the evaporation pan is 2000 mm, and the annual potential evapotranspiration are estimated to be about 1000 mm. Average, absolute minimum, average minimum, absolute maximum, and average maximum air temperature in the Talandasht region were reported as 14, -21, 6, 44, and 22 degrees Celsius, respectively. According to Selyaninov's classification, the climate of the region is semi-arid. Mahidasht meteorological station is adjacent to the Talandasht study area. Therefore, in order to check the monthly distribution of climatic data in the study area, the 30 years average data of this station, which is available in Table 1, was considered representative.

2.3. Water resources of the region

Talandasht is very poor in terms of water resources, and generally, there is no reliable water source on this plain. Few of springs that do not have an appreciable water supply and are not important from the point of view of agriculture and the wells dug in the settlements of this plain for the daily use of the people are the only sources of water available in this plain. The small amount of annual rainfall, unsuitable physiographic conditions, lack of suitable places to build water storage facilities, and the poverty of the aquifer in the region have all caused the lack of access to programmable water resources in this plain. Since rainfall, even in small amounts, occurs almost everywhere, it can be collected and used with the help of water harvesting methods before it becomes a flood or becomes polluted in the flow path. Unlike large centralized systems, such as dams, that require investment and advanced technology, water harvesting systems have simple technology and can be implemented on a small scale. For this reason, this method can be used without location restrictions. Rainwater harvesting restores the underground water reserves of the region. It not only increases access to water but also increases employment opportunities and improves socio-economic conditions in dry areas (Ammar et al., 2016: Ray-Shyan et al., 2018). After the successful implementation of the watershed project in the Talandasht area by Gol Nasar Agricultural Engineering Technical Services Company, which focused on the creation of Chinese dry dams (by stones in small waterways), gabion dams (in larger waterways with fences), and earth dams (to control water pollution and nutrition) artificially concentrated in seasonal watercourses (generally non-condensing with a height of 3-5 m), huge changes were made in water resources, especially groundwater. The result of these changes was the digging of four wells (one for drinking and three for agriculture) and the conversion of 80 hectares of dry land to irrigated land. If the irrigation system is converted to a drip irrigation system, the water level of the fields can be increased to about 200 hectares. In order to choose the best place, the socio-economic, physical conditions, and characteristics of the target area should be taken into account (Al-Adamat, 2008). Due to the lack of access to the soil hydrological groups of the Talandasht basin, this information was estimated by an innovative method by Di Paola et al. (2017) based on the slope of the area and geomorphological features.

2.4. Statistical analyses

Analytic Hierarchy Process (AHP) is multivariate analysis. AHP facilitates the decision-making process by providing a structure for organizing and evaluating the importance of different criteria and the preference of options for decision-makers.

In the AHP process, the stages of analysis include creating a hierarchical model, giving the model the ability to make group decisions, comparing two by two criteria and sub-criteria to determine their importance in decision-making, combining and integrating to determine the best options, and performing sensitivity analysis (Ameri Ekhtearabadi et al., 2011). This process is a suitable decision-making method for identifying GIS-based rainwater harvesting sites (Salavati et al., 2017). The method adopted to develop such a system includes criteria selection, data acquisition criteria classification, AHP development, relative weights calculation, sensitivity analysis and water quantity estimation. One of the indicative examples of AHP application is helping to locate underground water resources in the geographic information system (GIS) environment. Based on the review of sources and opinions of experts and professors, the influencing factors on the infiltration and storage of rainwater in the soil profile in the Talandasht watershed, in order of importance and priority, include slope percentage, hydrological groups, vegetation/land use, elevation classes, and Euclidean distance. It was considered from waterways (Table 2). Then the selected biophysical criteria were extracted using the digital model of the area's height with a resolution of 30 meters and entered into the process of hierarchical analysis. In the hierarchical approach, the most weight is assigned to the layer that has the most impact in determining the goal. In other words, the weighting criterion for each information unit is also based on the role it plays within that layer (Lopez and Zinck, 1991). Using the expert choice software, their importance coefficients

were extracted, and the obtained coefficients were used in the geographic information system. They were determined into four classes: very suitable, suitable, average, and unsuitable. Finally, based on the considered physical characteristics, the optimal sites were identified by a geographic information system and using a hierarchical analytical process for the Talandasht region.

3. Results and discussion

3.1. Slope

In this study, slopes of 5 to 15% were given the highest score, and slopes below 5% and above 60% were given the lowest score (Table 2). One of the effective factors in the amount of runoff and rainwater infiltration in the soil is the slope. The amount of sediment, the speed of water flow, and the materials needed to build dams depend on the amount of runoff (Adham et al., 2016). In order to investigate the land use characteristics of Talandasht, the extent of each slope class is given in Table 3. Figure 2 shows the slope layers of the study area. In Khairkhah's study (Khairkhah Zarkesh et al., 2015), a slope of 18 to 30% was given the highest score, and a slope of 0 to 2% and more than 30% was given the lowest score. Ammar et al. (2016) have recommended terracing as a suitable technique for rainwater storage for slopes of 5-30%.

Table 2. Effective layers in rainwater harvesting in the Talandasht region

Criterion valuation of layers	Euclidean distance from waterways	Altitude classes (meters above sea level)	Land use	Hydrological groups	Slope	Layers
4	0-1032	1456-1626	Forest lands	loamy sand-clay sand	5-15	very suitable
3	1032-2140	1626-1723	Pasture lands	loam-clay loam- hard layer deep in the soil	15-30	Appropriate
2	2140-3409	1723-1839	Scattered rainfed lands	Clay	30-60	medium
1	3409-5548	1839-2106	Drayland land	Salty soils - stone - asphalt road - concrete	<5 and >60	Unsuitable
	0.12	0.16	0.17	0.24	0.31	Coefficient obtained from AHP for each layer

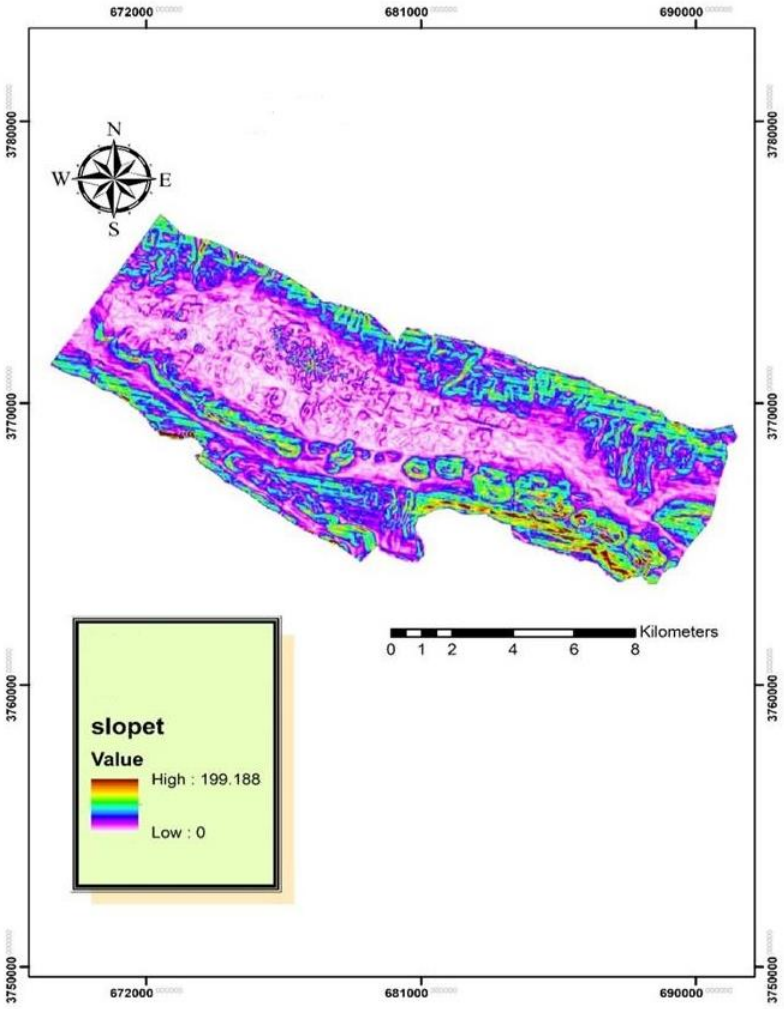

Figure 2. Slope layers

Table 3. Class and percentage of slope of Talandasht region

Slope classes	Area (ha)	Percentage (%)
0-2	1514	11.9
2-5	994	7.8
5-8	824	6.5
8-12	2330	18.3
12-15	97	0.8
15-30	3034	24
30-60	2483	19.6
>60	409	3.2
Total	12685	100

Soltani (2017), in the study of the Mekhoran and Khosroabad Sanghar watersheds of Kermanshah, concluded that in addition to the rainfall factor, which is one of the main factors in the discussion of rainwater storage, the slope and texture of the soil are more effective than other factors. Low slopes tending to zero disrupt the mechanism of runoff production and movement and increase the number of puddles and surface water retention, which prevents the collection of runoff in one place to the extent that maintains the rational-economic justification of the implementation of rainwater collection plans. It causes problems. On the other hand, the high slope is also considered an undesirable phenomenon. The high slope has caused land erosion and the loss of good soil in the catchment area, and it is not possible to create mechanical structures in places with a high slope (Keshavarz, 2012). Adham et al. (2016) recommend rainwater collection in areas with a slope greater than 5% because these areas are subject to high erosion due to the irregular distribution of runoff.

3.2. Hydrological groups

After preparing the soil hydrological maps and obtaining the user map, the infiltration curve related to the basin was prepared in the ArcGIS software environment. Figure 3 shows the hydrological groups of the study area. Soil hydrological groups were used to measure soil permeability, and hydrological groups 4 (D) and 1 (A) were given the highest and lowest points, respectively. Hydrological group D has the lowest permeability and the highest potential for runoff production, so it gets the highest score. Hydrological group A has the highest permeability and the lowest potential for runoff generation, so it gets the lowest score (Khairkhah et al., 2015: Sadeghi, 2011).

3.3. Land cover/use

Land use plays an important role in the infiltration and storage of precipitation (Keshavarz, 2012). In Talandasht, in addition to forest and pasture lands, out of a total of 12,685 hectares, 4,363 hectares (34.4% of the total area) are allocated to rainfed lands, and 1,636 hectares (12.9%) are allocated to scattered rainfed lands (Figure 4). Scattered rainfed lands are a part of non-agricultural lands that have been cultivated by carrying out agricultural operations. Therefore, from the total area of 5999 hectares to rainfed agriculture and vegetation in the study area of Talandasht, it includes forest and pasture cover with 5736 hectares (45.2%) of forest and 950 hectares (7.5%) of pasture. Examining the slope classes of the region and based on the principles of agriculture shows that slopes above 12% are not suitable for agriculture. Therefore, 1200 hectares of the land under rainfed cultivation should be changed and allocated to rainfed trees. Rainfed and irrigated gardens and agriculture have potential for rainwater harvesting, but residential areas are not prone to rainwater harvesting due to private ownership and permeable bed and due to the inability to collect runoff.

3.4. Pasture

Astragalus Euphorbia is the only grassland type in the Talandasht range. This type has been destroyed due to the overexploitation of vegetation. The dominant species of the type are self-expressing the intensity of destruction in the pasture type. Stable and high-quality species, such as *Dactylis glomrata*, *Agropyron spp*., and *Bromus tomentellus*, are few. *Stipa barbata* species at lower altitudes and *Festuca ovina* species at higher altitudes appear in spots. Among the shrub species, *Daphne mucronata* is relatively more abundant than the others.

After mounding and seeding operations, during the management operations of the Talandasht watershed, restoration was carried out on the level of degraded pastures and sloping lands of the region, which had poor coverage. The pastures were enriched by using the seeds of pasture species, such as clover and alfalfa, and grazing management was done by reducing pressure. Livestock was moved to pastures (Gol Nasar Consulting Engineers).

3.5. Forest

The forest types in the Talandasht area mainly include Iranian oak and Iranian-barnet oak, which has a coppice growth form. The areas that are located in the vicinity of the residential areas and generally have a relatively low slope and semi-deep soil have been destroyed and encroached, and wheat cultivation has been started under Ashkob. Since the power of the asexual life of the Iranian oak (*Quercus persica*) is strong and it reproduces in different ways (stem, root, and root), its complete removal is not easily possible, and even after a fire, root activity does not stop. In recent years, due to the replacement of oil, gas, and LPG fuels instead of firewood and the migration of villagers, and the implementation of the water management plan in the Talandasht watershed, the forest has been restored.

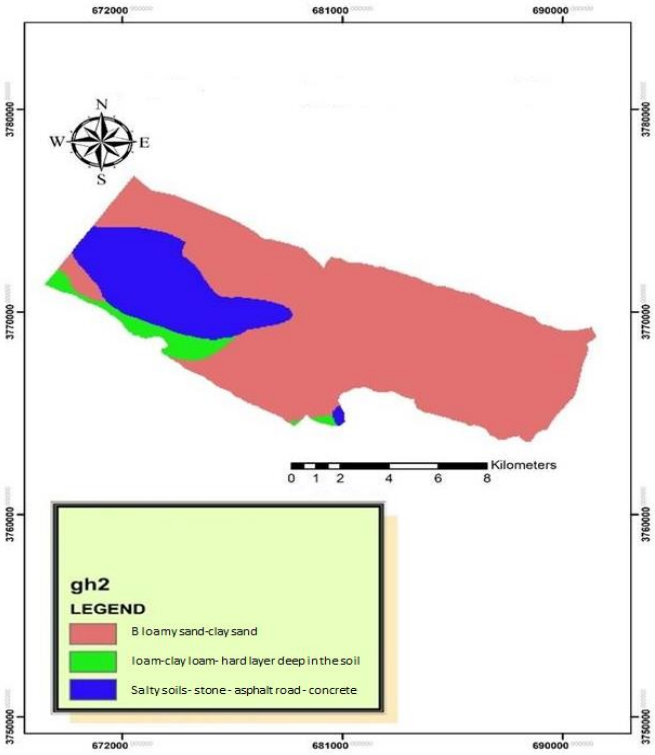

Figure 3. Hydrological groups

3.6. Agricultural landscape

The lack of reliable water sources in the region has caused agriculture in this plain to rely on seasonal rains, and rainfed cultivation of cereals and legumes is the only common agriculture in this plain. Rainwater harvesting by collecting and managing runoff increases water availability for domestic and agricultural use, as well as ecosystem capacity (Mekdaschi and Liniger, 2013). Table 4 shows the composition of crop cultivation in two periods before 1975 and after the implementation of the watershed project in 1985. By looking at Table 4 and comparing the two time periods before and after the implementation of the watershed project in Talandasht district, the magnitude of the project and its impact on biodiversity and crop diversity are determined. Cultivation of water crops, which was far from the mind, is signed, up to 80 hectares.

Also, the unprecedented cultivation of 20 hectares of saffron is extremely important from an economic point of view. Due to the increase in the area under the cultivation of legumes during the implementation of the ICARDA food security project in the west of the country, Talandasht, as one of the target areas, has caused the stability of production and increased production of protein and fodder (especially cowpea). The existing records of rainwater harvesting in the world show that this method was performed for the first time in the desert of occupied Palestine with an average rainfall of 90 mm and has greatly contributed to the production of fodder in the region.

3.7. Height

Creating a digital elevation model (DEM) of each region is an example of the spatial analysis of that region. Water resources management is a spatial problem. Water projects and especially the management and planning of droughts need to estimate locally available water (Hesari, 2013). Figure 5 shows the digital layers of the investigated area.

3.8. Euclidean distance from waterways

The distance from the waterway in the basin is the next effective factor in choosing suitable places for rain collection. This network expresses the direction of the runoff that is caused by rainstorms and flows on the surface of the basin (Sadeghi, 2011). The most basic method for creating a map of the distance to the waterway in GIS is the Euclidean distance tool. This tool shows the distance of each point in the area to the nearest river or waterway. Figure 6 shows well the distance of each point to the waterway. The map of the distance from the waterway was prepared in meters and divided into 0-1032, 1032-2140, 2140-3409, and 3409-5548classes. The floor of 0-1032 meters was given the highest score, and the floor of 3409-5548 meters was given the lowest score. The depth of runoff is an important criterion for choosing suitable sites for rainwater collection. The depth of runoff to evaluate the source of water during runoff is affected by the amount of rainfall and the distance from waterways. In this study, the rainfall were similar for the entire study area, and the same conditions were considered for the entire basin. Therefore, the runoff depth was more influenced by the Euclidean distance from the waterway. The longer the distance from the waterway is (for example, on the fourth floor, 3409-5548 meters), the amount and depth of the runoff increases and care must be taken in the construction of the channel or dam to control and store the runoff and prevent

erosion.Therefore, more than 10,000 hectares of the total area of Talandasht have a slope of more than 5%, and the runoff flows in it. By determining the appropriate storage location, it can be stored and used for further uses, especially supplementary irrigation and the development of rainfed gardens. Dense vegetation is associated with higher rates of absorption and infiltration, and therefore, lower runoff. The relationship between the order of the flow and the distance from the waterway is such that the greater the distance from the waterway, the more sub-branches join together, the volume of runoff increases and more care is needed in the management of the construction of the Chinese dry channel, gabion dam or earthen dam. It reduced the volume of runoff and minimized erosion and wastage of water (Khairkhah Zarkesh et al., 2015).

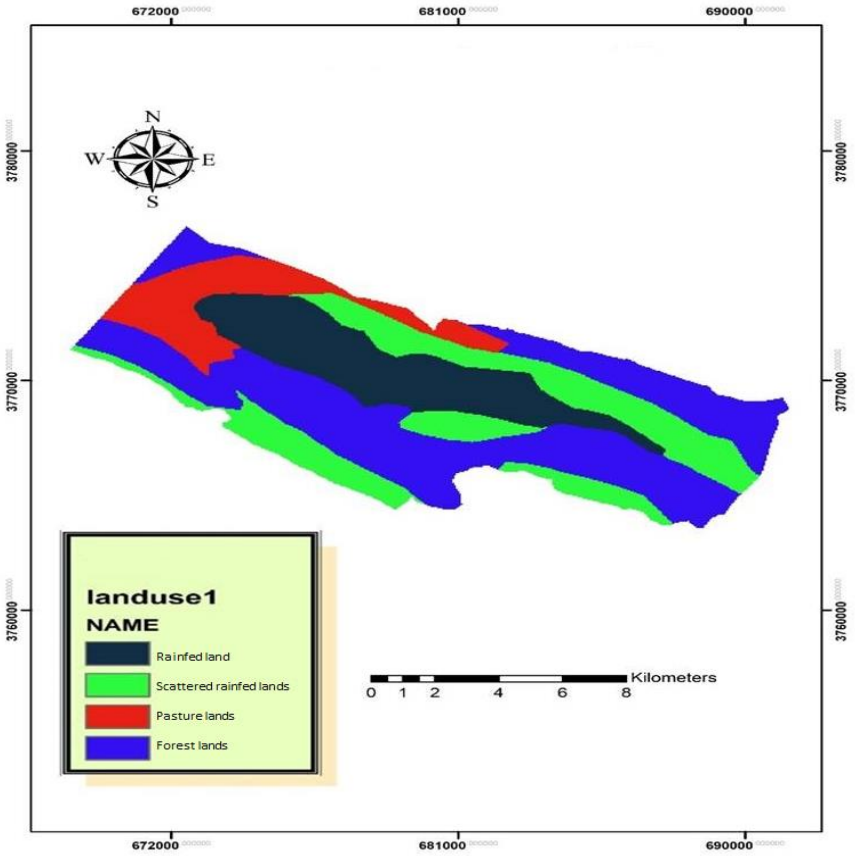

Figure 4. Land use / land cover

Table 4. Crop composition of the Talandasht region before (the year 1996) and after the implementation of watershed management project (the 90s)

The combination of crop cultivation before the year 1996	Area (ha)	The combination of crop cultivation after the watershed project (90s)	Area (ha)
Dryland wheat	3100	Dryland wheat	3272
Dryland barley	770	Dryland barly	950
Dryland spring peas	1549	Irrigated wheat	30
Black fallow	580	Spring peas	1420
		Expectational peas	60
		Forage Peas	20
		Lentils	40
		Bitter vetch	10
		Rain-fed Safflower	10
		Saffron	20
		Alfalfa	8
		Vegetables	20
		Vetch	40
		Rosa damascena	4
		Dryland almonds	20
		Dryland grapes	5
		Stubble fallow	70
Total	5999	Total	5999

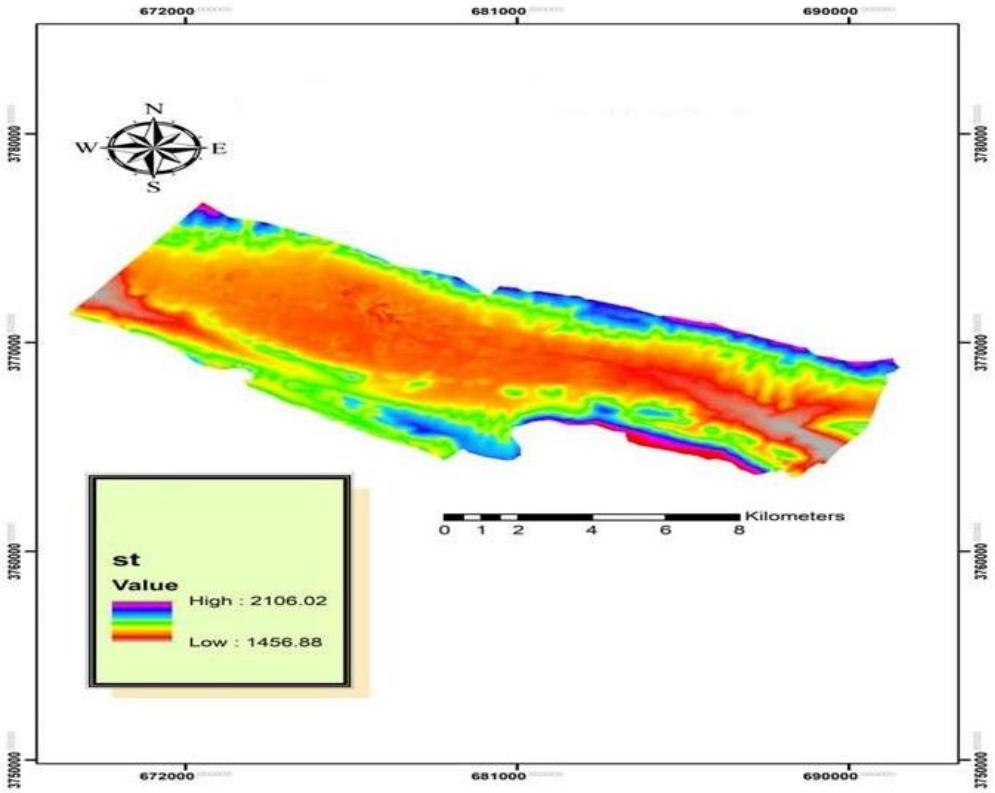

Figure 5. Digital height layer

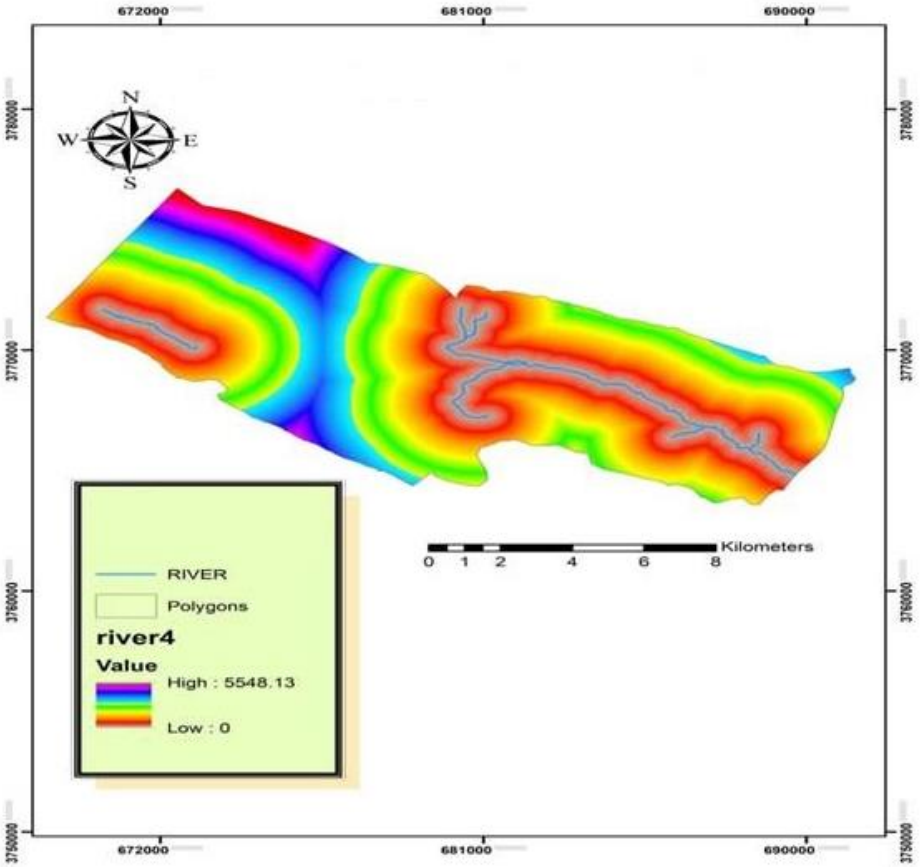

Figure 6. Euclidean distance from the waterway

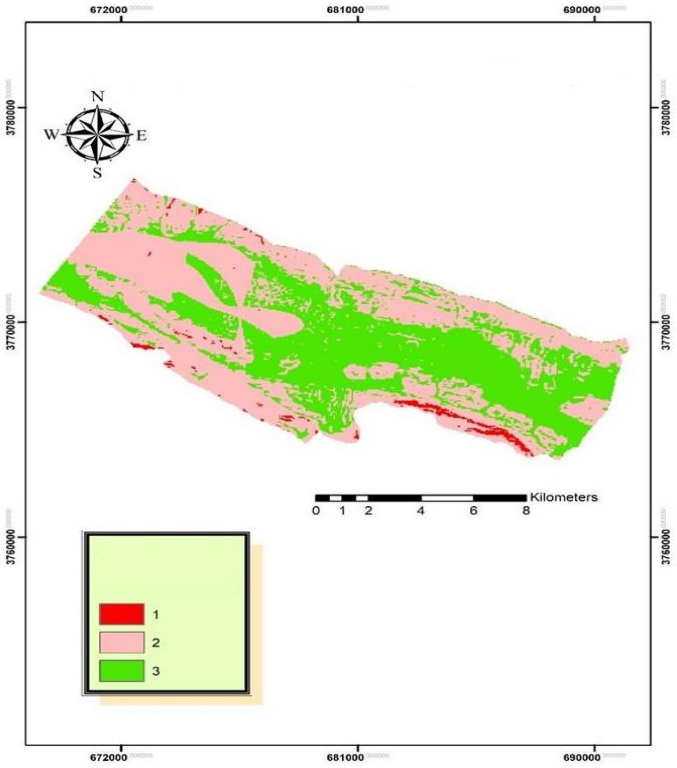

Figure 7. Final zoning of areas prone to storage of ecological compaction streams in rainfed agriculture

3.9. Final zoning of rainwater storage

After using GIS to prepare and classify the layers, the final map of rainwater harvesting potential was prepared (Figure 7). Finally, using the Raster calculator, each of the layers was multiplied by the weight obtained from AHP, and three basins, unsuitable, medium, and suitable for water storage, were determined. All the green spots that are prone to water storage are among the agricultural lands of the region. These lands have the potential to infiltrate and store rainwater, provided that farmers use soil management methods (such as vertical plowing, conservation tillage, conservation of residues, crop rotation, and use of organic fertilizers to increase soil organic matter therefore increasing soil water storage). The water stored with these methods is easily available to the plants. In addition, it costs less than other water storage methods and reduces soil erosion.

3.10. Possibilities of development and improvement and conclusions

Talandasht region has special conditions and great potential in terms of climate, topography, and soil. Especially with regard to the altitude above 1600 meters, which seems to be the best area for implementing watershed and aquifer projects above 1000 meters, and priority is given to areas above 1500 meters (due to low evaporation and the possibility of storing water in pools, canals and basins). Therefore, it seems that if rainwater is stored, the development of rain-fed gardening and supplementary irrigation of the region will be possible. Considering that Talandasht is an isolated area with a length of 30 km and a width of 2 km, the height of the plain is 1600 meters above sea level. Therefore, if a 40 km long canal (ditch) is created on two sides using level lines. At an altitude of 1650 to 1700 meters, an amount of 34300000 cubic meters of water can be collected annually and managed for supplementary irrigation and garden development.

4. Conclusion

It can be concluded that rainwater harvesting methods provide the ability to manage upstream water resources effectively. Stored water can be used as a source for supplementary irrigation in critical periods of water shortage and prevents damage to crop yield. The amount of rainwater harvesting is insignificant compared to building a dam or digging a well. However, these types of projects have more implementation potential in all parts of the country, are more compatible with the environment and attract more people's participation.

Conservative agriculture has good potential in smallholder farms in dry areas, as it is used in different regions of Asia and South America (Jat et al., 2012). In Talandasht, there is potential for conservative agriculture, and it is an opportunity to preserve and store water. Reducing the performance gap in rain-fed agriculture and dry areas to respond to the growing demand for human food, population increase, and climate change is one of the goals of water resources management. In addition, the need to increase food quality and performance stability also shows the need to pay attention to this matter. Also, in dry areas, ecological compression reduces soil degradation, carbon storage, water accumulation, and soil nitrogen binding and availability. Conservation agriculture and

livestock-agriculture integration are an opportunity to obtain different agroecosystem services in arid climates.

References

Adham, A., Wesseling, J. G., Riksen, M., Ouessar, M., & Ritsema, C. J. (2016). A water harvesting model for optimising rainwater harvesting in the wadi Oum Zessar watershed, Tunisia. *Agricultural Water Management*, *176*, 191-202. **doi:10.1016/j.agwat.2016.06.003**

Al-Adamat, R. (2008). GIS as a decision support system for siting water harvesting ponds in the basalt aquifer/NE Jordan. *Journal of Environmental Assessment Policy and Management*, *10*(2), 189–206. **doi:10.1142/s1464333208003020**

Al-Adamat, R., Alayyash, S., Amoush, H., Meshan, O., Rawajfih, Z., Shdeifat, A., Harahsheh, A., & Farajat, M. (2012). The combination of indigenous knowledge and geo-informatics for water harvesting siting in the Jordanian Badia. *Journal of Geographic Information System*, *4*, 366-376. **doi:10.1166/jcp.2010.1003**

Ameri Ekhtearabadi, A., Nikpour, M., & Shojaa Talatpa, F. (2011). Determination of proper places for the basin using analytical hierarchy process. Case study: Hamedan province. In *Proceedings of the First International Conference and 3rd National Conference on Dam and Hydroelectric Power Plants*, pp. 1-10. Tehran, Iran.

Ammar, A., Riksen, M., Ouessar, M., & Ritsema, C. (2016). Identification of suitable sites for rainwater harvesting structures in arid and semi-arid regions: A review. *International Soil and Water Conservation Research*, *4*(2), 108-120. **doi:10.1007/978-3-642-15479-9-5**

Bamne, Y., Patil, A., & Vikhe, D. (2014). Selection of appropriate sites for structures of water harvesting in a watershed using remote sensing and geographical information system. *International Journal of Emerging Technology and Advanced Engineering*, *4*(11), 270-275.

Bulcock, L. M., & Jewitt, G. P. W. (2013). Key physical characteristics used to assess water harvesting suitability. *Physics and Chemistry of the Earth*, *66*, 89–100. **doi:10.1016/j.pce.2013.09.005**

Di Paola, A., Rulli, M. C., & Santini, M. (2017). Human food vs. animal feed debate. A thorough analysis of environmental footprints. *Land Use Policy*, *67*, 652-659. **doi:10.1016/j.landusepol.2017.06.017**

Foley, J. A., Ramankutty, N., Brauman, K. A., Cassidy, E. S., Gerber, J. S., Johnston, M., Mueller, N. D., O'Connell, C., Ray, D. K., West, P. C., & Balzer, C. (2011). Solutions for a cultivated planet. *Nature*, *478*, 337–342. **doi:10.1038/nature10452**

García-Palaciosa, P., Alarcónb, M. R., Tenorioc, J. L., & Morenoc, S. S. (2019). Ecological intensification of agriculture in drylands. *Journal of Arid Environments*, *167*, 101-105. **doi:10.1016/j.jaridenv.2019.04.014**

Hesari, B. (2013). Investigation of upstream and downstream hydrological effects of supplementary irrigation development in rainfed areas in Karkheh basin. Doctoral dissertation, Ahvaz University. [In Persian]

Hobbs, P. R., Sayre, K., & Gupta, R. (2008). The role of conservation agriculture in sustainable agriculture. Philosophical Transactions of the Royal Society B: *Biological Sciences*, *363*(1491), 543-555. **doi:10.1098/rstb.2007.2169**

Jalili, J., Hesadi, H., & Hadidi, M. (2014). Artificial recharge of groundwater aquifers by surface drainage canals using AHP method. *Iranian Journal of Watershed Management Science and Engineering*, *8*(24), 29-36. [In Persian]

Jalili, K. H., Sadeghi, S. H. R., & Nikkami, D. (2007). Land use optimization of watershed for soil erosion minimization using linear programming (a case study of Brimvand watershed, Kermanshah province). *Journal of Water and Soil Science*, *10*(4), 15-27. [In Persian]

Jat, R. A., Craufurd, P., Sahrawat, K. L., & Wani, S. P. (2012). Climate change and resilient dryland systems: experiences of ICRISAT in Asia and Africa. *Current Science*, *102*(12), 1650-1659.

Kadam, A. K., Kale, S. S., Pande, N. J., Sankhua, R. N., & Pawar, N. J. (2012). Identifying potential rainwater harvesting sites of a semi-arid, basaltic region of western India, using SCS-CN method. *Water Resources Management*, *26*(9), 2537–2554. **doi:10.1007/s11269-012-0031-3**

Kahinda, J. M., Lillie, E., Taigbenu, A., Taute, M., & Boroto, R. (2008). Developing suitability maps for rainwater harvesting in South Africa. *Physics and Chemistry of the Earth*, *33*, 788–799. **doi:10.1016/j.pce.2008.06.047**

Kassam, A., Friedrich, T., Derpsch, R., Lahmar, R., Mrabet, R., Basch, G., González-Sánchez, E. J., & Serraj, R. (2012). Conservation agriculture in the dry Mediterranean climate. *Field Crops Research*, *132*, 7-17. **doi:10.1016/j.fcr.2012.02.023**

Keshavarz, A. (2012). Appropriate location of drinking water harvesting using fuzzy hierarchical analysis (FAHP) Case study: Birjand plain, Master's thesis, Birjand University. [In Persian]

Khairkhah Zarkesh, A., Mohammadi, F., & Meamarian, E. (2015). Determine areas prone to harvesting and storing rainwater using hierarchical analysis in the GIS environment. *Journal of Rainwater Basin Systems*, *14*(21), 3480.

Khan, M. D., & Khattak, M. (2012). Siting of rainwater harvesting locations in district Haripur using geographic information techniques. *Journal of Himalayan Earth Sciences*, *45*(2), 81-81.

Krois, J., & Schulte, A. (2014). GIS-based multi-criteria evaluation to identify potential sites for soil and water conservation techniques in the Ronquillo watershed, northern Peru. *Applied Geography*, *51*, 131–142. **doi:10.1016/j.apgeog.2014.04.006**

Kumar, M. G., Agarwal, A. K., & Bali, R. (2008). Delineation of potential sites for water harvesting structures using remote sensing and GIS. *Journal of the*

Indian Society of Remote Sensing, *36*(4), 323–334. **doi:10.1007/s12524-008-0033-z**

Lopez, J. H., & Zinck, J. A. (1991). GIS-assisted modelling of soil-induced mass movement hazards: A case study of the upper Coellop river basin, Tolima, Colombia. *ITC Journal*, *4*, 202-220.

Maestre, F. T., Eldridge, D. J., Soliveres, S., Kéfi, S., Delgado-Baquerizo, M., Bowker, M. A., García-Palacios, P., Gaitán, J., Gallardo, A., Lázaro, R., & Berdugo, M. (2016). Structure and functioning of dryland ecosystems in a changing world. *Annual Review of Ecology, Evolution, and Systematics*, *47*, 215–237. **doi:10.1146/annurev-ecolsys-121415-032311**

Mahmoud, S. H., & Alazba, A. A. (2014). The potential of in situ rainwater harvesting in arid regions: developing a methodology to identify suitable areas using GIS-based decision support system. *Arabian Journal of Geosciences*, *8*, 5167-5179. **doi:10.1007/s12665-014-3249-y**

Mekdaschi, R., & Liniger, H. (2013). *Water Harvesting: Guidelines to Good Practice*. Centre for Development and Environment.

Prăvălie, R. (2016). Drylands extent and environmental issues. A global approach. *Earth Science Reviews*, *161*, 259-278. **doi:10.1016/j.earscirev.2016.08.003**

Ray-Shyan, Wu, Molina, G. L. L., & Hussain, F. (2018). Optimal sites identification for rainwater harvesting in northeastern Guatemala by analytical hierarchy process. *Water Resources Management*, *32*(12), 4139-4153. **doi:10.1007/s11269-018-2050-1**

Sadeghi, S. H. (2011). Determining places prone to rainwater collection using DIS-based GIS support system Master's thesis, Birjand University. [In Persian]

Salavati, P., Fakheri fard, A., Asadi, A., & Asadi, S. (2017). Rain-runoff frequency analysis for designing reservoirs in order to collect surface water for the development of urban green space (case study: city of Tabriz). *Irrigation Sciences and Engineering*, *4*(2), 113-117. [In Persian]

Shamiri, A., & Ziadat, F. M. (2012). Soil landscape modeling and land suitability evaluation. The case of rainwater harvesting in a dry rangeland environment. *International Journal of Applied Earth Observation and Geo information*, *18*, 157-164. **doi:10.1166/jcp.2010.1003**

Soltani, A. (2017). Feasibility of susceptible areas for rainwater harvesting, based on AHP in GIS environment (a case Study: Khosroabad watershed, Iran). *Journal of Rainwater Catchment Systems*, *5*(2), 65-76. **doi:10.1007/978-3-642-15479-9-5**

Winnaar, G., Jewitt, G. P. W., & Horan, M. (2007). A GIS-based approach for identifying potential runoff harvesting sites in the Thukela River basin, South Africa. *Physics and Chemistry of the Earth*, *32*(15), 1058-1067. **doi:10.1016/j.pce.2007.07.009**

Ziadat, F., Bruggeman, A., Oweis, T., Haddad, N., Mazahreh, S., Sartawi, W., & Syuof, M. (2012). A participatory GIS approach for assessing land suitability for rainwater harvesting in an arid rangeland environment. *Arid Land Research and Management*, *26*(4), 297–311. **doi:10.1080/15324982.2012.709214**

Agriculture, Environment & Society

Journal homepage: www.aes.uoz.ac.ir

Designing a model for enhancing the capacity to implement sustainable production boom policies in the agricultural sector of Sistan and Baluchestan province

Reza Saidian [a], Mohammad Zia Aldini [*b], Seyed Mohammad Reza Hosseinipour [c]

[a] Ph.D Student of Public Administration, Majoring in Decision-Making and Public Policy, Department of Management, Rafsanjan Branch, Islamic Azad University, Rafsanjan, Iran
[b] Department of Public Administration, Rafsanjan Branch, Islamic Azad University, Rafsanjan, Iran
[c] Department of Economics, Rafsanjan Branch, Islamic Azad University, Rafsanjan, Iran

ARTICLE INFO

Article history:
Received: 5 September 2024
Accepted: 12 November 2024
Available online: 1 December 2024

Keywords:
Enhancing policy-making capacity
Policy implementation
Policy-making
Sustainable production

ABSTRACT

This study aimed to design a model to enhance the capacity for implementing sustainable production boom policies in the agricultural sector of Sistan and Baluchestan Province. This research is qualitative, employing literature review and interviews as methods for data collection. Initially, indicators were extracted through a review of texts and library research. The tools for gathering research findings included books, articles, theses, and other higher-level documents. Additionally, to collect expert opinions, a field method involving interviews was conducted with 25 specialists to review the indicators. The specialists were selected through purposive sampling, which enhances the transparency of the research process. To ensure the validity of the tools and confirm the accuracy of the findings from the researcher's perspective, valuable insights were obtained from 25 professors familiar with this field, academic experts, executive experts, and managers of commercial and production companies in Iran. After conducting three stages of coding (open, selective, and axial), the results indicated that enhancing the capacity to implement sustainable production boom policies in the agricultural sector of Sistan and Baluchestan Province includes six components: factors related to financial resource allocation, structural factors, factors related to policy implementers, factors related to the policy environment, technological factors, and enabling factors. Among these components**,** structural and financial factors were found to be the most critical and challenging in the context of Sistan and Baluchestan. Furthermore, the findings may be generalized to other regions with similar agricultural challenges and policy contexts. This study makes a significant contribution to the field of sustainable agriculture and policy implementation, particularly in the context of developing regions.

Highlights

- Explores advanced strategies to optimize energy efficiency in urban infrastructures for sustainable development.
- Proposes novel methodologies for reducing carbon footprints in metropolitan transportation systems.
- Highlights the role of AI in enhancing predictive maintenance for smart cities.
- Discusses innovative frameworks for integrating renewable energy into urban power grids.
- Advocates for multi-disciplinary collaboration in designing resilient, eco-friendly urban systems.

1. Introduction

Globalization is a complex set of multidimensional processes encompassing various fields such as economy, ideology, politics, culture, and environment, leading to increased interdependence among countries worldwide. Alternatives to globalization have been proposed, including the anti-globalization movement, reformed globalization, and sustainable development and production philosophy. The most rational alternative to globalization is sustainable production and development, emphasizing the necessity of environmental consideration and natural resource preservation alongside economic development and social

* Corresponding author.
E-mail address: mziaaddini@yahoo.com
https://doi.org/10.22034/aes.2025.495888.1094

progress (Koho et al., 2011). Today, public and private organizations face pressures from higher governmental organizations, stakeholder groups in society, technical standard requirements, criteria for participation in international and national projects, and greater awareness among community members. Therefore, they must pay attention not only to economic criteria such as profit generation and cost reduction but also to reducing environmental impacts and enhancing social welfare and development. One of the challenges facing industries is balancing economic and social progress with environmental preservation. While industries recognize the importance of sustainable development, they may not necessarily understand how to operationalize this concept (Tseng et al., 2009). Strategically, adopting sustainable production strategies at all levels large, small, and medium-sized industries is crucial; however, this can vary from industry to industry due to different organizational characteristics. The concept of sustainable production develops various items that may utilize minimal resources while being affordably safer for society. The sustainable production approach has been successfully implemented in dozens of industries worldwide (Shah et al., 2020).

In this context, public policies represent the tangible manifestation of governments' philosophies and doctrines regarding societal management. In other words, governments use public policies to weave their philosophies and doctrines into the fabric of society, thereby realizing their ideal community through these policies (Danaei Fard, 2016). Policy-making is an interpretation intertwined with government, state, society, and its public issues, evoking the actions of the government in effectively managing public affairs. Consequently, over the years, policy-making has gained attention as a scientific discipline among scholars, policymakers, and organizational managers (Heydari Hosseini, 2021). Policy-making plays a crucial role in achieving sustainable development by providing methods for achieving and managing objectives. Among various sectors, agriculture is considered one of the most important economic sectors in society (Vasyl'yeva, 2021). According to results from the labor force survey in 2015, approximately 50% of rural workers are engaged in agriculture. In 2005, the agricultural sector accounted for 24.7% of employment in the country, which decreased to 23.2% in 2006, 18.6% in 2011, and 17.9% in 2014. This annual decline in employment share is a concerning issue for production and the economy of the country. In this regard, the present study aims to design a model to enhance the capacity for implementing sustainable production boom policies in the agricultural sector of Sistan and Baluchestan Province.

Since the early 1950s, with the implementation of economic development programs, Iran's economy has largely shifted from agriculture toward an industrial and service-based economy. The industrial and service sectors, from 1967 to 2017, constituted an average of 13% and 50% of the total gross domestic product, respectively (Central Bank, 2020). This interannual change from 1967 to 2017 increased per capita energy consumption from 290 kilograms of crude oil equivalent to 2310 kilograms of crude oil equivalent (Ministry of Energy, 2020). Thus, national production has a direct impact on energy consumption in the country and is therefore one of the main factors driving energy demand (Soleimani, 2021). In a situation where we are facing economic crises, the salvation of the country lies in domestic production; as production flourishes, Iranian goods and services also thrive, consequently strengthening and preserving employment, production enterprises, labor force, and human capital (Hashemi Madani, 2019). Iran has not experienced sustainable growth during various development programs from the first to the fifth; specifically, it experienced an economic growth rate of 7.2% in the first program, 2.5% in the second, 5.8% in the third, 4.4% in the fourth, and -1.5% in the fifth program. The vulnerability of Iran's economy to global risks is a very important issue that depends on the country's foreign trade, which has fluctuated over different periods. After the war, Iran's share of foreign trade was approximately $20 billion annually, gradually increasing to $80 billion over the past decade due to reliance on unsustainable resources in global trade (Mirbagheri Hir and Abbasi, 2019).

Unfortunately, over the past century, political-social developments especially regional hydro-political equations and sometimes unilateral foreign government influences based on conditions prevailing in Iran and Afghanistan have resulted in about 95% of the Helmand River being located within Afghanistan. In all water disputes between the two countries, foreign experts often ruled in favor of Afghanistan. Consequently, Iran's share of water from Afghanistan has significantly diminished; according to the latest treaty between the parties in 1972, Iran's water rights from the Helmand River were set at 26 cubic meters per second, amounting to approximately 820 million cubic meters. This unprofessional decision has led to some of the greatest challenges currently facing Sistan. This volume of water is insufficient for irrigating the present arable lands of 200,000 to 250,000 hectares and cannot restore the dried wetlands of Hamoun with an area exceeding 380,000 hectares (Sarvari Nejad and Sargazi, 2021). Therefore, considering the issues raised, the research problem becomes apparent, and actions are taken to discover a model based on this phenomenon given the absence of such a specific model. The present research is responsible for conducting this study using a grounded theory research strategy. In this context, this research focuses on designing a model to enhance the capacity for implementing sustainable production boom policies in the agricultural sector of Sistan and Baluchestan Province.

2. Materials and Methods

To understand and explain complex social phenomena, qualitative data such as information gathered from interviews, participatory observation, documentation, questionnaires, etc., are utilized. Qualitative research focuses on human factors, valuing the perspectives of individuals under investigation. In this approach, researchers and participants are engaged in a reciprocal

relationship, where both description and explanation occur, relying on observable statements and behaviors for data collection.

In this study, the methodology includes a literature review and interviews. Initially, indicators were extracted through a literature study and library research methods. The tools used for gathering research findings in this section include books, articles, theses, and other higher-level documents. Additionally, to gather expert opinions through a field method involving interviews, 25 specialists were selected to review the indicators. To ensure the validity of the tools and to guarantee the accuracy of the findings from the researcher's perspective, the valuable insights of 25 professors familiar with this field and academic experts, as well as executive experts and managers of commercial and production companies in Iran, were consulted. Information regarding the experts is detailed in the table below.

Table 1. Demographic Information of Participants

Frequency	Class	Variable	Frequency	Class	Variable	Frequency	Class	Variable
10	40 to 45 years	Age	25	PhD	Education	15	Professors of Economics and Management	Place of Employment
15	Over 50 years		8	Female	Gender	10	Executive Experts and Managers of Commercial and Production Companies in Iran	
2	Under 10 years	Work Experience	17	Male				
16	11 to 20 years							
7	Over 20 years							

Given that this research utilized a literature review and expert interviews to identify the indicators, the indicators themselves inherently possess the necessary validity. In fact, to ensure the validity of the tools in the qualitative section of the research and guarantee the accuracy of the findings from the researcher's perspective, the valuable opinions of professors and academic experts knowledgeable in this field were incorporated. Additionally, participants were involved in the analysis and interpretation of the data.

Reliability refers to the consistency of the research findings. In interviews, reliability is addressed in stages such as the interview setting, transcription, and analysis. Moreover, when assessing reliability concerning interviewees, attention is given to how questions are directed. In transcription reliability, consistency within the subject matter during the transcription process, involving two individuals, is also crucial. In classifying interviews, attention to the percentages reported by two coders serves as a method for determining reliability. The level (percentage) of agreement within the subject matter between two coders (which should be 60% or more) for a single interview (control analysis) is also a method for assessing analysis reliability. In this study, test-retest reliability and inter-coder agreement methods were employed to calculate the reliability of the conducted interviews.

To calculate test-retest reliability, several interviews were selected as samples from those conducted, and each was recorded within a short and specific time interval. The codes identified during both time intervals for each interview were then compared. The retest method is used to assess the stability of the researcher's coding. In each interview, codes that are similar across both time intervals were marked as "agreement," while dissimilar codes were labeled as "disagreement." In this research, a reliability coefficient of 79% was obtained from the coding conducted, indicating its acceptability.

To calculate interview reliability using inter-coder reliability (ICR) with two coders, one of the professors in the relevant field familiar with coding was invited to participate as a secondary coder in the research. Subsequently, the researcher and this colleague coded three interviews together, calculating the percentage of inter-coder agreement, which serves as an indicator of analysis reliability. Thus, the reliability obtained from the two coders was found to be 75.75%.

The data analysis method involves theoretical coding as well as expert interviews using coding techniques. Examining backgrounds and simultaneously obtaining expert opinions can create a broad understanding of the subject matter, and expert opinions can lead to localizing indicators relevant to the research area. Theoretical coding refers to operations through which data are dissected, conceptualized, and re-arranged alongside each other. In this method, three main pillars—"concepts," "categories," and "propositions"—exist. This section is dedicated to a theoretical model and framework extracted from qualitative data derived from interviews with research participants.

3. Results

As mentioned, to identify components that reduce the failure of implementing sustainable production policies in the agricultural sector of Sistan and Baluchestan Province, this study utilized a literature review followed by expert interviews. Given that the data collected through interviews have reached theoretical saturation via continuous matching processes, after defining the main research questions (interviews) for which quantitative scales have been defined, coding of the collected interviews began, defining their characteristics and dimensions along with descriptive charts for these characteristics.

Strauss and Corbin describe open coding as "a part of the analysis that specifically pertains to naming and categorizing phenomena through careful examination of

data." In other words, in this type of coding, concepts within interviews and documents are classified based on their relation to similar topics. Therefore, the first step is to identify the semantic units, which are visible in Table 2.

Table 2. Identified Semantic Units

Interviewee Code	Index
I2.I3.I21.I5.I9	Financial System
I8.I10.I11.I12	Financial and Commercial Expansion
I2.I9.I12.I21	Creating Conditions for Attracting Green Investments
I22.I8.I8	Cost-Effective Management Practices
I9.I10.I13.I6	Revenue Collection and Attraction
I19.I23	Savings
I23.I5.I7.I11	Foreign Investment
I11.I1.I8	Green Resource Savings
I2.I9	Resilience
I6.I8.I7.I17	Leadership Policy
I24	Human Resource Development
I12	Green Missions and Strategies
I2	Integrating Decision-Making Centers and Preventing Multicentrism
I13	Updating Policies
I25	Increasing Literacy and Knowledge
I24	Reporting on the Performance of Managers and Institutions
I14	Attention to the Personality Traits and Behaviors of Policymakers
I2.I6.I7	Government Expenditure
I1.I5.I9	Pressure Groups
I15	Bureaucratic Society
I10.I5	Religious Culture
I16	Cultural Diversity and Changes in the World
I17	Considering Monetary and Banking Laws and Attention to Advantages and Capabilities
I18	Sustainable Consumption and Production Initiatives
I3.I14.I6	Rapid Technological Innovation
I19	Building Leadership Capacity
I20	Participation and Collaboration in Green Processes

Table 3. Creating Components (Axial Coding)

Index	Component
Financial System	
Financial and Commercial Expansion	
Creating Conditions for Attracting Green Investments	
Cost-Effective Management Practices	Factors Related to Financial Resource Allocation
Revenue Collection and Attraction	
Savings	
Foreign Investment	
Green Resource Savings	
Resilience	
Leadership Policy	
Human Resource Development	Structural Factors
Green Missions and Strategies	
Social Consulting	
Integrating Decision-Making Centers and Preventing Multicentrism	
Updating Policies	
Determining the Level of Collaboration with Businesses	Factors Related to Policy Implementers
Increasing Literacy and Knowledge	
Reporting on the Performance of Managers and Institutions	
Attention to the Personality Traits and Behaviors of Policymakers	
Government Expenditure	
Pressure Group	
Bureaucratic Society	
Environmental Regulations and Policies	
Religious Culture	Factors Related to the Policy Environment
Cultural Diversity and Changes in the World	
Considering Monetary and Banking Laws and Attention to Advantages and Capabilities	
Establishing Knowledge-Based Companies	
Sustainable Consumption and Production Initiatives	Technological Factors
Transferring Knowledge and Promoting Environmental and Green Education	
Rapid Technological Innovation	
Building Leadership Capacity	
Promoting a Culture of Work and Entrepreneurship	Enabling Factors
Supporting and Changing Policies	
Participation and Collaboration in Green Processes	

As shown, 28 codes were extracted from the interview process. At this stage, indicators extracted from the literature were also added to the interview indicators. The purpose of axial coding is to create relationships between the categories produced in the open coding stage. This process is generally based on coding and helps theorists facilitate the theory-building process. In this stage, after extracting semantic units from the interviews, axial coding and categorization of indicators were carried out.

As observed, in this stage, the initial codes extracted from the interviews were grouped based on conceptual proximity into similar categories. In this regard, six components emerged, as seen in Table 4. Finally, the coding process proceeded to selective coding. Selective coding is the process of selecting a main category, systematically relating it to other categories, validating these relationships, and completing categories that need further refinement and development. Selective coding, based on the results of open coding and axial coding, is the main stage of theory building. Accordingly, the final coding from this process is presented in the table below.

Table 4. Final Coding

Interviewee Code	Reference	Index	Component
I2.I3.I21.I5.I9	Khosravian (2021)	Financial Supply System	Factors Related to Financial Resource Allocation
I8.I10.I11.I12	Abounoori & Khajehzadeh (2020)	Financial and Commercial Expansion	
I2.I9.I12.I21	Abounoori & Khajehzadeh (2020)	Creating Conditions for Attracting Green Investments	
I22.I8.I8	Rezai & Shamseddini (2019)	Cost-Effective Management Practices	
I9.I10.I13.I6	Pollyn & Barinua & Johnagi (2016)	Revenue Collection and Attraction	
I19.I23	Dehghani & Naseh (2019)	Savings	
I23.I5.I7.I11	Khosravian (2021), Dehghani & Naseh (2019)	Foreign Investment	
I11.I1.I8	Dehghani & Naseh (2019)	Green Resource Conservation	
I2.I9	Amiri & Arshadi (2021)	Resilience	
I6.I8.I7.I17	Campos & Reich (2019)	Leadership Policy	
I24	Jahani & Farahani Fard (2020)	Human Resource Development	
I12	Pollyn & Barinua & Johnagi (2016)	Green Missions and Strategies	
I12	Bozorgi Nejad et al. (2021)	Social Consultation	
I2	Ghodarzi et al. (2021)		
I12	Ghodarzi et al. (2021)	Integrating Decision-Making Centers and Preventing Multicentralization	Structural Factors
I13	Ghodarzi et al. (2021)	Updating Policies	Factors Related to Policy Implementers
I13	Ghodarzi et al. (2021)	Determining Cooperation Levels with Businesses	
I25	Ghodarzi et al. (2021)	Increasing Literacy and Knowledge	
I24	Ghodarzi et al. (2021)	Reporting on the Performance of Managers and Institutions	
I14	Ghodarzi et al. (2021)	Attention to the Personality and Behavioral Traits of Policymakers	
I2.I6.I7	Le & Sarkodie (2020)	Government Expenditures	Factors Related to the Policy Environment
I1.I5.I9	Kazemi Rahbar et al. (2021)	Pressure Groups	
I15	Campos & Reich (2019)	Bureaucratic Society	
I15	Nathaniel et al. (2021)	Environmental Regulations and Policies	
I10.I5	Munawwaroh et al. (2019)	Religious Culture	
I16	Joniarta et al. (2019)	Diversity in Culture and Changes in the World	
I17	Ghodarzi et al. (2021)	Considering Monetary and Banking Laws and Paying Attention to Advantages and Capabilities	
I17	Farbod (2020)	Establishing Knowledge-Based Companies	Technological Factors
I18	Luthra et al. (2017)	Sustainable Consumption and Production Initiatives	
I18	Tsani (2021)	Knowledge Transfer and Promotion of Environmental and Green Education	
I3.I14.I6	Tsani (2021)	Rapid Technological Innovation	
I19	Pollyn & Barinua & Johnagi (2016)	Building Capacity in Leadership	Enabling Factors
I19	Hashemi Madani (2019)	Promoting a Culture of Work and Entrepreneurship	
I19	Pollyn & Barinua & Johnagi (2016)	Supporting and Changing Policies	
I20	Pollyn & Barinua & Johnagi (2016)	Participation and Collaboration in Green Processes	

Based on the studies conducted, the research options include six factors: financial resource allocation factors, structural factors, policy implementer factors, policy environment factors, technological factors, and enabling factors. Consequently, the research model is presented below.

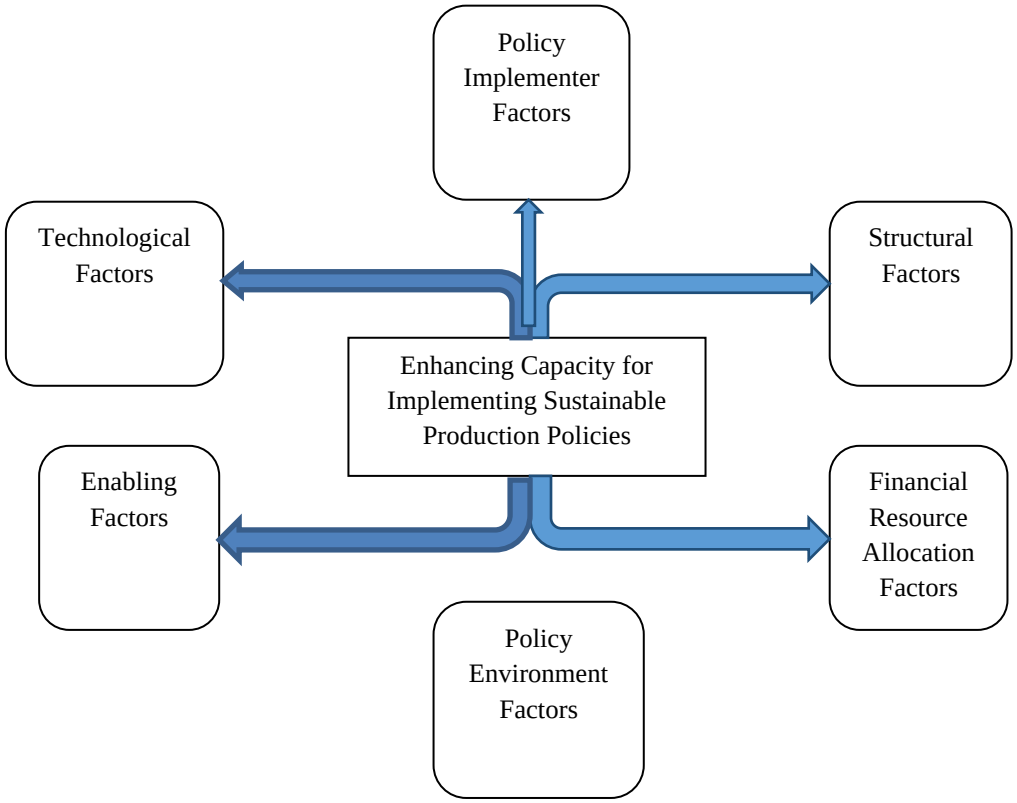

Figure 1. Conceptual Model of the Research

4. Conclusion

This study aimed to design a model for enhancing the capacity to implement sustainable production policies in the agricultural sector of Sistan and Baluchestan province. The findings revealed several critical factors influencing the successful implementation of these policies. The key components identified include financial resource allocation, structural factors, policy implementation capacity, the policy environment, technological advancements, and enabling factors such as leadership and entrepreneurship.

Among the financial resource allocation factors, the establishment of a sound financial supply system, attracting green investments, and expanding cost-effective management practices were found to be crucial for promoting sustainable agricultural practices. Structural factors, such as resilience, strong leadership, and human resource development, are vital for creating adaptable and effective policy frameworks. Additionally, factors related to policy implementers, including updating policies, fostering collaboration with businesses, and improving the literacy of policymakers, play a significant role in the policy's success.

The study also highlighted the importance of a supportive policy environment, which includes government expenditures, interest groups, and environmental regulations, as well as the promotion of technological advancements through knowledge-based companies and innovation. Furthermore, enabling factors such as promoting a culture of entrepreneurship and fostering green processes are essential for achieving long-term sustainability in agriculture.

Based on the findings, it is recommended that policymakers focus on improving financial systems to support sustainable agricultural practices, while also fostering partnerships between the public and private sectors. Farmers should seek collaborative opportunities with international organizations, government entities, and private companies to gain access to better resources and technologies.Additionally, the education and development system should be redesigned to prioritize human resource development, with a focus on training specialized personnel. A data-driven approach to policymaking, with measurable indicators aligned with global standards, is essential for improving the effectiveness of agricultural policies in the region. Policymakers should continue to empower leaders and encourage entrepreneurial activities to drive sustainable practices at all levels of the agricultural sector.

In response to reviewer feedback, several additional considerations have been integrated into the manuscript. The model presented in the study builds upon existing theories of sustainable agriculture, specifically applying

them to the unique context of Sistan and Baluchestan. This region faces distinct challenges that require tailored solutions. The incorporation of qualitative methods, such as expert interviews, deepens the analysis and enhances the understanding of how sustainable production can be effectively implemented in this region.

The revised version of the manuscript separates the Discussion and Conclusion sections. This change allows for a clearer comparison of the study's findings with existing literature, while also providing more precise, actionable recommendations for stakeholders. The Discussion section now highlights the theoretical and practical implications of the research, while the Conclusion focuses on summarizing the main findings and offering guidance on how to apply the model in practice.

Additionally, the model presented in the study is designed with broader applicability in mind. It can be adapted for use in other regions that face similar agricultural policy implementation challenges, particularly those with limited resources or underdeveloped infrastructure.

The manuscript now includes more comprehensive background information on the specific agricultural, environmental, and socio-economic challenges faced by Sistan and Baluchestan. This contextual information helps readers better understand the relevance of the study's findings and how they relate to the local conditions in the region.

Furthermore, the paper explicitly discusses the practical implications of the findings for key stakeholders, including farmers, policymakers, and other relevant parties. The paper emphasizes how stakeholders can leverage technological advances and create a supportive environment to promote sustainable agricultural practices.

Finally, additional visual aids, including tables and figures, have been incorporated into the manuscript. These visuals, such as the conceptual model, help to summarize key findings and illustrate the relationships between the various components of the proposed model.

References

Abounoori, A., & Khajehzadeh, M. (2020). Analysis of the impact of financial and trade expansion on economic growth in OPEC member countries. *Financial Economics*, *14*(51), 173-194.

Amiri, H., & Arshadi, V. (2021). Examining the simultaneous relationship between resilience and economic growth with emphasis on foreign investment. *Strategic and Macro Policies*, *9* (Special Issue 2021). **doi:10.30507/jmsp.2021.294256.2282**

Bozorgi Nejad, M., Memarzadeh, G., & Faqihi, A. (2021). Identifying and explaining the dimensions of modern public services in the policy-making cycle of Tehran Municipality with a neuro-fuzzy approach. *Journal of Development & Evolution Mnagement*, *1400*(44), 1-9.

Jahani, M. R., & Farahani Fard, S. (2020). The effect of trade and human resource development on Iran's economic growth with the aim of boosting production. *Strategic and Macro Policies*, *8*(32), 674-691. **doi: 10.30507/jmsp.2021.105735**

Heydari, F., & Hosseini, S. A. (2021). The process of justice-oriented policy-making of the Islamic Revolution in light of Mahdavi governance. Tenth National Conference on Management and Humanities Research in Iran.

Khosravian, S. (2021). Examining the position of the capital market in financing and its impact on boosting production. Fourth International Conference on Knowledge and Technology of the Third Millennium in Economics, Management and Accounting in Iran, Tehran.

Danaeefard, H. (2016). "The Getting Ride of" Public Policies in Iran: Conceptual Foundations, Charactrsitics, Antecedents and Concequences. *Journal of Science and Technology Policy*, *9*(2), 79-96. **dor: 20.1001.1.20080840.1395.9.2.7.1**

Dehghani, A., & Naseh, D. (2019). An equation for modeling the role of various factors and examining effective community policies for achieving production boom. *Shabak*, *49*, 53-61.

Sarvari Nejad, A., & Sargazi, H. (2021). Agricultural problems in the Sistan region and proposed solutions. National Conference on Resilience in Sistan, Zabol.

Solaymani, S. (2021). Impacts of technological innovation, economic growth, global oil price and trade openness on energy consumption in iran. *The Economic Research (Sustainable Growth and Development)*, *21*(2), 181-211. **dor: 20.1001.1.17356768.1400.21.2.4.4**

Farbod, D. (2020). The impact of establishing knowledge-based companies on boosting production (focusing on strengthening business environments in border areas). National Conference on Theoretical and Practical Aspects of Sustainable Development and Security in Border Areas with a Spatial Approach, Mashhad.

Godarzi, F., Hamidy, K., & Eslambolchi, A. (2021). Monitoring Key Success Factors in Comprehensive Banking Policy-Making: A Fuzzy Delphi Method (Case Study: Refah Bank). *Journal of Iranian Public Administration Studies*, *4*(1), 145-168. **doi: 10.22034/jipas.2021.289435.1188**

Mirbagheri Hir, M., & Abbasi, N. (2019). Examining the impact of production on economic growth with an endogenous approach. Fourth National Conference on Economics, Management and Accounting, Ahvaz.

Hashemi Madani, S. S. (2019). Entrepreneurship and production boom as a priority for the country in the importance of resistance economy and people's livelihoods. Payameh Qom Newspaper.

Campos, P. A., & Reich, M. R. (2019). Political Analysis for Health Policy Implementation. *Health Systems & Reform*, *5*(1), 1–12. **doi: 10.1080/23288604.2019.1625251**

Joniarta, W., Pinatih, D., & Pratiwi, N. (2019). The Dilemmatic Study of Local Policy Implementation towards "Bali Aga" Traditional Village in Culture Conservation. *International Journal of Social Sciences*

and Humanities, *3*(1), 153-159. **doi: 10.29332/ijssh.v3n1.278**

Koho, M., Tapaninaho, M., & Torvinen, S. (2011). Towards Sustainable Development and Sustainable Production in Finnish Manufacturing Industry. 4th International Conference on Changeable, Agile, Reconfigurable and Virtual Production (CARV2011), Montreal, Canada, 422-427. **doi:10.1007/978-3-642-23860-4_69**

Le, H. P., & Sarkodie, S. A. (2020). Dynamic linkage between renewable and conventional energy use, environmental quality and economic growth: Evidence from Emerging Market and Developing Economies. *Energy Reports*, *6*(4), 965–973. **doi: 10.1016/j.egyr.2020.04.020**

Luthra, S., Govindan, K., & Kumar, S. (2017). Structural model for sustainable consumption and production adoption — A grey-DEMATEL based approach. *Resources, Conservation & Recycling*, *125*, 198-207. **doi: 10.1016/j.resconrec.2017.02.018**

Munawwaroh, S., Larasati, E., Suwitri, S., & Warsono, H. (2019). Policy implementation of working culture development in ministry of religious affairs. *Management and Entrepreneurship: Trends of Development*, *4*(10), 43-57**. doi: 10.26661/2522-1566/2019-4/10-04**

Nathaniel, S. P., Murshed, M., & Bassim, M. (2021). The nexus between economic growth, energy use, international trade and ecological footprints. *Energy, Ecology and Environment*, *6*, 496–512. **doi:10.1007/s40974-020-00205-y**

Pollyn, B. S., Barinua, V., & Agi, C. J. (2016). Human capacity building and sustainable development in Nigeria: A value base analysis. *Best International Journal for African Universities*, *3*(2), 63-79.

Shah, N. H., Chaudhari, U., & Cárdenas-Barrón, L. E. (2020). Integrating credit and replenishment policies for deteriorating items under quadratic demand in a three echelon supply chain. *International Journal of Systems Science: Operations & Logistics*, *7*(1), 34-45. **doi:10.1080/23302674.2018.1487606**

Agriculture, Environment & Society

Journal homepage: www.aes.uoz.ac.ir

Forecasting wind speed in Zabol city: a comparative study of CNN, LSTM, and CNN-LSTM models

Tohid Bagherpoor [*a], Somayeh Kazemi Sormoli [b]

[a] Department of Agronomy, Faculty of Agriculture, University of Zabol, Zabol, Iran
[b] Department of Geo-information Engineering, School of Computer Science, China University of Geoscience (Wuhan), Wuhan, China

ARTICLE INFO

Article history:
Received: 4 October 2023
Accepted: 30 April 2024
Available online: 1 December 2024

Keywords:
Convolutional neural network
Hybrid models
Long short-term memory
Time series analysis
Wind speed prediction

ABSTRACT

One of the most essential concerns in renewable energy planning, weather forecasting, and environmental research is accurately predicting wind speed. This study evaluates and compares three machine learning methods: Long Short-Term Memory (LSTM), Convolutional Neural Network (CNN), and a hybrid CNN-LSTM. The dataset includes daily-averaged wind speed (m/s), the day of the year, and additional meteorological variables recorded at Zabol station from 2010 to 2021. The dataset was preprocessed using Min-Max normalization and then split into four seasonal subsets: spring, summer, autumn, and winter. Each season was further divided into distinct subsets for training, validation, and testing in a 7:2:1 ratio. Python 3.8 was utilized for model development and data preparation using TensorFlow and Keras libraries. Performance evaluation metrics included Pearson correlation coefficient, root mean square error (RMSE), mean absolute error (MAE), and mean directional absolute percentage error (MDAPE). The results highlight that the CNN-LSTM hybrid model achieves superior accuracy compared to the standalone CNN and LSTM models. CNN effectively captures spatial patterns, while LSTM manages long-term temporal dependencies. The integration of these strengths in the CNN-LSTM model enhances forecasting accuracy across diverse conditions. Notably, the CNN-LSTM model achieved the highest accuracy in autumn, with an R^2 value of 0.980, showcasing its robustness in capturing wind speed variations across diverse seasonal conditions. This research highlights the strengths and limitations of each model. The main objective of this study is to precisely predict wind speed to optimize energy production, improve weather forecasting, and evaluate environmental impacts. Future research could explore additional meteorological variables, hybrid modeling, improved preprocessing techniques, and the use of larger datasets.

Highlights

- A novel integrated model was introduced for wind speed prediction.
- The proposed model demonstrated superior performance compared to three benchmark models across four seasons.
- The research highlighted the timeliness and significance by pointing out the absence of comprehensive studies comparing CNN, LSTM, and CNN-LSTM models in wind speed prediction.

1. Introduction

Wind speed prediction (WSP) is crucial for various applications, including renewable energy generation, weather prediction, and disaster management. Despite significant advancements, accurately predicting wind speed remains challenging due to its highly nonlinear and dynamic nature.

Accurate WSP plays a vital role in various sectors, including renewable energy management, aviation, and agriculture (Bali et al., 2019; Neshat et al., 2021a). Timely and reliable wind speed predictions enable efficient energy production planning, optimized flight routes, and improved crop management. Traditional numerical weather prediction models often face challenges in accurately

* Corresponding author.
E-mail address: t.bagherpour@uoz.ac.ir
https://doi.org/10.22034/jelsa.2024.416818.1052

capturing the complex and non-linear nature of wind patterns.

Recent advancements in WSP have incorporated mainstream deep learning techniques like CNN (Hinton and Salakhutdinov, 2006) and LSTM (Hochreiter and Schmidhuber, 1997). For instance, Jaseena and Kovoor explored decomposition methods in WSP, determining that an empirical wavelet transform combined with Bi-LSTM yielded accurate and reliable results (Jaseena and Kovoor, 2021) . Yildiz et al. applied variational mode decomposition to extract time series features, reconstructing them into two-dimensional images for short-term wind power forecasting using a deep network model (Yildiz et al., 2021). Memarzadeh and Keynia utilized wavelet transforms for feature extraction in LSTM modeling (Memarzadeh and Keynia, 2020). Neshat et al. introduced a search-based CMA-ES model for hyperparameter tuning in LSTM training (Neshat et al., 2020). Bastos et al. integrated the U-Net semantic segmentation framework, widely utilized in medical image analysis, into WSP (Bastos et al., 2021). Additionally, hybrid models, which combine conventional time series models with machine learning, have gained traction in WSP, offering enhanced predictive power (Shobana Devi et al., 2021). However, these hybrid models cannot often capture spatiotemporal correlation data effectively.

As a result, machine learning models have gained significant attention for their ability to extract intricate patterns and make accurate forecasts. In this study, we focus on comparing three prominent machine learning models, namely CNN, Long LSTM networks, and the hybrid CNN-LSTM architecture, for WSP. By exploring the strengths and limitations of these models, we aim to contribute to the advancement of wind speed prediction (WSP) techniques and provide insights into the optimal choice of model for different forecasting scenarios. This research is motivated by the increasing need for reliable wind speed forecasts to support decision-making processes and facilitate the integration of renewable energy sources into the power grid. Moreover, understanding the comparative performance of these models can aid in designing more efficient operational strategies in sectors heavily reliant on wind speed information. To the best of our knowledge, no comprehensive study comparing CNN, LSTM, and CNN-LSTM models for WSP has been conducted in the literature, making this research timely and significant (Neshat et al., 2021b; Yang et al., 2022) .

WSP is of significant importance in various sectors. In renewable energy management, accurate predictions are crucial for optimizing wind farms and maximizing energy production (Kusiak et al., 2013). These forecasts allow operators to schedule maintenance, plan turbine operations, and make informed decisions on energy storage and distribution (Ali, 2012). Grid operators can integrate wind energy efficiently, ensuring a stable electricity supply (Sun et al., 2015). In the agricultural sector, wind speed forecasts contribute to improved crop management practices. Farmers use this information for irrigation, pest control, and harvest timing (Vanderwende and Lundquist, 2015). Accurate predictions help mitigate the risk of wind damage, optimize water usage, and enhance agricultural productivity.

CNNs have gained considerable attention in various domains, including computer vision and natural language processing. While initially designed for image analysis, CNNs have been successfully adapted for time series forecasting tasks. They excel at capturing local patterns and spatial dependencies through the use of convolutional filters. In time series forecasting, CNNs effectively extract temporal patterns and identify relevant features from the input data. By incorporating multiple convolutional layers, CNNs can learn hierarchical representations, enabling them to capture complex relationships within time series data (Dauphin et al., 2017).

LSTM networks, a type of recurrent neural network (RNN), are specifically designed to address the vanishing gradient problem and capture long-term dependencies in sequential data. LSTMs are well-suited for time series forecasting due to their ability to retain and propagate information across different time steps. With memory cells that selectively store and update information, LSTMs excel at capturing temporal dynamics and complex patterns in time series data(Hochreiter and Schmidhuber, 1997).

The CNN-LSTM model combines the strengths of both CNNs and LSTMs, making it a powerful approach for time series forecasting. By integrating CNN layers to extract relevant features and LSTM layers to model temporal dependencies, the CNN-LSTM architecture captures both spatial and temporal information effectively. This hybrid model benefits from the CNN's ability to learn local patterns and the LSTM's capacity to capture long-term dependencies. By combining these two architectures, the CNN-LSTM model provides a comprehensive representation of the input data, enabling accurate and robust predictions in complex time series forecasting tasks(Qiao et al., 2022). Overall, the CNN-LSTM model offers a valuable solution for accurate and comprehensive time series forecasting.

Several studies have explored the application of machine learning techniques for the WSP, showcasing their potential for improving the accuracy of predictions. Sheng-Xiang Lv and Lin Wang conducted a comprehensive review of deep learning models for the WSP and highlighted the advantages of utilizing neural network (NN)-based approaches. They discussed the successful application of CNNs and LSTM networks in capturing temporal patterns and extracting relevant features from wind speed data. The review emphasized the importance of model architecture selection and data pre-processing techniques in achieving reliable wind speed forecasts(Lv and Wang, 2022).

Liu et al. proposed the use of LSTM NNs for WSP and compared their performance against traditional time series models. Their study demonstrated the superior accuracy of LSTM networks in capturing the complex dynamics of wind speed data. The ability of LSTM networks to capture long-term dependencies in the time series data was particularly advantageous in WSP tasks. The authors also highlighted the importance of data preprocessing, including

feature selection and normalization, for improving the performance of the LSTM model(Liu et al., 2020).

In addition to individual models, hybrid architectures combining CNN and LSTM networks have shown promising results in WSP. Qiao et al. (2022) proposed a hybrid CNN-LSTM model that leverages the strengths of both architectures. Their study demonstrated that the CNN-LSTM model effectively captured spatial and temporal information from wind speed data, leading to improved forecasting accuracy compared to standalone CNN or LSTM models. The hybrid model's ability to extract spatial features through the convolutional layers and model temporal dependencies with the LSTM layers contributed to its superior performance(Qiao et al., 2022).

These previous studies collectively highlight the potential of machine learning techniques, including CNNs, LSTMs, and hybrid architectures, in improving the WSP accuracy. However, despite the advancements in this field, there is still a need for comprehensive comparisons between different models to identify the optimal approach for specific forecasting scenarios. Moreover, considering the dynamic and non-linear nature of wind speed data, it is crucial to investigate the impact of various input features and model configurations on the performance of machine learning models. The present study aims to address these gaps by comparing the performance of CNN, LSTM, and CNN-LSTM models and providing insights into their suitability for the WSP tasks.

In summary, the existing literature on WSP using machine learning techniques exhibits gaps in terms of comparative analysis between different models, exploration of input feature combinations, and the focus on longer-term forecasting horizons. This study aims to address these limitations by conducting a comprehensive comparison of CNN, LSTM, and CNN-LSTM models, investigating the impact of various input features, and extending the prediction horizon to one year. By filling these gaps, this research will contribute to the advancement of WSP methodologies and provide valuable insights for decision-makers in various industries relying on accurate long-term WSPs.

The remainder of the paper is organized as follows: Section 2 provides the dataset from Zabol City, Iran, and the models are implemented. Section 3 presents the obtained results. Section 4 concludes the paper by summarizing the key findings and suggesting future research directions.

2. Material and Methods

2.1. Data Collection and Pre-processing

The data used in this study were collected from a meteorological station located in Zabol, with a latitude of 31.05, a longitude of 61.48, and an altitude of 489 meters. The meteorological station, equipped with various sensors and instruments, measures wind speed, temperature, humidity, atmospheric pressure, and other relevant meteorological variables. The wind speed data used in this study were recorded at a specific frequency on the tutiempo.net website (TuTiempo.Net, 2010-2021), ensuring regular measurements and capturing the dynamic nature of wind patterns. The seven input variables (temperature, humidity, pressure, wind direction, solar radiation, etc.) were selected based on their demonstrated influence on wind speed, as supported by (e.g., Bali et al., 2019). Wind speed at 10 meters height was chosen as the target variable because it is a standard reference height in meteorological studies, ensuring consistency and comparability in results. The dataset comprises daily average wind speed measurements, spanning the period from 2010 to 2021. This time series dataset provides a valuable resource for the WSP research. With the availability of consistent and reliable data from the Zabol station, obtained from(TuTiempo.Net, 2010-2021), we aim to investigate the performance of various machine learning models in forecasting wind speed, contributing to the advancement of wind energy planning, weather prediction, and related fields.

The dataset comprises daily-averaged wind speed measurements spanning the period from 2010 to 2021 for 11 years. These wind speed measurements were recorded at the Zabol station, providing a consistent and reliable source of data obtained from (TuTiempo.Net, 2010-2021). Each entry includes the daily-averaged wind speed (m/s), day of the year, and additional relevant meteorological variables.

After pre-processing using Min-Max normalization, the dataset was split equally into four seasonal subsets: Spring, summer, autumn, and Winter. Each season was then divided into distinct subsets for training, validation, and testing in a 7:2:1 ratio(Qiao et al., 2022), corresponding to 720, 180 , and 90 days, respectively. (See Figure 1). The training and testing sets were used to evaluate and train various machine learning models, while the validation set was used to fine-tune model hyperparameters. The statistical indicators for wind speed across the four seasons using the test set, including mean, maximum, minimum, standard deviation, skewness, and kurtosis, are presented in Table 1.

Figure 2 compares the wind speed distributions across the four seasons: spring, summer, autumn, and winter, with important statistical characteristics summarized in Table 1. The figure visually represents the frequency and density of wind speeds, allowing for a clear comparison of seasonal wind behavior.

Table 1 displays the key statistical characteristics of the wind speed data for each season of the test set. The dataset consists of 90 samples for each season, and the table provides the maximum and minimum wind speeds, mean wind speeds, standard deviation (STD), skewness, and kurtosis values. The summer test set has the highest mean wind speed (39.33 m/s) and a relatively low standard deviation (9.07 m/s), indicating less variability and stronger winds. In contrast, the autumn test set has the largest standard deviation (14.87 m/s) and the widest range of wind speeds, highlighting greater variability and more extreme wind conditions. The spring and winter test sets show moderate mean wind speeds, with the spring test set having the most symmetric distribution (skewness of 0.19) and the winter test set being more positively skewed

(skewness of 1.01), indicating more frequent lower wind speeds. The skewness and kurtosis values help describe the shape and behavior of the wind speed distributions in each season.

These important results from Table 1 help explain the patterns observed in Figure 2, where the summer test set stands out with higher wind speeds and more concentrated distribution, while the autumn and winter test sets show more variability and extremes. The spring's wind speeds exhibit moderate turbulence, indicating balanced but varied wind behavior.

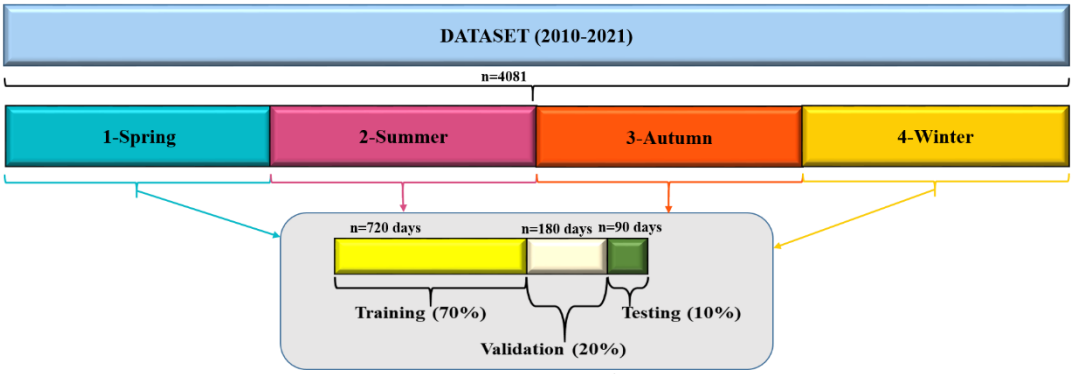

Figure 1. Dataset structure and division for the WSP (2010-2021)

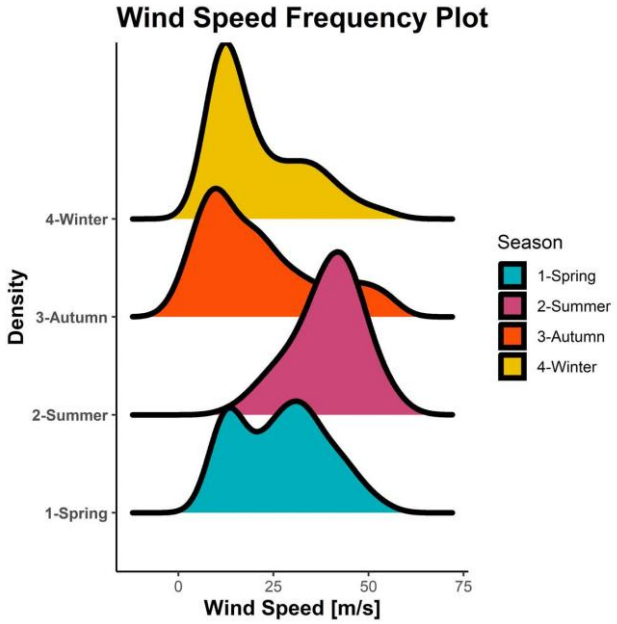

Figure 2. Wind speed frequency distribution across four seasons in 2021 (test set)

Table 1.Statistical characteristics of wind speed dataset for each season in 2021 (test set)

Season	Number of samples	Maximum (m/s)	Minimum (m/s)	Mean (m/s)	STD (m/s)	Skewness	Kurtosis
Spring	90	53.2	10	26.85	11.63	0.19	-0.96
Summer	90	59.1	14.3	39.33	9.07	-0.46	0.019
Autumn	90	55.2	0.9	20.88	14.87	0.83	-0.34
Winter	90	54.6	7	20.63	11.76	1.01	0.039

Before conducting any analysis or modeling, the collected wind speed data underwent a series of preprocessing steps. Missing values in the dataset were identified and treated using techniques such as linear interpolation or replacing them with the mean or median of neighboring values. Outliers, which could potentially affect the model's performance, were detected and either removed or adjusted. The wind speed data were then normalized using the Min-Max normalization to bring them to a common scale between 0 and 1, ensuring that all values fell within a standardized range by using the following equation (Radhika and Shashi, 2009):

$$y_{norm} = \frac{y - \min(y)}{\max(y) - \min(y)} \quad (1)$$

where y_{norm} is the scaled version of the unscaled variable y.

In addition to wind speed, other meteorological variables such as temperature, humidity, and atmospheric pressure were collected from the same meteorological station. These variables underwent similar preprocessing steps, including handling missing values, treating outliers, and normalization. The dataset was divided into training, validation, and testing sets to facilitate the modeling process. The partitioning was done chronologically, preserving the temporal order of the data and avoiding any leakage of information from future observations into the training or validation sets. By ensuring data quality through preprocessing and an appropriate train-test split, we can generate reliable datasets for training and evaluating the CNN, LSTM, and CNN-LSTM models. These steps lay the foundation for accurate WSP and contribute to advancements in wind energy planning, weather prediction, and related fields.

2.2. Proposed CNN, LSTM, and CNN-LSTM Architectures

A CNN is a sophisticated feed-forward NN that employs convolutional operations to autonomously extract features. Its architecture aligns with the principles of local perception, weight sharing, and the integration of multiple convolution kernels found in traditional NN models (Lecun et al., 1998). The CNN model is a deep learning architecture commonly used for image processing tasks, but it can also be applied to time series forecasting (Qiao et al., 2022). The CNN model consists of convolutional layers, pooling layers, and fully connected layers. In the context of WSP, the input data is treated as a one-dimensional (1D) sequence, where each data point represents a time step. The convolutional layers perform feature extraction by applying filters to the input sequence, capturing local patterns and spatial dependencies. The pooling layers reduce the dimensionality of the extracted features, aggregating the information across neighboring time steps. The fully connected layers at the end of the network combine the extracted features and generate the final predictions. The CNN model's architecture and hyperparameters, such as the number of filters, filter size, pooling size, and activation functions, can be tuned to optimize the model's performance for the WSP tasks (Karthik et al., 2020).

The CNN's layer inputs are sequentially derived from the preceding layer's outputs, with the initial layer being the time series data of wind speed. The convolution computation process unfolds as follows (Chen et al., 2021):

$$X_j^{(l)} = \mathrm{Re}\,LU\left(\sum_{i\in\Re_j} W_{i,j}^{(l)} * X_j^{(l-1)} + b_j^{(l)}\right) \quad (2)$$

where: $X_j^{(l)}$ is feature map j of layer l; $X_j^{(l-1)}$ is the output of the previous layer; * is the convolution operation; $W_{i,j}^{(l)}$ is the convolution kernel; and $b_j^{(l)}$ is the bias. All parameters are to be learned. The rectified linear unit (ReLU) stands as a widely employed non-linear activation function in NNs, defined by ReLU(X) = max(0,X). It serves the purpose of establishing intricate functional connections between intermediate outcomes and the characteristics of wind speed.

The fundamental architecture of a CNN comprises convolutional layers, pooling layers, and fully connected layers. Convolutional layers generate feature maps by applying moving kernels and activation functions to gridded input data through dot product calculations. Pooling layers, on the other hand, reduce the input data's size by selecting representative values (such as maximum or mean) from defined windows. To prevent excessive reduction in image size during the convolutional and pooling processes, padding techniques involving the addition of extra dummy data are commonly employed. Lastly, fully connected layers transform the spatial features from the previous layer, which are in a gridded format, into 1-D vectors. These transformed data are then input into densely connected NNs to produce the final output.

Many hyperparameters define a NN, but increasing the number of optimization variables extends the duration of the Bayesian optimization process (Frazier and Wang, 2016). Therefore, in this study, several hyperparameters were assigned fixed and conservative values. These selected hyperparameters primarily affect the network's training time rather than its accuracy, so sub-optimal values are unlikely to impact the final results' accuracy. To cut down on computation time, the networks trained during hyperparameter optimization were given random segments of 10% of the training and validation data, evenly distributed across the mean wind speed time histories. The hyperparameter optimization process was conducted twice for each network: initially, a broad range of values was used for each hyperparameter; subsequently, the range was narrowed significantly around the optimal value identified in the first round. The specific hyperparameter values for each NN are detailed in the following sections. Bayesian optimization was provided by the Skopt package in Python 3.8.12 with 120 rounds of optimization for each network.

The CNN employs an iterative backpropagation training process to extract the most effective feature maps from input data through hyperparameter optimization. In this research, the optimal input feature size, structure, and hyperparameters of the proposed CNN model were determined with a focus on both performance and efficiency, as illustrated in Figure 3. The input data, measuring 31 × 31 in size, consisted of features and was fed into the CNN. The CNN model was trained using the MAE loss function and the Adaptive moment estimation (Adam) optimizer. Following numerous tests with various combinations of structure and hyperparameters, the model incorporated two convolutional layers with filter sizes of 3 × 3 and capacities of 64 and 128 filters, respectively. A subsequent max-pooling layer with a 2 × 2 window size was connected, followed by a fully connected layer housing 64 nodes. The final output layer corresponds to the target output value. Throughout all convolutional and fully connected layers, the ReLU activation function was consistently employed in this investigation.

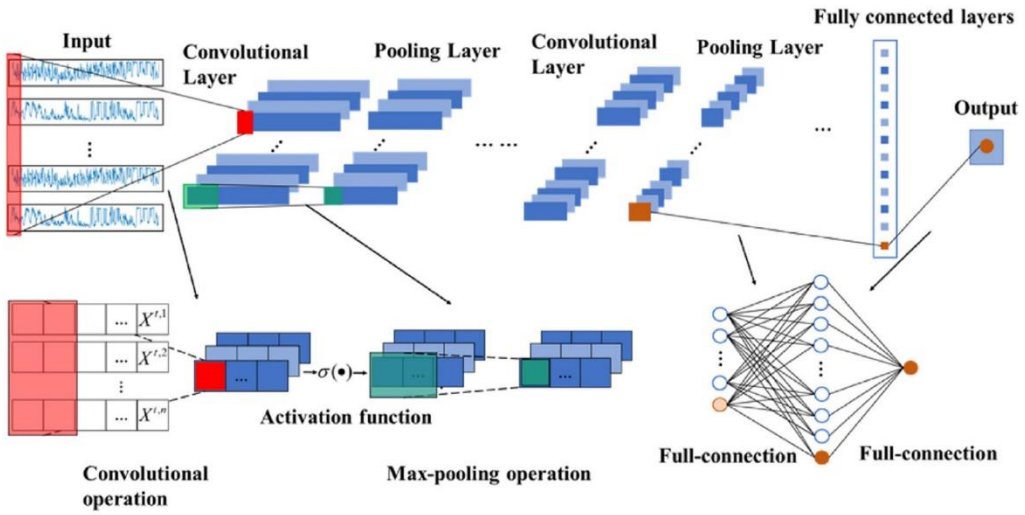

Figure 3. Architectures of CNN used in this study

The LSTM model is a type of RNN that is specifically designed to capture long-term dependencies and patterns in sequential data. Unlike traditional feed-forward NNs, LSTM models incorporate memory cells and gates, allowing them to retain and update information over multiple time steps. In the WSP, the LSTM model processes the input data sequentially, with each time step considered a sequence element. The model's architecture typically consists of LSTM layers, followed by fully connected layers. The LSTM layers use gates to control the flow of information and selectively remember or forget certain patterns over time. The fully connected layers combine the learned representations from the LSTM layers and produce the final WSPS. The LSTM model's architecture and parameters, including the number of LSTM cells, activation functions, and dropout rates, can be adjusted to optimize the model's performance for the WSP tasks.

The LSTM incorporates memory units within neurons to offer long-term memory capabilities and introduces a gating mechanism to regulate the flow of information to subsequent stages. This gating mechanism comprises an input gate $i(t)$, a forget gate $f(t)$, and an output gate o(t). These three gates, along with the candidate hidden states $\tilde{c}(t)$, can be represented similarly as follows (Chen et al., 2021):

$$\begin{bmatrix} i(t) \\ f(t) \\ o(t) \\ \tilde{c}(t) \end{bmatrix} = \begin{bmatrix} \sigma \\ \sigma \\ \sigma \\ \varphi \end{bmatrix} \left(W_{(*)} \begin{bmatrix} x(t) \\ s(t-1) \end{bmatrix} + b_{(*)} \right) \tag{3}$$

where $(*) \in \{i, f, o, \tilde{c}\}$ σ represents the sigmoid function yielding values within the range [0, 1]; φ denotes the hyperbolic tangent non-linear function, tanh(); $x(t)$ stands for the input at time t; $s(t-1)$ represents the external state from the previous time step; and b is an offset term. The hidden state from the previous time, c (t-1), and the candidate hidden state at the current time $\tilde{c}(t)$ are combined to form the complete state for the subsequent time step, which is expressed as:

$$c(t) = f(t) \cdot c(t-1) + i(t) \cdot \tilde{c}(t) \tag{4}$$

The calculation for obtaining the output of the current unit, which simultaneously serves as the hidden layer for the subsequent state s(t), is as follows (Hou et al., 2022):

$$s(t) = o(t) \cdot \tanh[c(t)] \tag{5}$$

In detail, the LSTM model incorporates essential components, including a memory cell (c), an input gate (i), a forget gate (f), and an output gate (o). These components work in tandem to significantly enhance the NN's capacity to handle lengthy, sequential data. The interplay between these elements is illustrated in Figure 4. Specifically, the input gate regulates the influence of new input on the memory cell (c), the forget gate governs the influence of the memory unit in retaining the prior value, and the output gate regulates the impact of the output memory cell. By utilizing an LSTM cell, the inputs $x(t)$ and $s(t)$ can be used to compute $s(t)$, which is then transmitted to the subsequent layer and forwarded to the fully connected layer to derive the output value.

During the training of the LSTM model, the number of epochs was set to 150. Training sets were processed using mini-batch gradient descent. After forming the mini-batches, gradients were calculated for each batch, followed by parameter updates. The mean square error (MSE) was selected as the loss function. The optimization algorithm used was Adam, with a learning rate of 0.001, known for its effectiveness in practical applications. This algorithm adjusted the model's weights and bias parameters. Each LSTM layer was configured with 100 neurons, and the model included two LSTM layers with 50 units each, utilizing ReLU activation and dropout regularization.

The CNN-LSTM model combines the strengths of both CNN and LSTM architectures, aiming to capture both spatial and temporal patterns in the input data. This model is well-suited for time-series forecasting tasks where both local patterns and long-term dependencies are important. The CNN-LSTM architecture typically starts with a few convolutional layers to extract spatial features from the input sequence. The output from the convolutional layers is then reshaped into a three-dimensional representation to be fed into the LSTM layers.

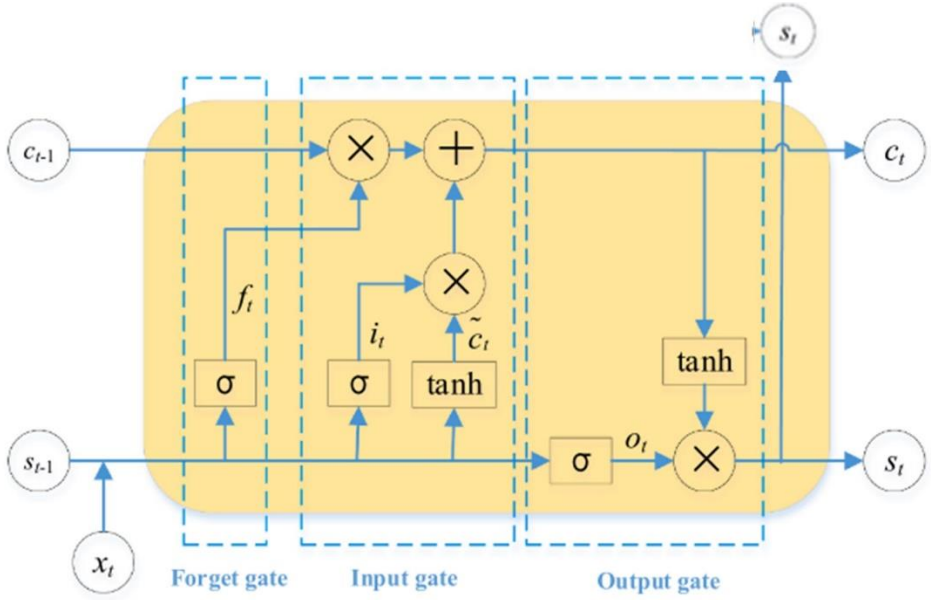

Figure 4. The basic LSTM cell

2.2. Evaluation metrics

Model performance was evaluated using appropriate evaluation metrics, such as root mean squared error (RMSE), mean directional absolute percentage error (MDAPE) or mean absolute error (MAE), Pearson correlation coefficient (PCC), and the coefficient of determination (R^2). These metrics provided quantitative measures of the models' accuracy in predicting wind speed. The models were also assessed based on their ability to capture temporal patterns and produce reliable long-term forecasts. The performance of each model was compared using statistical tests or other benchmark models to determine if the proposed CNN-LSTM model outperformed the individual CNN and LSTM models in the WSP. These metrics include:

- RMSE: It is the square root of the average squared difference between the predicted and actual wind speed values and provides a more interpretable measure of prediction error(Liu et al., 2019).

$$RMSE = \sqrt{\frac{1}{N}\sum_{i=1}^{N}(X_{predicted} - X_{observed})^2} \quad (6)$$

- MAE: It calculates the average absolute difference between the predicted and actual wind speed values, providing a measure of the average magnitude of the prediction error(Liu et al., 2019).

$$MAE = \frac{1}{N}\sum_{i=1}^{N}\left|X_{predicted} - X_{observed}\right| \quad (7)$$

- MDAPE: It quantifies the average absolute percentage difference between the predicted and actual wind speed values. MDAPE provides a measure of the average percentage error in capturing the magnitude of wind speed changes (Lv and Wang, 2022).

$$MDAPE = median(\sum_{i=1}^{N}\frac{\left|X_{observe} - X_{predicted}\right|}{X_{observed}}) \times 100\% \quad (8)$$

- PCC: The PCC is a widely used statistical measure that quantifies the strength and direction of the linear relationship between two continuous variables. It ranges from -1 to 1, with negative values indicating a negative linear relationship, positive values indicating a positive linear relationship, and 0 suggesting no linear relationship. PCC is calculated by comparing the covariance of the two variables to the product of their standard deviations. It is a valuable tool for researchers and analysts in various fields to assess and quantify associations between variables, though it assumes linearity and may not capture more complex relationships(Yang et al., 2022).

$$PCC = \frac{\sum_{i=1}^{N}((X_{observe} - \bar{X})(X_{predicted} - \bar{X}_{predicted}))}{\sqrt{(\sum_{i=1}^{N}(X_{observe} - \bar{X})^2 \sum_{i=1}^{N}(X_{predicted} - \bar{X}_{predicted})^2)}} \quad (9)$$

- R^2 (R-squared): R-squared is a statistical measure that reflects how well the predicted wind speed values align with the actual measured values (Yang et al., 2022).

$$R^2 = 1 - \frac{\sum_{i=1}^{N}(X_{observe} - X_{predicted})^2}{\sum_{i=1}^{N}(X_{observe} - \bar{X})^2} \quad (10)$$

where $X_{predicted}$ is the prediction results, $X_{observed}$ is the real data, N is the number of real data, and $\bar{X}_{predicted}$, $\bar{X}$ is the average of the prediction result and real data, respectively. These metrics provided measures of accuracy, prediction error magnitude, the proportion of variance explained by the models, and the average absolute percentage difference between predicted and actual values. It is important to consider that lower values of MAE and RMSE are indicative of better performance. The R^2 ranges from 0 to 1, and a value closer to 1 signifies a stronger alignment between the model's predictions and the actual measured values.

2.3. Experimental setup

In this study, the proposed network models were trained and evaluated using specific hardware and software environments. The hardware consisted of an Intel Core i7-8750H processor and an Nvidia GeForce GTX 1070 GPU, providing powerful computing ability and memory bandwidth. Deep learning frameworks like TensorFlow or PyTorch were utilized for model implementation and training. The Nvidia GeForce GTX 1070 GPU accelerated the training process due to its parallel processing capabilities. Python, along with libraries like Pandas and NumPy, was used for data manipulation and preprocessing tasks. This hardware and software setup ensured efficient analysis and reduced computational time.

3. Results and discussions

To assess the performance of our proposed CNN-LSTM model, we conducted comparative experiments using three individual models: CNN, LSTM, and CNN-LSTM(Chen et al., 2021). These experiments aimed to assess the generalization ability of the model across different seasons (spring, summer, autumn, and winter).

As shown in Table 2, the performance of all four models was evaluated using key metrics such as MAE, RMSE, MDAPE, PCC, and R^2. The results indicate that the proposed CNN-LSTM model consistently outperforms the other models in single-task prediction across all seasons. The CNN-LSTM model by Chen et al. (2021) displayed the second-best performance, followed by LSTM, with the CNN model showing the least favorable results.

Table 2. Assessing the precision of the four models in forecasting one step ahead.

Season	Model	Evaluation metrics				
		MAE	RMSE	PCC	MDAPE (%)	R^2
Spring	CNN	0.131	0.159	0.59	29.05	0.480
	LSTM	0.123	0.156	0.62	29.88	0.560
	CNN-LSTM (Chen et al.,2021)	0.408	0.525	-	-	0.934
	CNN-LSTM (proposed model)	0.047	0.056	0.95	10.36	0.966
Summer	CNN	0.107	0.135	0.47	16.78	0.472
	LSTM	0.096	0.116	0.53	14.91	0.554
	CNN-LSTM (Chen et al.,2021)	0.469	0.579	-	-	0.923
	CNN-LSTM (proposed model)	0.048	0.062	0.93	7.21	0.950
Autumn	CNN	0.150	0.210	0.51	40.06	0.492
	LSTM	0.144	0.201	0.58	37.06	0.579
	CNN-LSTM (Chen et al.,2021)	0.186	0.311	-	-	0.979
	CNN-LSTM (proposed model)	0.052	0.064	0.97	16.94	0.980
Winter	CNN	0.167	0.237	0.23	42.45	0.481
	LSTM	0.144	0.200	0.37	36.64	0.571
	CNN-LSTM (Chen et al.,2021)	0.393	0.495	-	-	0.964
	CNN-LSTM (proposed model)	0.048	0.062	0.95	14.71	0.975

These findings strongly validate the effectiveness and generalization capabilities of the model developed in this study. In the spring season, the proposed CNN-LSTM model demonstrated remarkable accuracy with the lowest MAE (0.047) and RMSE (0.056) values and a PCC of 0.95, indicating a strong linear relationship between predicted and actual wind speeds. The model also achieved the lowest MDAPE (10.36%) and a high R^2 (0.966), reflecting its excellent predictive capabilities. These trends were observed consistently across all seasons, highlighting the robustness of the model in predicting wind- related variables under diverse conditions(Schepers and Snel, 2007; Yang et al., 2022).

Graphical representations of the forecast results for each models across seasons are presented in Figures 5-8. These visuals highlight the challenges posed by abrupt changes in wind speed, which significantly impact forecasting accuracy. Figure 5 demonstrates that the proposed CNN-LSTM model outperforms the individual CNN and LSTM models, especially in spring, by closely following the wind speed changes. The CNN model, typically used for image data processing, struggles with time series data, showing large deviations between predicted and actual wind speeds. The limitation is likely due to the CNN's relatively small receptive field, which hinders effective extraction of long-range temporal features. Similarly, the LSTM model shows slight improvements, but it also fails to accurately predict sharp wind speed changes(Yang et al., 2022).

Incorporating LSTM improves predictions slightly, especially in periods of stable wind speeds. However, combining LSTM with CNN (i.e., single-task CNN-LSTM) significantly enhances performance, as illustrated in Figures 6-8. Similar to the findings of Qiao et al. (2022), who demonstrated the effectiveness of their MS-CDL model in handling sudden changes in wind speed over complex terrains, our proposed CNN-LSTM model also excels at managing sharp fluctuations without requiring multi-site data input. The model's ability to maintain high accuracy under such conditions underscores its robustness and efficiency in the WSP for diverse environments (Schepers and Snel, 2007; Yang et al., 2022).

Table 2 demonstrates that during the summer season, the proposed CNN-LSTM model exhibits outstanding predictive performance, with an MAE of 0.048 and an RMSE of 0.062. The model also achieves a high R^2 value of 0.950, indicating a strong correlation between the predicted and actual wind speeds. Figure 6 further highlights the model's effectiveness in closely tracking wind speed fluctuations, particularly during the peaks and troughs. This superior performance underscores the model's ability to handle sudden changes in wind speed, making it a reliable option for summer WSP. This model captures the rapid variations in wind speed, especially during abrupt changes, far more accurately than other models.

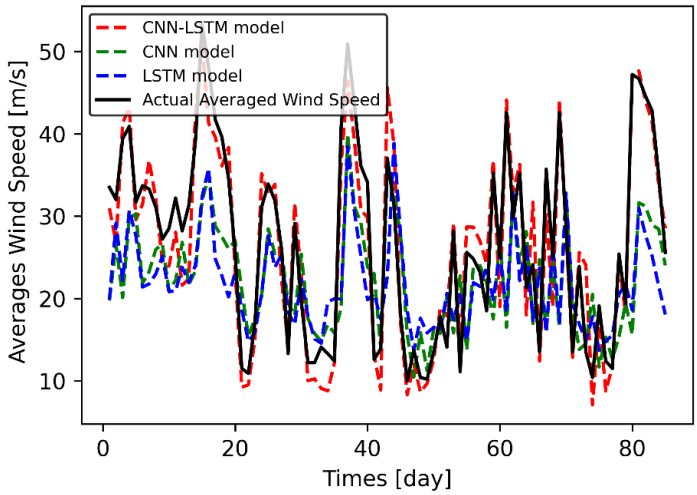

Figure 5. Comparison of CNN, LSTM, CNN-LSTM (proposed) model, and actual wind speed values on the spring test set

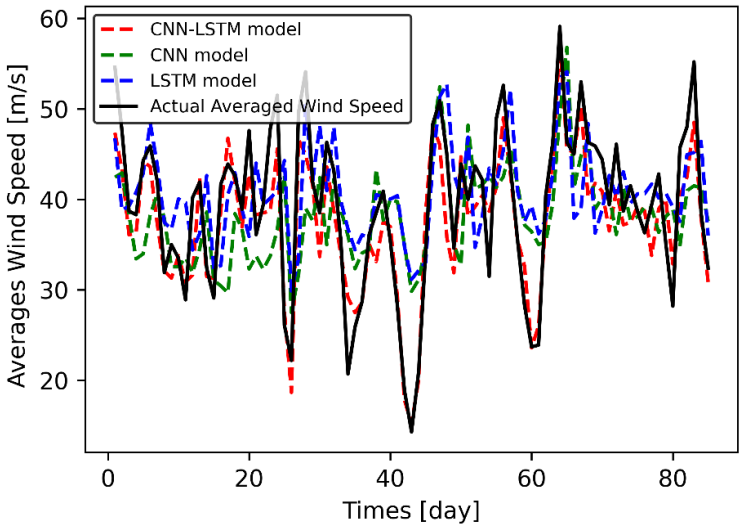

Figure 6. Comparison of CNN, LSTM, CNN-LSTM (proposed) model, and actual wind speed values on the summer test set

In the autumn season, as shown in Figure 7, the proposed CNN-LSTM model delivered its strongest performance, achieving an MAE of 0.052 and an RMSE of 0.064. The R^2 value of 0.980 demonstrates the model's exceptional accuracy in predicting wind speed, even during the most challenging conditions when frequent and abrupt changes occur. This result is consistent with Liu et al. (2020), who found that hybrid models incorporating signal decomposition techniques and feature selection methods achieve superior forecasting performance for multi-step predictions, further validating the use of hybrid architectures like CNN-LSTM (Liu et al., 2020; Yang et al., 2022).

In the winter season, the proposed CNN-LSTM model continues to outperform other models with an MAE of 0.048 and an RMSE of 0.062. The high R^2 value of 0.975 indicates its robustness in capturing sudden wind speed changes and delivering highly accurate predictions. Figure 8 shows that, unlike the CNN and LSTM models, which exhibit notable discrepancies, the proposed CNN-LSTM model closely aligns with the actual wind speed, maintaining precision even during sudden fluctuations. This demonstrates that the proposed model is the most dependable option for winter forecasting, where wind speed changes tend to be more unpredictable and difficult to predict(Qiao et al., 2022).

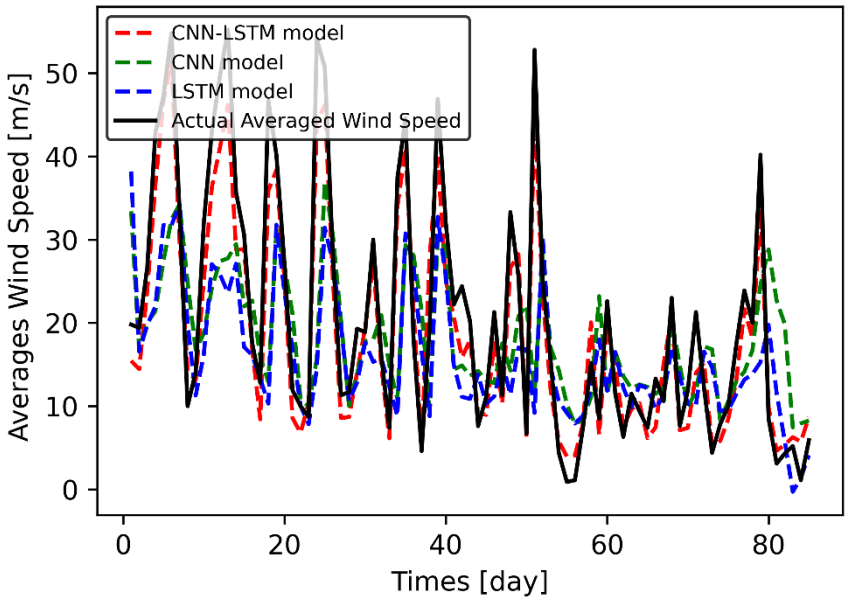

Figure 7. Comparison of CNN, LSTM, CNN-LSTM (proposed) model, and actual wind speed values on the autumn test set

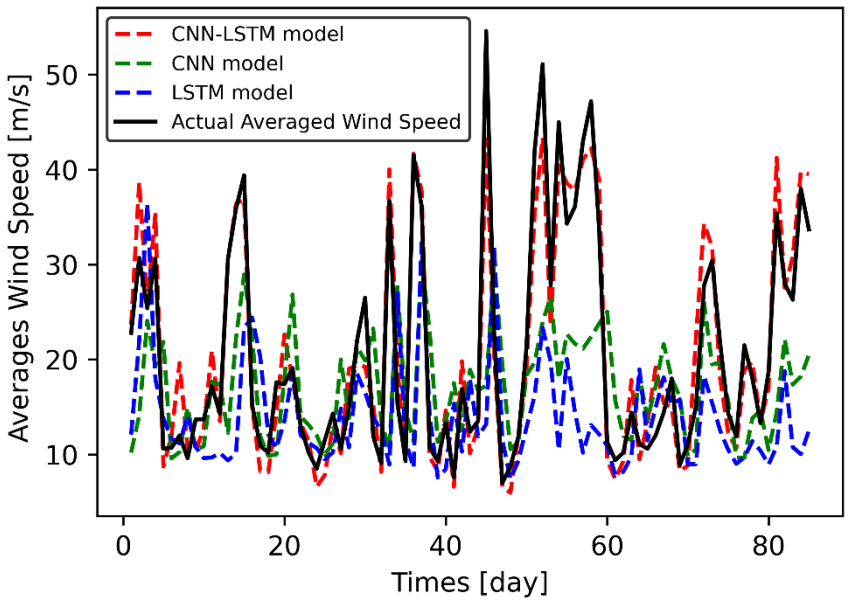

Figure 8. Comparison of CNN, LSTM, CNN-LSTM (proposed) model, and actual wind speed values on the winter test set

Figure 9 illustrates the R^2 values for each model in this study across the four distinct seasons: spring, summer, autumn, and winter. These figures provide a comprehensive overview of the model's performance in terms of achieving an exact fit between forecasted and real wind speed data. Notably, our proposed approach, employing CNN with LSTM, consistently stands out as the top-performing model, attaining an exceptional R^2 value of 0.98 for the autumn. This remarkable R^2 value underscores the exceptional accuracy with which our proposed method aligns the forecasted and actual wind speed data, thereby demonstrating its superior predictive capabilities.

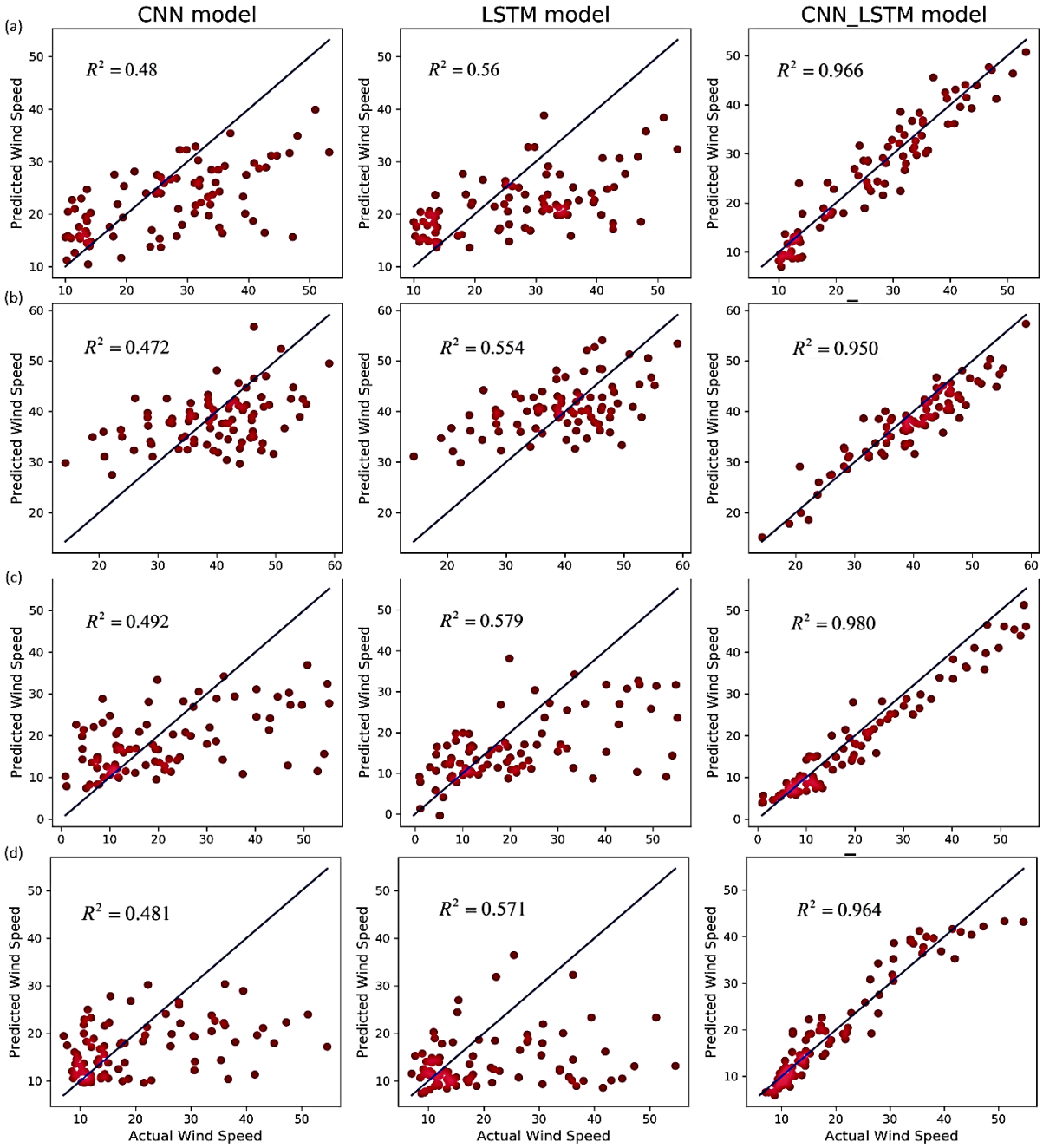

Figure 9. The comparison of a different forecasting model in (a) spring, (b) summer, (c) autumn and (d) winter seasons.

4. Conclusions

In this study, we conducted the interpretation and analysis of the results, which shed light on the performance of the CNN, LSTM, and CNN-LSTM models in the context of WSP. The superior performance of the CNN-LSTM model can be attributed to its ability to capture both the spatial and temporal characteristics of the wind speed data.

4.1 Contribution of the CNN-LSTM Model in WSP

By incorporating convolutional layers, the CNN component of the model effectively captures spatial patterns and local features, such as wind direction and geographic influences. On the other hand, the LSTM

component captures the temporal dependencies and long-term trends in the data. The integration of these two components in the CNN-LSTM model results in a more comprehensive representation of the complex interactions influencing wind speed variations.

Furthermore, the CNN-LSTM model's ability to leverage the strengths of both CNN and LSTM architectures addresses some of the limitations of the individual models. While the CNN model focuses on spatial features, it may overlook temporal dependencies, and vice versa for the LSTM model. The CNN-LSTM model overcomes this limitation by combining both aspects, enabling a holistic understanding of wind speed patterns. This integration proves to be particularly valuable in the WSP, where both spatial and temporal factors play significant roles.

The results also highlight the importance of considering appropriate evaluation metrics in the WSP. The MAE, RMSE, MDAPE, PCC, and R^2 provide valuable insights into the accuracy, precision, and linear relationship between predicted and actual wind speed values. These metrics help in assessing the model's performance in capturing the overall wind speed patterns and in quantifying the errors associated with the predictions. By employing these metrics, we can better understand the strengths and limitations of the models and make informed decisions regarding their suitability for the WSP tasks.

Additionally, the findings suggest that the CNN-LSTM model has the potential to advance WSP in various applications. Accurate WSPs are crucial for industries such as renewable energy, aviation, and environmental monitoring. The ability to forecast wind speed accurately can optimize energy generation and distribution, improve flight safety, and enhance environmental impact assessments. The CNN-LSTM model's superior performance in the WSP offers practical benefits in these domains and provides an avenue for more precise and reliable decision-making.

However, despite the promising results, it is important to acknowledge the limitations of the study. The performance of the models may vary depending on the specific characteristics of the dataset, such as geographic location, period, time and data quality. Furthermore, the choice of hyperparameters and the architecture of the models can significantly impact their performance. Future research should focus on addressing these limitations by conducting comparative studies across different datasets, exploring different architectural variations, and considering additional factors that may influence the WSPs, such as topography and meteorological conditions.

In conclusion, the interpretation and analysis of the results demonstrate the effectiveness of the CNN-LSTM model in the WSP. Its ability to capture both spatial and temporal features, coupled with its superior performance in terms of accuracy and correlation, makes it a promising approach for the WSP tasks. These findings contribute to the advancement of WSP techniques and highlight the potential for improving decision-making in industries reliant on accurate WSPs. Further research and experimentation are needed to refine and optimize the models, taking into account the specific characteristics and requirements of different WSP applications.

4.2 Limitations and Future Work

While the CNN-LSTM model shows superior performance, it also presents challenges such as higher computational complexity and longer training times. Scalability and generalizability remain concerns, especially with varied datasets. Future work will focus on addressing these limitations through optimization techniques and exploring ensemble models for enhanced robustness and sensitivity.

References

Ali, M. H. (2012). *Wind energy systems: Solutions for power quality and stabilization*: Crc Press.

Bali, V., Kumar, A., & Gangwar, S. (2019). Deep learning based wind speed forecasting- a review. Paper presented at the 9th International Conference on Cloud Computing, Data Science & Engineering (Confluence), Noida, India. **doi: 10.1109/confluence.2019.8776923**

Bastos, B. Q., Oliveira, F. L. C., & Milidiu, R. L. (2021). U-convolutional model for spatio-temporal wind speed forecasting. *International Journal of Forecasting, 37*(2), 949-970. **doi: 10.1016/j.ijforecast.2020.10.007**

Chen, Y., Wang, Y., Dong, Z., Su, J., Han, Z., Zhou, D., Zhao, Y., & Bao, Y. (2021). 2-d regional short-term wind speed forecast based on cnn-lstm deep learning model. *Energy Conversion and Management, 244*, 114451. **doi: 10.1016/j.enconman.2021.114451**

Dauphin, Y. N., Fan, A., Auli, M., & Grangier, D. (2017). *Language modeling with gated convolutional networks*. Paper presented at the the 34th International Conference on Machine Learning, Sydney, Australia.

Frazier, P. I., & Wang, J. (2016). Bayesian optimization for materials design. *Information science for materials discovery and design*, 45-75. **doi: 10.1007/978-3-319-23871-5_3**

Hinton, G. E., & Salakhutdinov, R. R. (2006). Reducing the dimensionality of data with neural networks. *SCIENCE, 313*(5786), 504-507. **doi: 10.1126/science.1127647**

Hochreiter, S., & Schmidhuber, J. u. (1997). Long short-term memory. *Neural Computation 9*(8), 1735-1780. **doi: 10.1162/neco.1997.9.8.1735**

Hou, J., Wang, Y., Zhou, J., & Tian, Q. (2022). Prediction of hourly air temperature based on cnn–lstm, geomatics. *Natural Hazards and Risk, 13*(1), 1962-1986. **doi: 10.1080/19475705.2022.2102942**

Jaseena, K. U., & Kovoor, B. C. (2021). Decomposition-based hybrid wind speed forecasting model using deep bidirectional lstm networks. *Energy Conversion and Management, 234*. **doi: 10.1016/j.enconman.2021.113944**

Karthik, R., Hariharan, M., Anand, S., Mathikshara, P., Johnson, A., & Menaka, R. (2020). Attention embedded residual cnn for disease detection in tomato leaves. *Applied Soft Computing, 86*, 105933. **doi: 10.1016/j.asoc.2019.105933**

Kusiak, A., Zhang, Z., & Verma, A. (2013). Prediction, operations, and condition monitoring in wind energy. *Energy*, *60*, 1-12. **doi: 10.1016/j.energy.2013.07.051**

Lecun, Y., Bottou, L., Bengio, Y., & Haffner, P. (1998). *Gradient-based learning applied to document recognition.* Paper presented at the in Proceedings of the IEEE. **doi: 10.1109/5.726791**

Liu, H., Duan, Z., Wu, H., Li, Y., & Dong, S. (2019). Wind speed forecasting models based on data decomposition, feature selection and group method of data handling network. *Measurement*, *148*, 106971. **doi: 10.1016/j.measurement.2019.106971.**

Liu, H., Yu, C., Wu, H., Duan, Z., & Yan, G. (2020). A new hybrid ensemble deep reinforcement learning model for wind speed short term forecasting. *Energy*, *202*, 117794. **doi: 10.1016/j.energy.2020.117794**

Lv, S.-X., & Wang, L. (2022). Deep learning combined wind speed forecasting with hybrid time series decomposition and multi-objective parameter optimization. *Applied Energy*, *311*, 118674. **doi: 10.1016/j.apenergy.2022.118674**

Memarzadeh, G., & Keynia, F. (2020). A new short-term wind speed forecasting method based on fine-tuned lstm neural network and optimal input sets. *Energy Conversion and Management*, *213*, 112824. **doi: 10.1016/j.enconman.2020.112824**

Neshat, M., Nezhad, M. M., Abbasnejad, E., Mirjalili, S., Groppi, D., Heydari, A., . . . Wagner, M. (2021a). Wind turbine power output prediction using a new hybrid neuro-evolutionary method. *Energy*, *229*. **doi: 10.1016/j.energy.2021.120617**

Neshat, M., Nezhad, M. M., Abbasnejad, E., Mirjalili, S., Tjernberg, L. B., Astiaso Garcia, D., Alexander, B., & Wagner, M. (2021b). A deep learning-based evolutionary model for short-term wind speed forecasting: A case study of the lillgrund offshore wind farm. *Energy Conversion and Management*, *236*, 114002. **doi: 10.1016/j.enconman.2021.114002**

Neshat, M., Nezhad, M. M., Abbasnejad, E., Tjernberg, L. B., Garcia, D. A., Alexander, B., & Wagner, M. (2020). An evolutionary deep learning method for short-term wind speed prediction: A case study of the lillgrund offshore wind farm. *ArXiv*, *abs/2002.09106*. **doi: 10.48550/arxiv.2002.09106**

Qiao, D., Wu, S., Li, G., You, J., Zhang, J., & Shen, B. (2022). Wind speed forecasting using multi-site collaborative deep learning for complex terrain application in valleys. *Renewable Energy*, *189*, 231-244. **doi: 10.1016/j.renene.2022.02.095**

Radhika, Y., & Shashi, M. (2009). Atmospheric temperature prediction using support vector machines. *International Journal of Computer Theory and Engineering*, 55-58. **doi: 10.7763/ijcte.2009.V1.9**

Schepers, J. G., & Snel, H. (2007). Model experiments in controlled conditions. *ECN Report: ECN-E-07-042*, *484*.

Shobana Devi, A., Maragatham, G., Boopathi, K., Lavanya, M. C., & Saranya, R. (2021). *Long-term wind speed forecasting—a review*. Paper presented at the Artificial Intelligence Techniques for Advanced Computing Applications, Singapore. **doi: 10.1007/978-981-15-5329-5_9**

Sun, W., Liu, M., & Liang, Y. (2015). Wind speed forecasting based on feemd and lssvm optimized by the bat algorithm. *Energies*, *8*(7), 6585-6607. **doi: 10.3390/en8076585**

TuTiempo.Net. (2010-2021). Global climate data, from https://en.tutiempo.net/climate

Vanderwende, B., & Lundquist, J. K. (2015). Could crop height affect the wind resource at agriculturally productive wind farm sites? *Boundary-Layer Meteorology*, *158*(3), 409-428. **doi: 10.1007/s10546-015-0102-0**

Yang, R., Liu, H., Nikitas, N., Duan, Z., Li, Y., & Li, Y. (2022). Short-term wind speed forecasting using deep reinforcement learning with improved multiple error correction approach. *Energy*, *239*, 122128. **doi: 10.1016/j.energy.2021.122128**

Yildiz, C., Acikgoz, H., Korkmaz, D., & Budak, U. (2021). An improved residual-based convolutional neural network for very short-term wind power forecasting. *Energy Conversion and Management*, *228*, 113731. **doi: 10.1016/j.enconman.2020.113731**

Agriculture, Environment & Society

Journal homepage: www.aes.uoz.ac.ir

Monitoring and evaluating land use changes using remote sensing techniques and satellite images (case study: Bam plain)

Maryam Safavi [a], Somayeh Galdavi [*b], Hadi Dehghan [b]

[a] Ph.D Student of Water Resources, Birjand University, Birjand, Iran
[b] Department of Water Sciences and Engineering, Kashmar Higher Education Institute, Kashmar, Iran

ARTICLE INFO

Article history:
Received: 24 April 2024
Accepted: 6 July 2024
Available online: 1 December 2024

Keywords:
Bam plain
Change detection
Land use
MLC
Remote sensing techniques

ABSTRACT

One way to effectively manage geographical space, natural resources, and the environment is through the use of land use maps. Understanding the quantitative and qualitative characteristics of changes in land use is crucial for environmental planning, land use, and sustainable development. The study aims to assess the potential of Landsat satellite data in identifying, detecting, and monitoring changes in land use. This involves using various digital processing techniques on satellite images to produce maps. The focus is on evaluating both the quantitative and qualitative changes in land use in the Bam Plain in Kerman province. To conduct research using Landsat satellite images from 2003 to 2018, a land use map for the year 2018 was prepared using the maximum likelihood algorithm, neural network, and support vector machine. The accuracy of the algorithms for this year was then discussed. The evaluation of the classification results shows that maximum likelihood classification has an overall accuracy of 95% and a kappa coefficient of 94%, which is higher than the accuracy of 93% and kappa of 91% for neural network classification, as well as the accuracy of 88% and kappa of 85% for support vector machine classification. Then, Using the maximum likelihood algorithm, which had high accuracy, the map of other years was also prepared. then the map of changes for each period was also obtained, which showed the changes in land use during the 5-year periods of 2003-2008, 2008-2013, and 2013-2018. although these maps revealed fluctuations in land area over the mentioned periods, during the last 15 years (2003-2018) significant changes were observed in the extent of barren and Salty lands in the study area. In 2003, these lands covered approximately 6811.91 Km^2, which accounted for about 38.52% of the study area. This area expanded to 6877.17 Km^2 in 2018, covering approximately 38.91% of the study area. During this period, agricultural lands and pastures diminished due to overuse. The results of this research assist managers and decision-makers in making more informed decisions regarding changes in land use, as well as the control, protection, and sustainable use of land.

Highlights

- The potential of Landsat satellite data in identifying, detecting, and monitoring changes in land use was investigated.
- The focus is on evaluating the quantitative and qualitative changes in land use in the Bam Plain in Kerman province.
- land use maps were prepared using the maximum likelihood algorithm, neural network, and support vector machine.
- The result of land use change detection showed significant changes in the extent of barren and Salty lands.
- During this period, agricultural lands and pastures diminished due to overuse.

1. Introduction

Understanding changes in land use and analyzing its patterns is essential for managing and evaluating natural resources. The monitoring of changes in land use over time is achieved through remote sensing, which offers shorter time intervals, lower costs, and greater accuracy (Lausch & Herzog, 2002). Land use has always been one of the most

* Corresponding author.
E-mail address: s.galdavi@kashmar.ac.ir, s.galdavi@yahoo.com
https://doi.org/10.22034/jelsa.2024.459150.1067

important factors through which humans have influenced their environment. Historically, the most significant change in land use that human has made has been the destruction of forests and their conversion to agricultural lands and settlements (Galdavai et al., 2013). Effective land management requires accurate and current information in the form of a map. Considering the widespread and unregulated changes in land use, including the depletion of natural resources in recent years, it is essential to analyze the evolving patterns of land use over time using satellite images. On the other hand, Satellite data is repeatable, up-to-date, and covers a wide area, making it increasingly utilized. In recent years, the efficiency of satellite data and geographic systems capabilities have drawn researchers' attention to studying land use changes. Monitoring land use changes is essential for ecology, deforestation, sustainable resource management, urbanization, and modeling climate change impacts (Galdavi et al., 2024). With recent advances in remote sensing and satellite technology, the latest geographic information is now more accessible and affordable for users. As a result, the use of remote sensing has become more common due to reduced costs and time compared to ground mapping. For several decades, the integration of remote sensing and geographic information system technology has been utilized to observe, monitor, and the dynamics of land use and land cover change (Longley et al., 2010).

Today, the investigation of land use changes, including Urban changes, is related to the conversion of forest, range, agricultural, and orchard lands into residential areas and urban facilities through the process of revealing changes using multi-temporal remote sensing images (Galdavi et al., 2013; Galdavi et al., 2015 and Shayesteh et al., 2018), which increases the speed Checking and accuracy of the results replace expensive, time-consuming and often less accurate methods. Remote sensing, along with geographic information systems (GIS), is a valuable tool for monitoring changes in land coverage on both regional and global scales in developing countries. RS and GIS are superior and efficient technologies for studying environmental changes and managing resources. Today, remote sensing images are considered the most up-to-date information for studying land cover and land use (Galdavi et al., 2013). The use of images is crucial for creating accurate land use maps due to providing up-to-date information, a variety of shapes, digitality, and the possibility of processing. Remote sensing techniques can display and present land cover classes by classification processes. Land use plans affect certain changes that have specific consequences for the structure and function of the ecosystem in the landscape pattern (Zhang & Li, 2022).

Numerous studies have been conducted in the field of monitoring land use and land cover changes using satellite data such as Landsat, Spot, and IRS. Among these studies, Singh (1989) compared the techniques of image difference, image ratio, normalized vegetation index difference, and post-classification comparison. The result showed the image difference method had the highest accuracy, while the comparison method after classification had the lowest accuracy in monitoring forest changes in the northeastern region of India. Gao et al. (2006) utilized Landsat TM and ETM+ satellite images to identify land use changes in Northeast China in 1995, 1990, and 2000. The analysis revealed an increase in urban areas, water bodies, and forests. Agricultural lands predominantly transitioned into urban areas, water bodies, and forests, while forest and grassland areas converted to agricultural lands.

Fan et al. (2008) used TM 1998 and ETM^{+} 2003 images to investigate land use and land cover changes in the Pearl River Delta. They employed the maximum likelihood classification method, and the temporal and spatial changes in land use and land cover from 1998 to 2003 were revealed using the post-classification method. Jabbar and Zhou (2011) used remote sensing techniques and geographic information systems to identify ecological changes in Basra province, located in the south of Iraq, from 1990 to 2003. They found that processes such as desertification, salinity, urbanization, destruction of vegetation, and destruction of wetlands were the main factors contributing to the ecological degradation of the region. Hussain et al. (2013) used pixel-based algorithms and object-oriented methods to detect changes in a high-spatial-resolution images. They concluded that the object-oriented method has higher potential for change detection. Galdavi et al. (2013) detected urban changes by integrating multi-temporal remote sensing data over a 19-year period in the Gorgan region of Golestan province in northern Iran. The findings revealed a predominant conversion of agricultural lands into residential areas. Arulbalaji and Gurugnanam (2014) utilized remote sensing data to observe land use changes in the Salem area of South India. They noted that the most significant changes took place in the central part of the study area. These changes were attributed to the socio-economic development of the region, which has implications for water and mineral resources.

Madurapproma et al. (2015) identified land use changes in the Pipsten Creek 4 basin in North Dakota by using remotely sensed data and a supervised classification method from 1976 to 2011. They stated that the remotely sensed data digitized land cover changes and could be considered as a necessary input in land management policies.

Ramezani et al. (2018) conducted a study on land use changes in Esfrain (North Khorasan) over a period of four decades using Landsat images. They employed the supervised classification method and post-classification comparison to analyze the changes. The study achieved a kappa coefficient of approximately 87% and an overall accuracy of 90%. The findings indicated significant changes in irrigated lands and residential areas during the study period. Arekhi (2014) documented the land use changes in the Abdanan region over a 25-year period. The findings indicated a decrease in average and good range coverage between 1985 and 2010, suggesting a trend of degradation in the region due to the replacement of these ranges with poor ranges and barren lands. In a study, Yousefi et al. (2011) monitored land use changes in Marivan City using Landsat images from TM and ETM sensors for 16 years with the reclassification method. The

results showed that the most changes are related to agricultural and forest lands. These changes include reducing the forest and agricultural lands and increasing residential areas during the studied period of this region.

Shaisteh et al. (2018) detected the changes in Kurdkovi city in Golestan province from 1987 to 2015. They created land use maps for 1987, 2000, and 2015 using Landsat satellite time series images. Subsequently, they identified changes in the city using the post-classification method. The results indicated that 333 hectares approximately were added to the urban areas during the study period. The study also found that agricultural and forest areas contributed the most to the increase in urban lands, with 306 hectares and 27 hectares of land conversion, respectively. Galdavi et al. (2024) identified and monitored forest land changes in 20 years in the Gorgan region of Golestan province. For this purpose, land use maps were prepared in two 10-year periods using satellite images, and the changes revealed by the post-classification method. The results showed a decrease in the extent of forest lands in the studied period, and the main reason was the development of residential areas and agricultural lands in the region.

A review of past research showed that using remote sensing data is most useful and highly effective for identifying land use changes over time. Therefore, in the current research, using remote sensing (RS) and geographic information system (GIS) data, land use changes and their trend in Bam Plain have been studied.

2. Materials and methods

2.1. The study area

The city of Bam is located in the Kerman province and has a population of over 300,000 people. Bam experiences a dry desert climate. The main occupations of the residents are agriculture and horticulture. Water for drinking and agriculture is mainly sourced from underground water Aqueducts and wells. Bam Plain is a closed rectangular plain located at approximately 58°21' east longitude and 29°6' north latitude. It is situated in the southwest-northeast direction, about 207 Km southeast of the capital of Kerman province. Bam Plain is located on the edge of the Lut desert, which is considered one of the dry areas of the country. In these plain, deep and semi-deep wells are very popular due to the existence of many agricultural lands. The study area is a part of the Lut desert catchment area with a hot desert climate. Its height above mean sea level is 960 meters, and its area is 9921 Km^2, of which 4357 Km^2 includes plains.

2.2. Data

The research utilized Landsat satellite images and 1:25000 topographic maps. The images have been requested from the USGS website and received at the L1T correction level. The specifications of the images used can be found in Table 1. Since the study area is located in two frames two images were received for each year. These images were then mosaiced after necessary corrections and clipped using the area's border.

Table 1. Specifications of satellite images used in the research

	Date of Images	Pass and row number	Satellite	Sensor	Resolution (m)
1	2003	159-40	LANDSAT_5	TM	30
		158-40	LANDSAT_5		
2	2008	159-40	LANDSAT_7	ETM	30
		158-40	LANDSAT_7		
3	2013	159-40	LANDSAT_8	OLI	30
		158-40	LANDSAT_8		
4	2018	159-40	LANDSAT_8	OLI	
		158-40	LANDSAT_8		

After preparing satellite images for the study area, ENVI 5.1 was used during different stages of image processing. Also, the Maximum Likelihood Classifier (MLC), neural network, and support vector machine methods were used to investigate land use changes and evolutions.

2.3. Pre-processing of satellite images

The quality of the satellite data was assessed for geometric and radiometric errors, such as striations, non-overlapping scan lines, repeated pixels, and atmospheric errors like cloud patches. Pre-processing involves correcting these distortions and errors to extract primary information and prepare the data for further processing (Akbari et al., 2016). In this research, to check the geometric condition of the images, the layers of Roads and Rivers were extracted from 1:25000 topographic maps and placed on the satellite images. Also, there are different methods for atmospheric correction, and in this research, the Dark Subtract method was achieved using ENVI software. In this method, a constant value is subtracted from the total value of pixels in a band. The turbidity reduction method assumes that the non-zero values for clean and deep water in the near-infrared band are caused by atmospheric path radiance (Lp). In this case, the constant value Lp is subtracted from all the values of the surface pixels (Akbari et al., 2016).

2.4. Classification of satellite images

Land use classification methods were used to process the images. Classification methods are divided into two categories: Supervised classification and Unsupervised Classification. Supervised methods need basic information such as the number of classes, their characteristics, and also several known examples of each class. In contrast to the unsupervised methods, most of them are automatic methods that do not need known samples and decide on their classification based on the values of the pixels themselves (Fatemi and Rezaei, 2016). The classification algorithms used in this research are of the supervised type,

which includes maximum likelihood, neural network, and support vector machine.

The maximum likelihood algorithm for classification is based on variance and covariance. This method assumes that all training areas have a normal distribution. To ensure representative samples, it is important to use as many samples as possible to cover a wide range of spectral characteristics. In maximum likelihood classification, the pixel is assigned to the class with the highest probability of belonging to that class (Akbari et al., 2016).

Support vector machine (SVM) is a binary classifier. In the case of two classes, the SVM method tries to create a hyperplane that maximizes the distance of each class to the hyperplane. Point data that is closer to the hyperplane are used to measure this distance. Therefore, these point data are called support vectors. In general, SVM is a binary and linear classifier which, by developing it and using kernel functions, is also used as a multi-class and non-linear classifier. In this research, the RBF kernel (Radial Basis Function) was used due to its widespread use in land use change studies with data from different satellites and also its better performance than other kernels. RBF kernel was determined from the formula (Eq. 1):

$$k(xi, xj) = \exp(-\gamma \left\| xi, xj \right\| 2), \quad \gamma > 0 \qquad (1)$$

In this formula; xi and xj are sets of training data and γ is a parameter defined by the user as kernel assumption. γ is the inverse of the number of spectral bands of the sensor (Akbari et al., 2016).

The first step in supervised classification is determining the type and number of classes. This classification is based on prior knowledge and used as training examples in data classification. The study area includes agricultural lands, rangelands, barren lands, built lands, and water areas. These classes are defined based on visits to the area, differences in satellite image reflections, and past similar studies. For each type of land cover and land use, any number of training samples can be defined with an ID, but in general, there should be a suitable number of cells for each type of land use for statistical analysis. An important rule is that the number of cells of each training sample or all training samples of a land use class should not be less than ten times the number of bands (Salman Mahiny and Kamyab, 2010). The land use map for the year 2018 was produced after determining training points using maximum likelihood methods, the neural network, and vector machine support. Then, the accuracy of the mentioned methods was evaluated for choosing the best algorithm. After that, the maps of other years were also determined with the best algorithm.

2.5. Evaluation of classification accuracy

Evaluation of classification results is one of the important steps of classification, which shows the level of correctness in classification. According to most well-known researchers, no classification can be relied upon until its accuracy has been evaluated, except when sampling pixels as a pattern of spectral or informative classes, evaluating the spectral reflectance of the classes, and distinguishing Their adaptability can also be done at the same time. The accuracy of the classification indicates the level of confidence in the extracted map, and it should be at least 85 in the land use maps obtained from remote sensing images (Akbari et al., 2016). Error evaluation and estimation of classification accuracy are usually based on statistical parameters that are extracted from the error matrix, one of the most common methods of expressing the classification accuracy is to prepare the classification error matrix. The error matrix compares the relationship between known reference data (ground truths) and the relevant results of an automatic classification class by class. Based on the error matrix, several parameters are extracted to express accuracy and error, which include total accuracy, producer accuracy, user accuracy, and kappa coefficient. Based on the accuracy of the manufacturer and the user, two errors of omission and commission can also be obtained. From the point of view of theory, total accuracy probabilities cannot be a good criterion for evaluating classification results. Because the role of chance is significant in this index. The overall accuracy is obtained from the sum of the elements of the main diameter of the error matrix divided by the total number of pixels according to the following relationship (Akbari et al., 2016).

In this regard:

$$OA = \frac{1}{N} \sum P_{ii} \qquad (2)$$

- OA overall accuracy
- N number of test pixels
- ΣPii sum of elements of the main diameter of the error matrix

Due to the defects in the overall accuracy, the kappa index is often used in executive works where the comparison of classification accuracy is considered. Because the kappa index focuses on the incorrectly classified pixels, the kappa index is calculated from the following relationship (Bonyad & Hajyghaderi, 2008).

$$Kappa = \frac{\text{po} - \text{pc}}{1 - \text{pc}} \qquad (3)$$

That in the above formula:

po – correctly observed

pc – expected agreement

The producer's accuracy is the probability that a pixel in the classified image is in the same class on the ground, and the user's accuracy is the probability that a certain class on the ground is in the same class on the classified image. They are calculated through the following formula (Bonyad & Hajyghaderi, 2008).

$$\text{PA} = \frac{ta}{ga} * 100 \qquad (4)$$

$$\text{UA} = \frac{ta}{n_1} * 100 \qquad (5)$$

that in the above formulas:

PA – Class A accuracy percentage for manufacturer's accuracy

ta - number of correct pixels classified as class a

ga - the number of classes a pixel in ground reality

UA – Class an accuracy percentage for user accuracy

n1 - the number of pixels of class a as a result of the classification based on the two mentioned accuracies, the two errors assigned 1 and omitted 2 are defined as follows (Fatemi and Rezaei, 2016).

Ce = 1- UA

Oe = 1- PA

The assigned error (Ce), which is calculated based on the accuracy of the user, is equivalent to the percentage of pixels that do not belong to the desired class, but the classifier considers them to be part of that particular class. The omitted error (Oe) is related to the percentage of pixels that belong to the desired class in the ground reality and are classified as other classes**.**

2.6. Change Detection

The change detection process is determining the changes in a subject or a phenomenon in a certain period (Coppin et al., 2004). In this study, after ensuring the acceptable accuracy of the maps and extracting the land use maps produced with the best algorithm in the desired years from the method of comparison after classification to prepare the matrix of land use changes for the period of 2003- 2008, 2008-2013, and 2013-2018 have been used. In this method, based on equation (7), the intensity of changes was determined by comparing the changes in the type of land use between the images of two different times. The result of this method is an image that shows the changes in land use between two dates (Singh, 1989). In this method, the area and percentage of the classes from the total will be determined in each year, and the amount of their changes in the investigated period.

$$DN = x(t1) * 10 + x(t2) \quad (7)$$

3. Results and discussion

In this research, 4 satellite images have been used at different times for detecting Changes in Land use and Land cover types in Bam Plain. The results of investigating the radiometric quality and geometric control of the images showed that the images had good quality. Also, the images overlayed with the vector layers of roads and rivers for investigating the geometry which showed they are spatially located in the correct place. After that, maximum likelihood supervised classification (MLC), neural network, and support vector machine were used to prepare land use maps. For this purpose, according to the existing Land uses in the region, training samples were prepared for 5 classes, including agricultural lands, urban lands, range lands, Salty lands, and bare lands, and based on the land use maps were extracted. Then, the accuracy of land use maps was assessed. For this purpose, land use maps and ground samples were analyzed in ENVI 5.1 software and the results of the error matrix for 2018 for all three algorithms of the neural network, maximum likelihood, and support vector machine was indicated in Tables 2 and 3. According to the result, the land use maps prepared by the all three algorithms have had high accuracy, however, the maximum likelihood algorithm has higher accuracy and precision than other algorithms (Table 3). This result is consistent with the findings of several researchers, including Akbari et al. (2016), Alizadeh et al. (2015), Morgan et al. (2015), and Madhura and Venkatachalam (2015). By comparing the accuracy of different supervised classification methods, the mentioned researchers stated that the maximum likelihood method has a suitable accuracy.

Table 2. Accuracy assessment of classification for Land use map 2018

Methods	Total accuracy (%)	kappa coefficient
Maximum likelihood	95.65	94.44
Neural network	93.11	91.25
Support vector machine	88.76	85.57

Table 3. Statistical characteristics of producer and user accuracy for OLI image for 2018

Methods	Maximum likelihood		Support vector mac		Neural network	
Accuracy Classes	Producer (%)	User (%)	Producer (%)	User (%)	Producer (%)	User (%)
Agriculture	94.55	94.55	92.73	94.44	94.55	92.86
Bare	98.78	96.43	100.00	95.35	90.24	96.10
Range	98.78	98.31	93.55	90.63	93.55	100.00
Salty lands	93.55	100.00	95.24	75.47	95.24	100.00
Urban	91.43	86.49	40.00	73.68	94.29	73.33

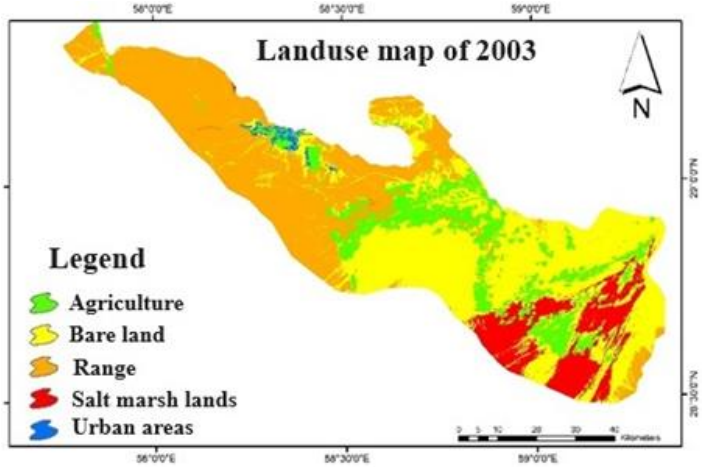

Figure 1. Land use map of 2003

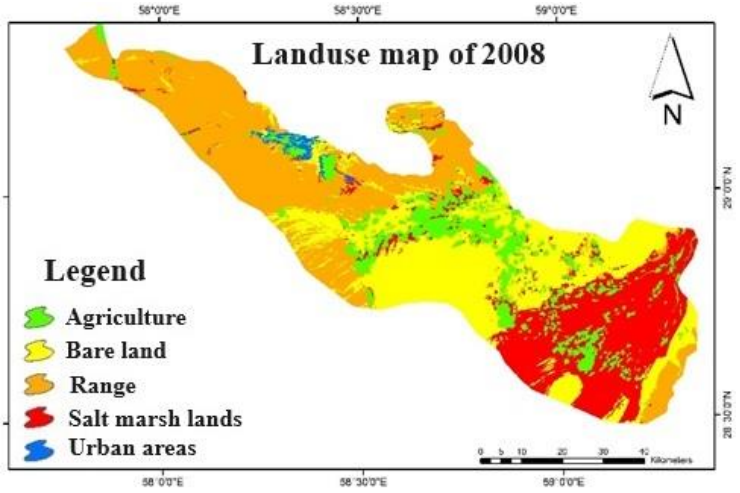

Figure 2. Land use map of 2008

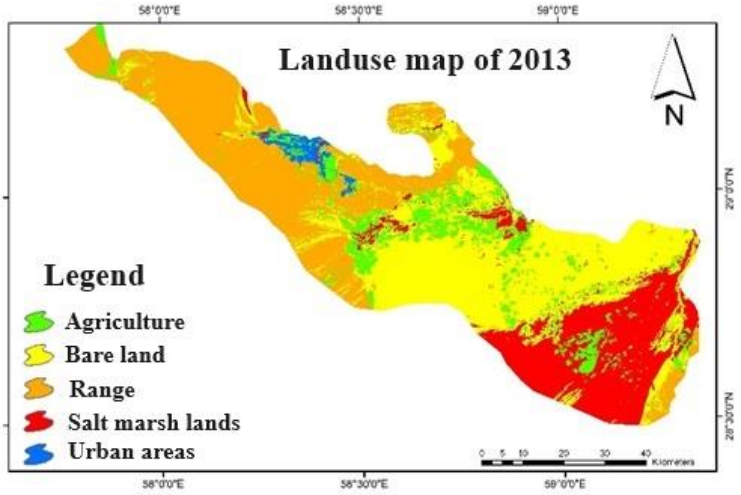

Figure 3. Land use map of 2013

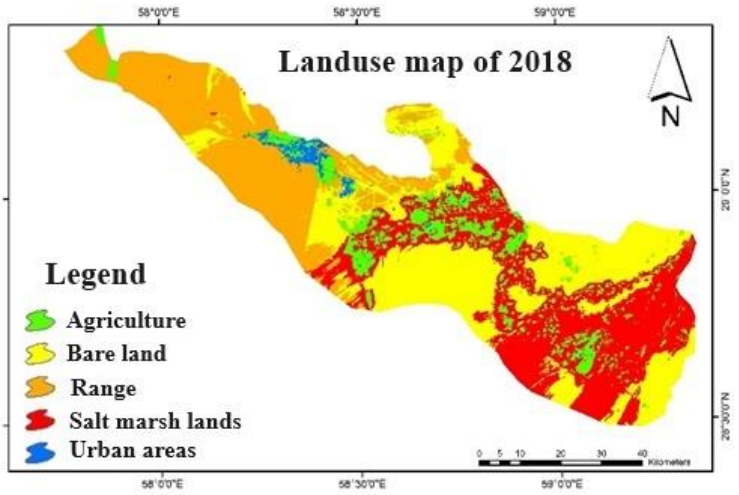

Figure 4. Land use map of 2018

The producer's and user's accuracy for all types of land use in images classified by the investigated algorithms - except urban in the neural network and support vector machine algorithm - were estimated above 80%, which is an acceptable level. After choosing the best algorithm, land use maps for other studied years were also prepared and their accuracy was evaluated. The accuracy of these maps was more than 80%, which is very accurate when compared with studies such as Lefsky and Cohen (2003). They have stated that overall accuracy and kappa coefficients greater than 0.7 are very good and less than 0.4 are poor. Figures 1 to 4 show the land use maps of the studied years.

After preparing the land cover/use map of three time periods, the area of five classes of land cover/use was obtained (Table 4). The results show a decrease in range and agricultural lands and an increase in bare and Salty lands. In 2003, the total of bare and Salty lands was 50%, and in 2018, these lands reached nearly 63%. After preparing the land cover/use map of three time periods, the area of five classes of land cover/use was obtained (Table 4). The results show a decrease in pasture and agricultural lands and an increase in barren and saline lands. In 2003, the total of barren and saline lands was 50%, and in 2018, these lands reached nearly 63%. On the other hand, range and agricultural lands have been reduced, which is the result of the indiscriminate destruction of them and their transformation into bare and Salty lands.

Table 4. Area of land uses for the years 2003, 2008, 2013, and 2018

Type of land use	The area of land use in the map of 2003		The area of land use in the map of 2008	
	Area (Km^2)	Area (%)	Area (Km^2)	Area (%)
Agriculture	661.3606	13.20	660.6602	12.432
Bare Lands	1987.5751	39.67	1515.885	30.266
Range	1811.7372	36.16	1743.775	34.816
Salty lands	515.2188	10.28	1084.828	21.659
Urban areas	33.7453	0.673	41.3296	0.825
Type of land use	**The area of land use in the map of 2013**		**The area of land use in the map of 2018**	
	Area (Km^2)	Area (%)	Area (Km^2)	Area (%)
Agriculture	553.0828	11.04	532.3891	10.62
Bare Lands	1795.5394	35.84	1698.828	33.91
Range	1584.4821	31.36	1268.6685	25.32
Salty lands	1007.2589	20.10	1441.1678	28.77
Urban areas	70.1349	1.40	69.4448	1.38

Finally, maps of land use changes in the periods of 2003-2008, 2008-2013, and 2013-2018 were prepared (Figures 5 to 7). According to the results, in the period from 2003 to 2018, range lands decreased and Salty lands and bare lands increased, which indicates the general trend of destruction in the region by replacing range and agriculture with Salty lands and bare lands. Most conversions have been related to agriculture to saline lands due to excessive use of agricultural lands over time, these lands have been destroyed and turned into saline lands and no longer can be used for agriculture. Likewise, the bare lands of the region have also turned into Salty lands over time, in 2018 nearly 29% of the region is salty lands, which cannot be cultivated or converted to other uses. Table 5 shows the rate of conversion of each user to another user.

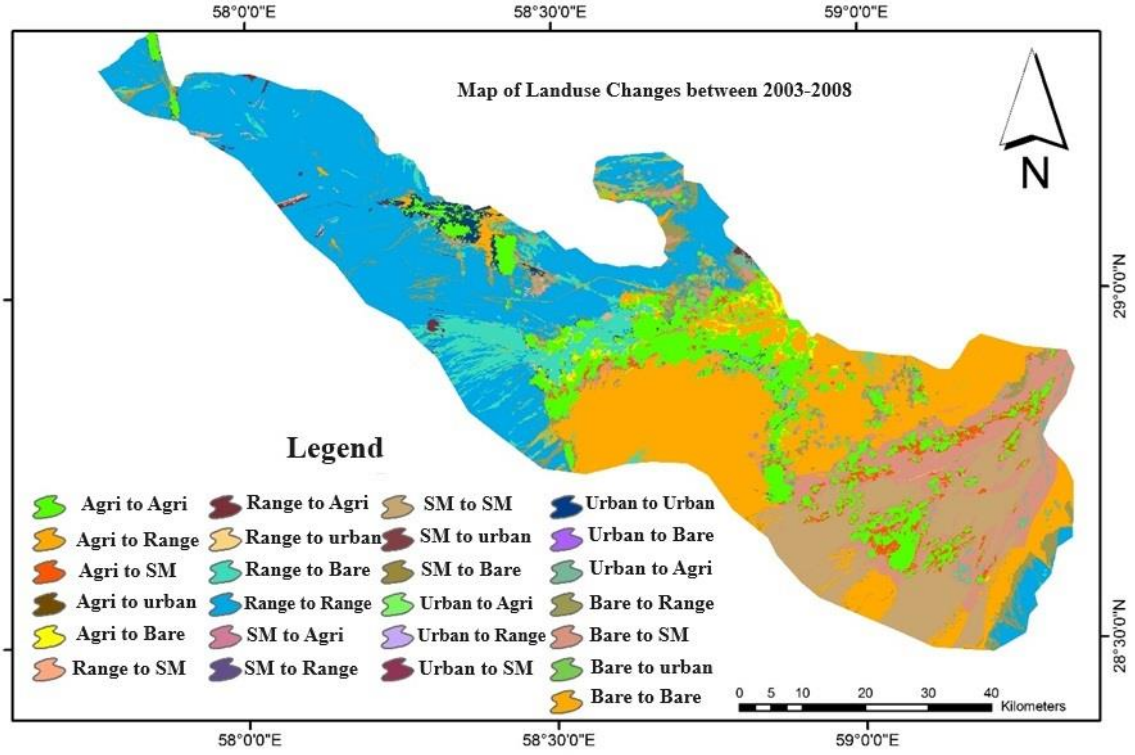

Figure 5. Map of Land use changes between 2003-2008

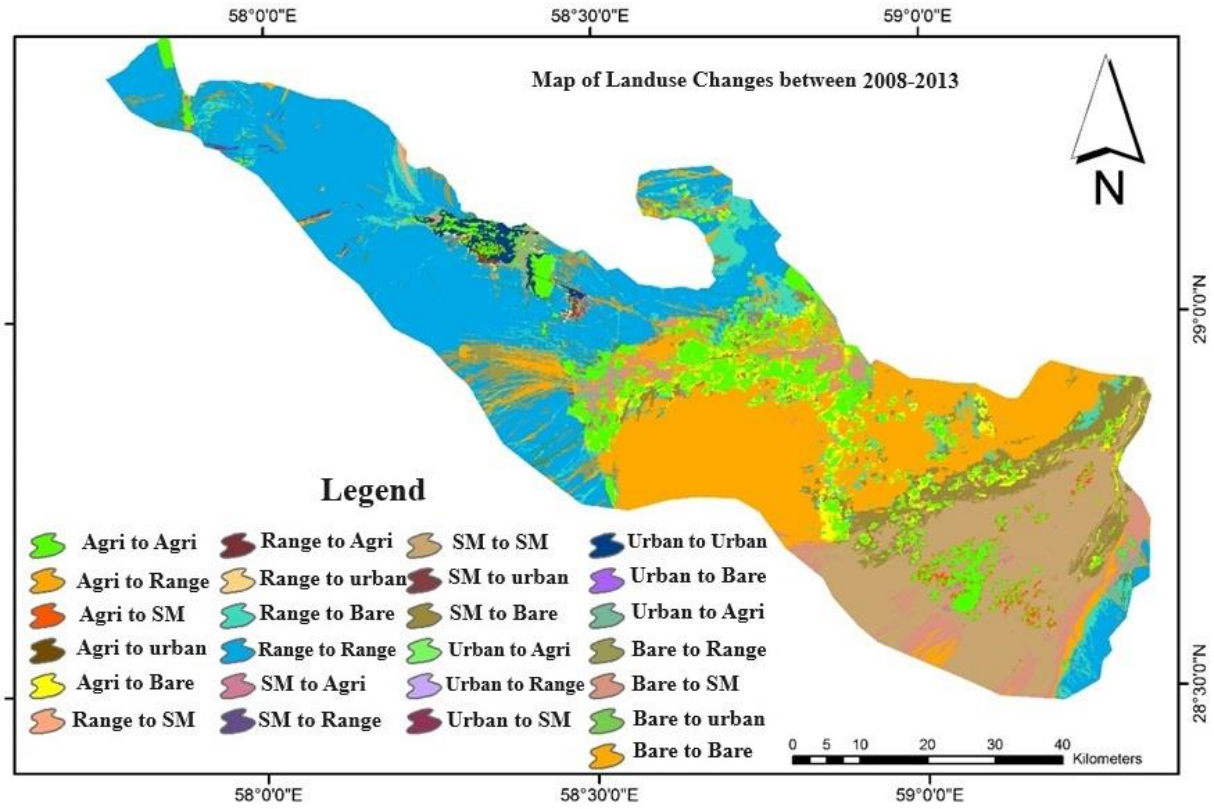

Figure 6. Map of Land use changes between 2008-2013

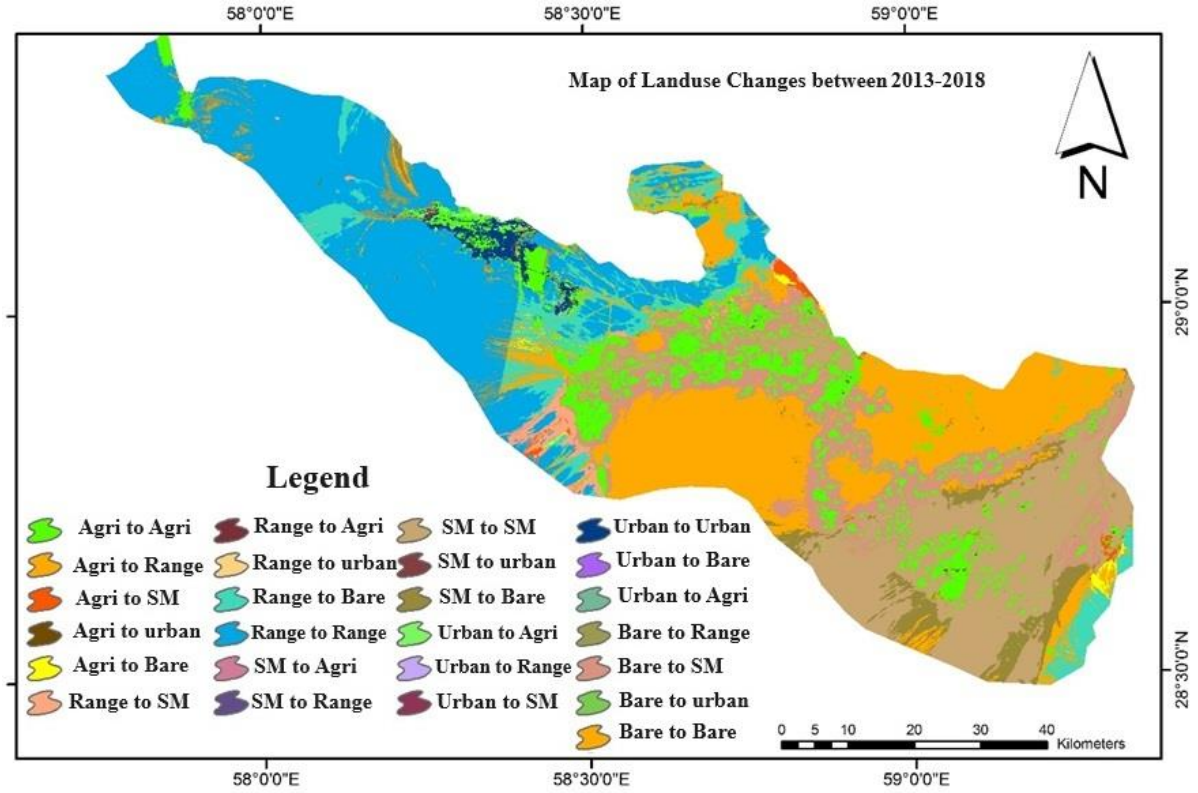

Figure 7. Map of Land use changes between 2013-2018

Land use changes predominantly involve agricultural and range land, which are decreasing in trend. Conversely, changes in bare, saline, and urban areas are increasing. Over the 15-year study period, 131 square kilometers of agricultural land changed, with the most significant changes occurring in the initial period. Overall, the majority of agricultural land changes involve the transformation of these lands into barren and salty lands. In

the initial period, the majority of land use change occurred in range land, with 5% of its total area transforming into bare land. Subsequently, more range land became bare, resulting in a total change of nearly 17% over three periods. The investigation suggests that the changes in range and agricultural lands are due to irresponsible land use practices in the region. The majority of bare lands have been transformed into salty lands, with approximately 23% of the bare lands of the region now being salty.

Table 5. The results of land use change detection in the studied time periods

	Abbreviation signs in Figures 5-7	Land use changes between 2003-2008		Land use changes between 2008-2013		Land use changes between 2013-2018	
		Area ($Km^{2)}$	Area (%)	Area ($Km^{2)}$	Area (%)	Area ($Km^{2)}$	Area (%)
Agriculture to Agriculture	Agri to Agri	519.5165	10.37	417.2871	8.33	495.9823	9.89
Agriculture to Bare	Agri to Bare	36.3884	0.72	157.7443	3.149	20.789	0.41
Agriculture to Range	Agri to Range	5.7236	0.114	11.6768	0.23	11.8249	0.23
Agriculture to Salty lands	Agri to SM	95.8575	1.913	28.9984	0.57	23.3024	0.46
Agriculture to urban	Agri to urban	3.8518	0.076	7.0084	0.139	1.1842	0.023
Bare to Agriculture	Bare to Agri	78.3657	1.56	50.2944	1.0041	14.5967	0.29
Bare to Bare	Bare to Bare	1218.7605	24.333	1114.8652	22.258	1176.3436	23.47
Bare to Range	Bare to Range	224.3512	4.47	133.8194	2.671	68.1544	1.36
Bare to Salty lands	Bare to SM	461.7773	9.219	206.602	4.124	529.6474	10.57
Bare to urban	Bare to urban	3.618	0.072	10.3219	0.206	6.7973	0.135
Range to Agriculture	Range to Agri	24.2581	0.484	52.9098	1.0563	3.2844	0.065
Range to Bare	Range to Bare	255.7302	5.105	248.3279	4.957	332.584	6.63
Range to Range	Range to Range	1512.7309	30.203	1428.619	28.522	1187.8403	23.70
Range to Salty lands	Range to SM	17.7987	0.355	6.7718	0.135	59.4998	1.18
Range to urban	Range to urban	0.7944	0.0158	7.2862	0.145	1.2736	0.025
Salty lands to Agriculture	SM to Agri	0.0695	0.0013	30.8569	0.616	4.5639	0.091
Salty lands to Bare	SM to Bare	4.855	0.0969	273.9336	5.469	168.9238	3.37
Salty lands to Range	SM to Range	0.9023	0.0180	9.6894	0.193	0.6725	0.0134
Salty lands to Salty lands	SM to SM	509.3736	10.170	764.7601	15.26	828.7074	16.53
Salty lands to urban	SM to urban	0.0148	0.00029	5.5517	0.110	4.3913	0.087
Urban to Agriculture	Urban to Agri	0.4504	0.0089	1.383	0.0276	13.9618	0.278
Urban to Bare	Urban to Bare	0.1504	0.0030	0.0303	0.00060	0.1875	0.0037
Urban to Range	Urban to Range	0.0674	0.00134	0.0052	0.00010	0.1764	0.0035
Urban to Salty lands	Urban to SM	0.021	0.00041	0.0068	0.00013	0.0108	0.00021
Urban to Urban	Urban to Urban	33.0506	0.659	39.9201	0.7970	55.7984	1.113

4. Conclusion

In this research, satellite images of Landsat 5, 7, and 8 were used in the study area between 2003 and 2018 to investigate land use changes in the Bam Plain. First, the pre-processing of satellite images, including geometric, radiometric, and atmospheric corrections was achieved. Then land use maps were prepared in four time periods 2003, 2008, 2013, and 2018. For this purpose, 5 classes including agriculture, range, urban, salty land, and bare were considered. So, supervised classification methods of maximum likelihood, neural network, and support vector machine were used to extract land use Maps in 2018. The results of calculating the total accuracy, kappa coefficient, producer, and user accuracy of the prepared land use maps showed that the maximum likelihood method (MLC) has a good accuracy for determining land use in the region. Therefore, the maps of other considered years were also extracted by the maximum likelihood method and then the change maps were prepared for three periods 2003-2008, 2008-2013, and 2013-2018. The most changes are related to agricultural and range lands in this area. The trend of changes in agriculture and range is decreasing, and the trend of changes in bare, saline, and urban lands is increasing. Over the 15-year study period, 131 Km^2 of agricultural lands have been changed in use. The most change of range land was to bare land and the most change of bare land was to salty land.

References

Akbari, E., Zangane Asadi, M. A., & Taghavi, E. (2016). Change detection land use and land cover regional neyshabour using Different methods of statistical training theory. *Geographical Planning of Space Quarterly Journal*, *6*(20), 35-50.

Alizadeh, M., Mirzaei, R. A. & Kia, S. H. (2015). A comparative study of multiple classification methods to prepare land use map (case study: watershed of Ken and Karaj rivers). *Geography and Sustainability*, *6*(20), 103-89.

Arekhi, S. (2014). Prediction of spatial land use changes based on LCM in a GIS environment (A case study of Sarabeleh (Ilam), Iran. *Iranian Journal of Forests and Rangelands Protection Research*, *12*(1), 1-19.

Arulbalaji, P., & Gurugnanam, B. (2014). Geospatial Science for 16 Years of Variation in Land Use/Land Cover Practice Assessment around Salem District, South India. *Journal of Geosciences and Geomatics*, *2*(1), 17-20**.**

Bonyad, A., & Hajyghaderi., T. (2008). Inventorying and Mapping of Natural Forest Stands of Zanjan Province Using Landsat ETM+ Image Data. *Journal of Water*

and Soil Science, *11*(42), 627-638. **doi: 20.1001.1.24763594.1386.11.42.51.5**

Coppin, P. I., Jonckheere, K., Nackaerts, M. B. (2004). Digital change detection methods in ecosystem monitoring: a review. *Remote Sensing*, *25* (9), 1565–1596. **doi: 10.1080/0143116031000101675**

Fan, F., Wang, Y., & Wang, Z. (2008). Temporal and spatial change detecting (1998–2003) and predicting of land use and land cover in Core corridor of Pearl River Delta (China) by using TM and ETM^+ images. *Environmental Monitoring and Assessment*, *137*(1), 127-147. **doi: 10.1007/s10661-007-9734-y**

Fatemi, S. B., & Rezaei, Y. (2016). Basics of Remote Sensing. Azadeh Publications, 350 pp.

Galdavi, S., Mohammadzadeh, M., Salmanmahiny, A., & Najafi Nejad, A. (2013). Urban change detection using multi-temporal remotely sensed imagery (Case study: Gorgan Area, Northern Iran). *Environment and Urbanization Asia*, *4*(2), 339-348. **doi: 10.1177/0975425313511161**

Galdavi, S., Mohammadzadeh, M., Salmanmahiny, A., & Najafi Nejad, A. (2024). Monitoring and modeling forest land changes in Gorgan region using Geomod model. *Environmental Science and Technology*, *25*(10), 1-16. **doi: 10.30495/jest.2023.75920.5927**

Galdavi, S., Mohammadzadeh, M., Salmanmahiny, A., Najafi Nejad, A. (2015). Predicting of Urban Growth Pattern Using Logistic Regression Model in Gorgan Area. *Town and Country Planning*, *7*(1), 96-117. **doi: 10.22059/jtcp.2015.54783**

Gao, J., Liu, Y., & Chen, Y. (2006). Land cover changes during agrarian restructuring in Northeast China. *Applied Geography*, *26*, 312–322. **doi: 10.1016/j.apgeog.2006.09.001**

Hussain, M., Chena, D., Chenga, A., Weib, H., & Stanley, D. (2013). Change detection from remotely sensed images: From pixel-based to object-based approaches. *ISPRS Journal of Photogrammetry and Remote Sensing*, *18*, 283–292. **doi: 10.1016/j.isprsjprs.2013.03.006**

Jabbar, M.T., & Zhou, X. (2011). Eco-environmental change detection by using remote sensing and GIS techniques: a case study Basrah province, south part of Iraq. *Environmental Earth Sciences*, *64*(5), 1397-1407. **doi:10.1007/s12665-011-0964-5**

Jensen, J. R. (2004). Digital change detection: Introductory digital image processing: A remote sensing perspective, Prentice-Hall, New Jersey. 505-512.

Lefsky, M. A., & Cohen, W. B. (2003). Selection of remotely sensed data. In M. A ulder and S. E Franklin (Eds), Remote Sensing of Forest Environments: Concepts and case studies. *Boston: Kluwer Academic Publishers*, 13 – 46. **doi: 10.1007/978-1-4615-0306-4_2**

Longley, P. A., Goodchild, M., Maguire, D. J., & Rhind, D. W. (2010). Geographic Information Systems and Science. 3rd Edition, *England: Wiley*, 560 pp.

Madhura, M., & Venkatachalam, S. (2015). Comparison of Supervised Classification Methods on Remote Sensed Satellite Data: An Application in South India. *International Journal of Science and Research*, *4*(2), 1407-1411.

Madurapperuma, B., Rozario, P., Oduor, P., & Kotchman, L. (2015). Land-use and land-cover change detection in Pipestem Creek watershed, North Dakota. *International Journal of Geomatics and Geosciences*, *5*(3), 416-426.

Morgan, R. S., Rahim, L. S., & El-Hady, M. (2015). A Comparison of Classification Techniques for the Land Use/ Land Cover Classification. *Global Advanced Research Journal of Agricultural Science (GARJAS)*, *4*(11), 810-818.

Ramezani, N., Jafari, R., & Izanello, A. (2018). Investigation of land use changes in the city of Esfarayen (North Khorasan) in the last 4 decades. *Iranian Journal of Remote Sensing and GIS*. *3*(2), 19-37.

Salman Mahiny, A. R., & Kamyab, H. R. (2010). Remote sensing and applied geographic information systems with Idrisi software. *Mehramhadis Publications*. 610 pp

Shayesteh, K., Abedian, S., & Galdavi, S. (2018). Urban expansion modeling using Logistic regression method based on Geomod model (Case study: Kordkuy city). *Geography and Development*, 16 (51), 43-64. **doi:10.22111/gdij.2018.3875**

Singh, A. (1989). Digital Change Detection Techniques Using Remotely Sensed Data. *International Journal of Remote Sensing*, *10*(6), 989-1003. **doi: 10.1080/01431168908903939**

Sonneveld, B. D. J. S. (2003). Formalizing expert judgments in land degradation assessment: A case study for Ethiopia. *Land Degradation & Development*, *14*, 347–361. **doi: 10.1002/ldr.564**

Yousefi, S., Moradi, H. R., Hosseini, S. H., & Mirzaee, S. (2011). *Journal of Applied RS & GIS Techniques in Natural Resource Science*, *2* (3), 97-105.

Zhang, C., & Li, X. (2022). Land Use and Land Cover Mapping in the Era of Big Data. *Land. 11*, 1692. **doi: 10.3390/land11101692**

Agriculture, Environment & Society

Journal homepage: www.aes.uoz.ac.ir

Evaluation of the effect of foliar zinc sulfate application on quality characteristics, yield, and yield components of barley cultivars under irrigation water salinity conditions

Amir Kazemi Arpanahi [a], Mehrdad Mahlooji [*b,c], Seyed Keyvan Marashi [c], Mani Mojaddam[c], Tayeb Saki nejad [c]

[a] Ph. D. student, Department of Agronomy, Ahvaz branch, Islamic Azad University, Ahvaz, Iran
[b] Horticulture Crops Research Department, Isfahan Agricultural and Natural Resources Research and Education Center, AREEO, Isfahan, Iran
[c] Department of Agronomy, Ahvaz branch, Islamic Azad University, Ahvaz, Iran

ARTICLE INFO

Article history:
Received: 3 October 2024
Accepted: 27 November 2024
Available online: 1 December 2024

Keywords:
Harvest index
Leaf chlorophyll
Leaf proline
Micronutrients

ABSTRACT

In order to evaluate the effect of zinc sulfate fertilizer on quality characteristics, yield and yield components of barley cultivars under irrigation water salinity (salinity over 6 dS/m), this research was conducted as split-plots in randomized complete blocks design with three replicates in Kabutarabad Agricultural Research Station in Isfahan. Foliar application of zinc sulfate concentration at three levels (0, 0.5 and 1%) was considered as main factor and three cultivars of Armaghan (stress sensitivity), Goharan (drought tolerant), and Mehr (salinity tolerant) were considered as sub-factors. The results demonstrated that foliar application of zinc sulfate at concentration of 1% significantly increased the chlorophyll b content by 14.8% compared to a lower concentration (0.5%). The highest chlorophyll a content (1.85 mg/g), leaf content (45.9 mg/kg), and grains/spike (37.2) with foliar application of 1% zinc sulfate was observed in Mehr cultivar. Given foliar application of 1% zinc sulfate, Mehr and Goharan cultivars had 21.3% and 15.3% higher leaf proline than Armaghan cultivar, respectively. Foliar application of zinc sulfate at concentration of 1% in Mehr, Goharan, and Armaghan cultivars significantly increased grain yield by 22.2%, 25.7% and 29.0%, respectively, compared to the non-foliar application of sulfate fertilizer. Generally, the results of the present study suggested that under irrigation water salinity conditions, Mehr cultivar is superior to Goharan and Armaghan cultivars in response to foliar application of zinc sulfate and the photosynthetic pigments produced higher yield and yield components.

Highlights

- Foliar 1% zinc sulfate boosts barley yield by 22-29% under saline conditions.
- Mehr cultivar excels with higher chlorophyll and yield with zinc sulfate.
- Zinc sulfate at 1% increases chlorophyll b by 14.8% vs. 0.5% concentration.
- Mehr and Goharan show 21.3% and 15.3% more proline than Armaghan with zinc.

1. Introduction

Barley, scientifically known as *Hordeum vulgare* L, is an annual grass (belonging to the Gramineae) is the fourth most important cereal after wheat, rice, and corn. Barley needs a less fertile soil than wheat and is more adaptable to different types of soils. It is more salinity tolerant than other cereals, however, some varieties of bread wheat (such as: Narin, Barzegar, …) and durum wheat (Mahan, Sana,…) are more tolerant. The soil should not be drowned and its sandy or acidity should not be lower than 6% (barley is sensitive to acidic soil conditions). Nearly half of the cultivated barley is used as livestock feed. The grains are usually mixed with other foods to produce livestock feed (Winch, 2009). Soil nutrient deficiency, leaching, and drought are the most important factors to reduce barley yield (Tigre et al., 2014).

* Corresponding author.
E-mail address: mmahlooji2000@yahoo.com
https://doi.org/10.22034/aes.2025.492027.1090

Foliar application is another way for rapid supply of nutrients for plants. In this method, nutrients are directly available to air organs and fruit. Given the various effective factors on soil absorption of nutrients, foliar application is an effective method in correcting plant nutrition disorders (Khan et al., 2003). Foliar nutrition is a method to reduce the stability of chemical fertilizers in the soil and as a result decrease environmental hazards, including soil and water contamination, and provides nutrients to the plant in a controlled manner (Kannan, 2010). Nowadays, in addition to macronutrients, micronutrients are also taken into consideration as an important tool to achieve maximum yield per unit area (Mosavi et al., 2007).

Zinc is an essential micronutrient involved in the activity of various enzymes. Carbonic anhydrase, which catalyzes the reversible conversion of carbon dioxide and water to carbonic acid, contains zinc element and needs zinc for activity (Weisany et al., 2012). Zinc plays a role in protein metabolism, gene expression, structural and functional integrity of biological membranes, and photosynthetic carbon metabolism. Zinc is involved in regulating the opening of stomata given its role in keeping membrane integrity. In zinc deficiency, K+ content of stomatal guard cells is reduced (Tester and Davenport, 2003).

Continuous cultivation, annual overuse of phosphorus fertilizers, leaching and other conditions of calcareous soils, including large amounts of calcium carbonate, Alkaline pH, and not using micronutrient-containing and organic fertilizers reduces the storage of this element in the soil and thus its yield (Seyed Sharifi et al., 2015). Zinc deficiency could not be entirely and definitively solved through consuming zinc-containing fertilizers in cases of subsoil constraints, surface soil dryness, and diseases. Therefore, using efficient genotypes for zinc uptake could be an effective and sustainable solution for further production of crops under zinc deficiency conditions (Sadeghzadeh, 2013). Durable and efficient genotypes in absorbing and using zinc can be considered as a complement for soil use and foliar application of zinc, particularly when farmers are not aware of zinc deficiency in their field soil or do not have access to zinc fertilizer. In addition to reducing the use of chemical fertilizers, applying cultivars with high efficiency of zinc element could increase the quantity and quality of the product with the minimum amount of available zinc (Sadeghzadeh and Rengel, 2011).

Salinity of water and soil resources is one of the most important agricultural issues in Iran. Under salinity conditions, the provision of nutrients in the soil solution is reduced due to the high concentration of chlorine, sodium, and also calcium ions and leads to eating disorder and imbalance of plant nutrients. Therefore, the role of proper nutrition is highly important under these conditions to ensure the proper growth and increase plant yield while maintaining the balance of nutrients (Ahmadi et al., 2006). Zinc is one of the most effective micronutrients for plants grown in calcareous, saline, and sodium soils at high pH. Today, treatments that can be used to grow plants in saline soils is of great interest to many researchers. Zinc is one of the significant elements in reducing salinity stress and toxic effects of sodium and chlorine in plants (Vojodi Mehrabani et al., 2018). Therefore, in this regard, this research was conducted with an aim of investigating the foliar application of zinc sulfate fertilizer on morphophysiological properties, yield, and yield components of barley under saline irrigation conditions and also determining the most appropriate cultivar.

2. Materials and methods

This experiment was conducted in a split-plot design with three replications at Kabutarabad Agricultural Research Station in Isfahan (51º40'N, 32º93'E), and an altitude of 1541 meters above sea level with very hot dry climate, arid summers, and semi-cold winters in accordance to Koppen classification. Mean annual precipitation and temperature were 122 mm and 16.1°C, respectively, at the experimental site. Some physicochemical properties of the test site soil are presented in Table 1.

Table 1. Some physical and chemical properties of field soil

Clay	Silt	Sand	O.C	pH	EC	Absorbable phosphorus P (available)	Absorbable potassium K (available)	Absorbable copper Cu (available)	Absorbable zinc Zn (available)	Absorbable manganese Mn (available)	Absorbable iron Fe (available)	Absorbable boron B (available)
%					dS/m	mg/kg						
38	46	16	0.95	7.1	13.2	11.5	304	0.76	0.30	7.64	1.22	1.68

Three foliar application of zinc sulfate concentration [control (0%), 0.5% (2 kg/ha of zinc sulfate or equivalent to 659 g/ha of zinc) and 1% (4 kg/ha of zinc sulfate or equivalent to 1319 g/ha of zinc)] were the main plots, and the barley (*Hordeum vulgare* L.) cultivars [Armaghan (stress-sensitive), Goharan (drought-tolerant), and Mehr (salt-tolerant)] were the subplots. Some physicochemical characteristics of the soil and irrigation water quality are shown in Table.1. Mean annual precipitation and temperature were 122 mm and 16.1°C, respectively, at the experimental site. Seeds were sown with the density rate of 450 seeds m^{-2} on 5 November by a cereal row planting machine (Wintersteiger Plotman, Austria). Each subplot consisted of six rows, 6 m in length, and was spaced 20 cm apart. To irrigate the plots, water was delivered a local well (with water salinity over 6 dS/m). Foliar application of zinc sulfate was conducted at tillering stage with an interval of 7 days and in 3 turns.

2.1. Proline content

Three flag leaves were randomly sampled from each testing unit and the proline content was measured by Bates (1973) technique. In this method, 400 mg of fresh leaf of the plant previously stored at -20 ° C was transferred to a

mortar and pounded by adding 10 ml of 3% sulfosalicylic acid. Then, the resulting solution was passed through a filter paper and 2 ml of the filtered solution, 2 ml of ninhydrin solution, and 2 ml of acetic acid solution were poured into a test tube. The solution was stirred and kept in water bath at temperature of 90 ° C for 1 h. Solution-containing tubes were immediately placed on ice to stop the reaction and then 4 ml of toluene was added to the solution and stirred for 15 to 20 s. After being stirred, a two-phase solution was formed and the upper phase contained proline. Toluene solution was used to calibrate the spectrophotometer. After calibration, the samples were read at wavelength of 520 nm. Proline content obtained during this method was obtained based on micromoles of proline per gram of fresh leaf (Bates, 1973).

2.2. Chlorophyll a and b content

The concentrations of chlorophyll a, chlorophyll b and totalchlorophyll were calculated using the following equation (Arnon, 1949):

Total Chlorophyll: $20.2(A_{645}) + 8.02(A_{663})$, Chlorophyll a: $12.7(A_{663}) - 2.69(A_{645})$, Chlorophyll b: $22.9(A_{645}) - 4.68(A_{663})$

2.3. Agronomy measurement and statistical analysis

In order to determine plant height, spike length, grains/spike, 1000-grain weight, biological and grain yield, a number of 10 plants were randomly harvested from plants in testing plot and weighed by a scale with a precision of 0.01 g. Harvest index was also obtained from dividing grain yield by biological yield. Eventually, the data were analyzed using MSTATC after being collected and the means were compared with LSD test at a probability level of 5%. Trait correlation coefficients were also estimated by SPSS software.

3. Results and discussion

3.1. Chlorophyll a

Results of analysis of variance on data indicated that in addition to the main effects of zinc sulfate and cultivar, the interaction of these factors on chlorophyll a was also significant at probability level of 1% (Table 2). Results of comparing the means demonstrated that the highest chlorophyll a content (1.85 mg/g) was observed with foliar application of 1% zinc sulfate in Mehr cultivar, which was significantly different from all treatments (Table 3). This result could be attributed to the superiority of Mehr cultivar under salinity conditions and also to the positive effect of zinc element in improving growth and consequently increasing photosynthetic pigments of the plant. Foliar application of 1% zinc sulfate in Mehr cultivar significantly increased chlorophyll a by 46.8% compared to the control (no foliar application). Under 1% zinc sulfate conditions, Mehr cultivar had 9.4% and 16.3% higher chlorophyll a than Goharan and Armaghan cultivars, respectively. The results of the interaction of the factors indicated that the lowest chlorophyll a content (0.64 mg/g) belonged to Armaghan cultivar and under zinc sulfate fertilizer conditions (Table 3). In this regard, the results of research showed that zinc sulfate uptake increased chlorophyll a, so that foliar application of the largest amount of this substance (1%) increased the aforementioned trait by 22.88% compared to the control (Fallah, 2019). Foliar application of zinc sulfate increased the chlorophyll a content in both safflower cultivars and the lowest chlorophyll a content in both cultivars was observed in the control treatment (Moradi Telavat et al., 2015). In another study, the results indicated that foliar application of zinc sulfate increased the chlorophyll a content in safflower compared to the control treatment (Jamshidi et al., 2017). Zinc synthesis the chlorophyll via protecting the sulfhydryl group. Porphobilinogen is a chlorophyll precursor that is required for forming magnesium and zinc (Cakmak, 2000).

Trait correlation results showed that chlorophyll a content is positively and significantly correlated (0.92**) with grain yield (Table 4). In this regard, the results demonstrated that cantaloupe leaf chlorophyll had a positive and high correlation of 87% with plant yield (Nasiri Dehsorkhi et al., 2020). In a research carried out to investigate the effects of foliar application of zinc sulfate on the mung bean growth and yield under water stress, the results of correlation showed that chlorophyll a and b are positively and significantly related to biological and grain yield (Makarian et al., 2017).

Table 2. Analysis of variance of studied traits in barley cultivars affected by foliar application of zinc sulfate

Source of variation (SOV)	Degrees of freedom (df)	Mean squares (MS)					
		Chlorophyll a	Chlorophyll b	Proline content	Zinc content	Plant height	Spike length
Replication	2	0.31**	0.09ns	8361.48**	29.07ns	4.54ns	0.47ns
Zinc sulfate	2	1.37**	2.05**	12371.7**	397.66**	505.28**	0.10ns
Error (a)	4	0.007	0.01	62.75	4.47	5.35	0.89
Cultivar	2	0.38**	0.17**	2243.51**	30.97**	28.29ns	0.19ns
Zinc sulfate × cultivar	4	0.02**	0.02ns	416.46**	9.62**	6.61ns	0.58ns
Error (b)	12	0.005	0.009	65.37	1.32	8.50	0.23
Coefficient of variation C.V (%)	-	5.10	8.43	3.97	3.23	4.36	10.08

ns, * and ** represent the insignificance and significance at probability levels of 5% and 1%, respectively

Table 2 Continued.

Source of variation (SOV)	Degrees of freedom (df)	Mean squares (MS)					
		1000-grain weight	Grains/spike	Spikes/m^2	Biological yield	Grain yield	Harvest index
Replication	2	17.22ns	5.55ns	2446.17ns	1504331.2**	197428.9ns	0.11ns
Zinc sulfate	2	66.65ns	167.77**	29412.8**	3489440.2**	3378907.2**	61.29*
Error (a)	4	14.97	5.15	597.14	56298.5	41655.4	3.41
Cultivar	2	21.73ns	26.64**	3484.24**	183636.4*	586173.1**	34.99**
Zinc sulfate × cultivar	4	18.06ns	3.09*	788.74*	126331.1*	51030.2*	4.76*
Error (b)	12	6.99	0.94	234.33	36113.9	15325.6	0.88
Coefficient of variation C.V (%)	-	7.43	3.05	3.05	1.24	2.29	2.67

ns, * and ** represent the insignificance and significance at probability levels of 5% and 1%, respectively.

3.2. Chlorophyll b

Results of analysis of variance showed that foliar application of zinc sulfate significantly affect the chlorophyll b content (probability level of 1%) (Table 2). Results demonstrated that chlorophyll b is also increased with increasing levels of zinc fertilizer, so that the highest level of aforementioned trait was observed in foliar application of 1% zinc sulfate. The lowest chlorophyll b content (0.56 mg/g) was observed in the control treatment (no foliar application of zinc sulfate). Foliar application of zinc sulfate at a concentration of 1% significantly increased the chlorophyll b content by 14.8% compared to a lower concentration (0.5%) (Figure 1).

In this regard, the results of research showed that cantaloupe leaf chlorophyll is also increased with increasing levels of zinc fertilizer, so that the highest leaf chlorophyll was obtained from foliar application of 4 g/L zinc sulfate under weeding conditions (Nasiri Dehsorkhi et al., 2020). Hydrolytic activity of cellular organelles such as chloroplasts, mitochondria, cytoplasm. and apoplastic space depend on the presence of zinc (Hellubust and Caraigie, 1978).

Table 3. Results of interaction of zinc sulfate and barley cultivars on studied traits

Levels of zinc sulfat (%)	Cultivars	Traits							
		Chlorophyll a (mg.g^{-1} FW)	Proline content (µg.g^{-1} FW)	Zinc content (mg/kg)	Grains/spike	Spike/m^2	Biological yield (kg/ha)	Grain yield (kg/ha)	Harvest index (%)
0	Armaghan	0.64f	164.5e	27.5e	24.2f	415.7f	14699.9de	4530.5f	30.8e
	Goharan	0.91e	165.4e	28.5e	27.5e	422.4f	14677.8de	4764.0e	32.4e
	Mehr	1.26cd	171.3de	29.1e	29.8d	482.0e	14656.7e	5003.3d	34.1d
0.5	Armaghan	1.24d	183.5d	36.0d	31.8c	501.7de	15701.1bc	5078.6d	32.3e
	Goharan	1.38c	199.0c	36.8cd	32.2c	516.8cd	15393.2c	5508.1c	35.7cd
	Mehr	1.59b	225.5b	37.9cd	34.0b	524.3cd	15012.0d	5865.2b	39.0a
1	Armaghan	1.59b	214.9b	38.5bc	34.7b	535.4bc	15851.9ab	5847.4b	36.9c
	Goharan	1.69b	247.9a	40.0b	35.2b	558.3ab	16104.5a	5989.0ab	37.2bc
	Mehr	1.85a	260.8a	45.9a	37.2a	563.5a	15806.3ab	6118.5a	38.7ab

Based on the LSD test, means with common letter in each column are not significantly different at the probability level of 5%.

Table 4. Correlation coefficients between the studied barley traits

	1	2	3	4	5	6	7	8	9	10	11	12
1- Chlorophyll a	1											
2- Chlorophyll b	0.86**	1										
3- Proline content	0.88**	0.81**	1									
4- Zinc content	0.70**	0.85**	0.58**	1								
5- Plant height	0.62**	0.72**	0.58**	0.71**	1							
6- Spike length	-0.22ns	-0.10ns	-0.22ns	0ns	-0.06ns	1						
7- 1000-grain weight	-0.68**	-0.57**	-0.60**	-0.43*	-0.41*	-0.22ns	1					
8- Grains/spike	0.84**	0.85**	0.67**	0.86**	0.69**	-0.15ns	-0.58**	1				
9- Spikes/m^2	0.73**	0.80**	0.54**	0.89**	0.65**	-0.12ns	-0.45*	0.85**	1			
10- Biological yield	0.75**	0.74**	0.80**	0.53**	0.69**	-0.22ns	-0.42*	0.60**	0.52**	1		
11- Grain yield	0.92**	0.90**	0.83**	0.80**	0.72**	-0.11ns	-0.65**	0.88**	0.78**	0.67**	1	
12- Harvest index	0.80**	0.78**	0.66**	0.75**	0.56**	-0.03ns	-0.62**	0.82**	0.73**	0.36ns	0.93**	1

ns, * and ** represent the insignificance and significance at probability levels of 5% and 1%, respectively.

According to the results of analysis of variance, barley cultivars also suggested a significant impact ($p \leq 0.01$) on chlorophyll b content of plant leaf (Table 2). The highest (1.21 mg/g) and lowest (0.95 mg/g) chlorophyll b content was found in Mehr and Armaghan cultivars, respectively. However, Mehr and Goharan cultivars were in a statistical group in terms of significance level. Chlorophyll b content in Mehr and Goharan cultivars was 27.3% and 21.0% higher than Armaghan cultivar, respectively (Figure 1). In this regard, the research results suggested that by approaching the final stages of growth, the salinity tolerant genotype of barley showed a higher chlorophyll number,

while semi-susceptible genotypes of Morocco and Nosrat were reduced by 7.02 and 5.91, respectively (Mahlooji, 2017). Researchers have said that chlorophyll is less degraded in salinity-tolerant cultivars (Kumar Parida and Bandhu Das, 2005).

Trait correlation study (Table 4) showed that chlorophyll b content was positively and significantly correlated with zinc content in the leaf at the level of 1% (0.85 **). In this regard, results of research showed that zinc content in grape leaf was positively correlated with fruit yield, chlorophyll a at the level of 5%, chlorophyll b, and total chlorophyll at the level of 1% (Vatankhah et al., 2016). Chlorophyll biosynthesis needs zinc element, and while preventing chlorophyll degradation, it increases chlorophyll a and b by producing indole acetic acid, which results in increasing photosynthesis and grain yield (Hemantaranjan and Grag, 1988).

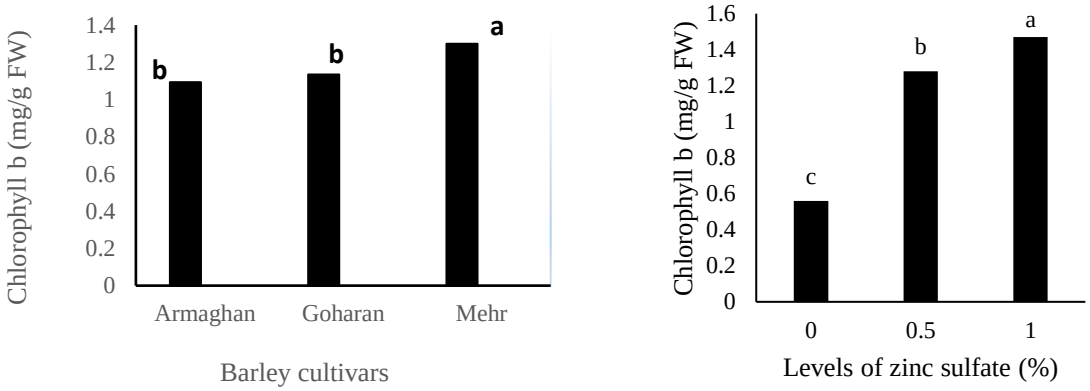

Figure 1. Comparing the means of chlorophyll b content affected by foliar application of zinc sulfate (Right) and barley cultivars (Left)

3.3. Proline leaf

Results of analysis of variance (Table 2) indicated that the main effects of fertilizer, cultivar, and also interaction of these two factors on leaf proline content were significant at the probability level of 1%. Results of the interaction of the studied factors showed that the highest leaf proline content (260.8 µg/g) is belonged to Mehr cultivar with foliar application of 1% zinc sulfate, however, as shown in Table 3, Mehr and Goharan cultivars are in a statistical group. At foliar application of 1% zinc sulfate, Mehr and Goharan cultivars had 21.3% and 15.3% higher leaf proline content than Armaghan cultivar, respectively. (Table 3). In this regard, the research results showed that the difference between barley cultivars for flag leaf proline content was significant at probability level of 1% and leaf proline content in salinity tolerant and semi-tolerant cultivars was higher than semi-salinity sensitive cultivar (Mahlooji, 2017). The researchers said that barley cultivars with high Fv/Fm ratios and the highest potential for proline production under stress conditions could have lower yield reduction (Mamnoei and Seyed Sharifi, 2010).

Results of the present research indicated that the lowest leaf proline content was observed in absence of zinc sulfate fertilizer, and with foliar application of zinc fertilizer, in particular at higher concentration (1%), leaf proline content in all three cultivars was significantly increased. Foliar application of 1% zinc sulfate in Mehr, Goharan and Armaghan cultivars significantly increased leaf proline content by 52.2%, 49.8% and 30.6%, respectively, compared to no foliar application of zinc fertilizer (Table 3).

Increasing proline content in the plants under salinity stress is in fact a reaction of the plant to dehydration in the root environment. Proline helps to regulate osmosis during stress and retain the basic structure of macromolecules and membranes during increased dehydration. In addition to osmotic regulation, proline has other tasks such as protecting plasma membranes and eliminating hydroxyl and reactive oxygen radicals (Sun et al., 2013). On the one hand, using zinc element with impact on production of osmolytes such as proline leads to a discount on stress effects, and on the other hand, indirect prevention of degradation of chlorophyll leads to continued growth and optimal distribution of osmolytes in the plant (Abbasi and Shekari, 2016). Results of the research demonstrated that highest proline content was obtained in the severe stress treatment with foliar application of 1% zinc sulfate (Fallah, 2019). In a research conducted to investigate the foliar application of zinc element on mung bean under drought stress conditions, the results showed that foliar application with 10 g zinc nano-oxide had the greatest impact on leaf proline content by 32% increase compared to the control (Makarian et al., 2017).

3.4. Leaf zinc content

Results of analysis of variance demonstrated that in addition to the main effects of the studied factors (fertilizer and cultivar), the interaction was also significant at probability level of 1% on the leaf zinc content (Table 2). Results showed that in the absence of zinc fertilizer, there was no significant difference between cultivars in terms of leaf zinc content and all three cultivars were in a statistical group. However, leaf zinc content was significantly increased with foliar application of zinc sulfate, in particular at higher concentrations (1%). Foliar application of 1% zinc sulfate in Mehr, Goharan and Armaghan cultivars increased the leaf zinc content by 57.7%, 40.3% and 0.40%, respectively, compared to the absence of fertilizer (Table 3). Increasing zinc concentration in leaf is due to direct effect of foliar application of this element,

which is easily absorbed by leaf (Vatankhah et al., 2016). Results of a research showed an increasing trend with increasing concentration of zinc sulfate fertilizers and zinc nanoclates of zinc concentration in Abujahl watermelon leaf (Nikbakht et al., 2021). In another research, the highest concentration of zinc in grape leaf (49.1 mg/kg) was obtained from foliar application of 0.2% zinc sulfate, which was significantly different from the control treatment (Vatankhah et al., 2016). In a research conducted to investigate the effect of zinc fertilizer on grain corn under salinity stress, the results showed that the highest use of zinc increased the zinc and potassium in plant air organs by 27.7% and 5%, respectively, compared to the absence of zinc (Karmollachaab and Gharineh, 2013).

Results of the present research showed that the highest leaf zinc content was observed with foliar application of 1% zinc sulfate, which was significantly different from all treatments. In foliar application of 1% zinc sulfate, Mehr cultivar had 14.7% and 19.2% higher leaf zinc content than Goharan and Armaghan cultivars, respectively (Table 3). In studying the effect of irrigation water salinity and foliar application of zinc fertilizer on barley genotypes, the results indicated that reaction of barley cultivars to zinc element in air organs was significant at the probability level of 1%, so that the highest concentration of zinc element was observed in the four-salt genotype (salinity tolerant) (Mahlooji, 2017). Results of correlation showed that leaf zinc content had a positive and significant correlation with grain yield (0.80**) at probability level of 1% (Table 4). In this regard, researchers said that adding zinc fertilizer under salinity conditions might lead to further growth and increased wheat yield by improving the nutrient status in plants and reducing the effects of salinity (Ahmadi et al., 2006). In a research conducted to investigate the effect of humic acid and zinc sulfate on fruit yield and concentration of elements in grape leaf, the results showed that grape leaf zinc content had a positive correlation with fruit yield at the level of 5% (Vatankhah et al., 2016).

3.5. Plant height

Results showed that among the sources of variation, merely the foliar application of zinc sulfate could affect the plant height at probability level of 1% and the cultivar factor as well as fertilizer and cultivar interaction had no significant effect on this trait (Table 2). Results of comparing the mean levels of zinc fertilizer showed that the highest (74.8 cm) and lowest (0.60 cm) plant height were related to 1% zinc fertilizer and control (no fertilizer), respectively (Figure 2). Foliar application of zinc sulfate at concentration of 1 and 0.5% significantly increased the plant height by 24.6% and 9.3%, respectively, compared to the control. Plant height with foliar application of 1% zinc sulfate also showed a 14% increase compared to 0.5% (Figure 2).

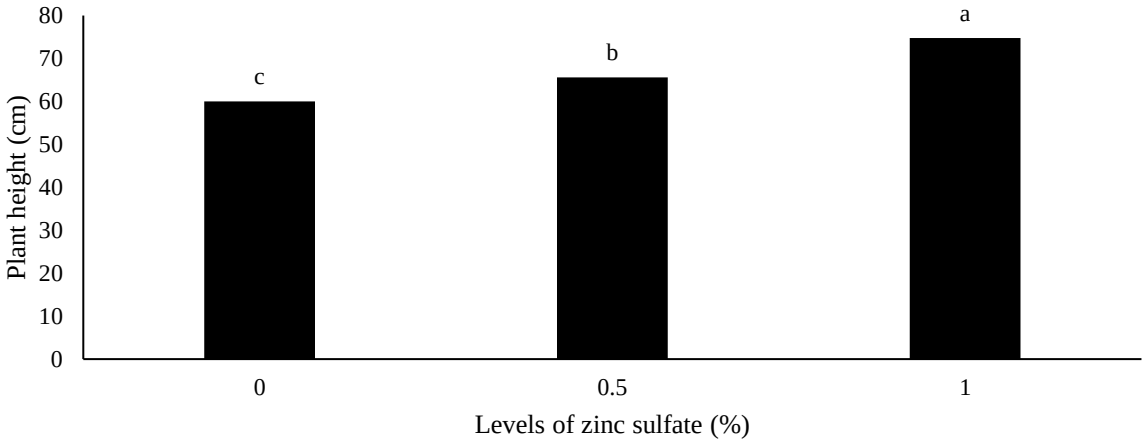

Figure 2. Comparing the means of plant height affected by foliar application of zinc sulfate

Zinc element plays a basic role in the growth, height, and yield of crops as well as in the synthesis of the hormone auxin, nitrogen metabolism processes, and the activity of enzymes. Effect of zinc application in increasing plant height could be mostly associated with effect of this factor on synthesis of tryptophan as a constituent of indole acetic acid (IAA) or plant growth hormone (Brennan, 2007). Research results demonstrated that the highest wheat height was observed at foliar application of zinc sulfate at a concentration of 1%, which was increased by 0.5% compared to foliar application and by 14.3% and 5.6% compared to control, respectively (Fallah, 2019). In another research, consuming 10 and 20 mg of Zn/kg soil under severe salinity stress increased the corn plant height by 8.1 and 12.1% (Karmollachaab and Gharineh, 2013).

Results of trait correlation showed that plant height is positively correlated (0.72**) with grain yield (Table 4). The higher height referred to better light reception by the flag leaf and second upper leaf (which play the most significant role in providing photosynthetic substance to fill the forming grains), which is associated with fertility and formation of more grains per spike (Hoseini Ebrahimi et al., 2016). A positive and significant correlation of grain yield with plant height is reasonable, due to possible increasing height by providing optimal growth conditions and a greater green area that increased CO2 uptake and production of photoassimilates, which led to production and accumulation of substances in fertilization, grain formation, and filling and largely increased the yield (Dadashi et al., 2010). In this regard, the research results

suggested that height of red bean plant is positively and significantly related (0.89**) to grain yield (Varnaseri Ghandali et al., 2020). Study of correlation of traits showed that cumin plant height had a positive and significant relationship with grain yield; so that the highest correlation was related to plant height and grain yield (Nasiri Dehsorkhi et al., 2018). Results of estimating correlation coefficients also showed that plant height is positively and significantly correlated with biological yield by 69% (Table 4). Research results showed that leaf uptake of iron, zinc, and manganese micronutrients increases dry matter yield in corn with increasing plant height (Whitty and Chambliss, 2005).

3.6. Yield components

Results indicated that in addition to the main effects of the studied factors (at probability level of 1%), their interaction at probability level of 5% had a significant effect on grains/spike (Table 2). Results of comparing the mean interaction of factors showed that the highest grains/spike belongs to foliar application of 1% zinc sulfate in Mehr cultivar and the lowest mean grains/spike was observed in Armaghan cultivar and the absence of zinc fertilizer (Table 3). Results showed that grains/spike was increased with increasing levels of zinc fertilizer, so that the highest mean grains/spike in all three cultivars was related to zinc fertilizer concentration of 1%. Foliar application of 1% zinc sulfate in Mehr, Goharan and Armaghan cultivars significantly increased grains/spike by 24.8%, 28.0% and 43.3% compared to no foliar application (Table 3). In this regard, the research results showed that the difference between the studied barley cultivars was statistically significant on grains/spike, so that the highest grains/spike belonged to the four-salt genotype (stress tolerant) (Mahlooji, 2017). Plant nutrition with zinc, due to increasing carbohydrate storage of pollen grains, has increased the lifetime of pollen grain, as a result, it increased pollination and formation of more grains in the plant (Hafeez et al., 2013). Researchers said that sterilization of spike flowers in plants growing in zinc-deficient soils is more severe and adding zinc reduces the spike sterility problem (Bagci et al., 2007). In a research, the highest grains/spike in barley was obtained from the treatment of 60 kg/ha of zinc sulfate fertilizer and the lowest grains/spike was obtained from no fertilizer treatment (Seyed Hayat Gheyb et al., 2019).

Results of estimating the correlation of traits showed that the grans/spike had a negative and significant correlation (level of 1%) with 1000-grain weight (Table 4). In this regard, research results showed that the correlation between 1000-grain weight and grains/spike of barley was negative and significant (Nikkhah et al., 2015). In another research, researchers found that grains/spike in barley showed a significant and negative correlation with 1000-grain weight and number of plants. Therefore, it can be concluded that with increasing number of plants, 1000-grain weight is increased but the grains/spike was reduced (Soleimani et al., 2017). The study of correlation of traits showed that grains/spike had a significant and positive correlation (0.88**) with grain yield (Table 4). Grains/spike determines the capacity of the plant's reservoirs. The higher number of grains, there are more reservoirs for processed substances and any factor that can increase this component will increase the yield.

Results of analysis of variance (Table 2) showed that the main effects of fertilizer and cultivar at probability level of 1% and their interaction at probability level of 5% affected spikes/m^2. According to the results of comparing the means, the lowest spike/m^2 belonged to Armaghan cultivar in the absence of zinc fertilizer, although as shown in Table 3, Armaghan and Goharan cultivars are in a statistical group in terms of significance. Results demonstrated that no significant difference was observed in terms of spikes/m^2 at lower concentrations of zinc sulfate fertilizer (0.5%), however, Mehr cultivar produced more spikes compared to Armaghan at higher concentrations (1%). In foliar application of 1% zinc sulfate, Mehr cultivar produced 5.2% more spikes/m^2 compared to Armaghan cultivar (Table 3).

Different mechanisms are involved in response of various plant cultivars to utilization of nutrients (Baligar et al., 2001; Erenoglu et al., 2002; Karimian and Moafpouryan, 1999). Such mechanisms include root-related interactions to increase the usability of soil zinc to be absorbed by root, increased uptake and transfer of zinc from root to air organs, zinc intracellular meronomy variation in plant air organs to have a larger part of zinc in the cytoplasm, and increased efficiency of biochemical use of zinc in plant cells (Malian et al., 2014).

It seems that zinc fertilizer in the plant with increasing photosynthesis, photosynthetic substances, and auxin hormone increases vegetative growth and improves fertile spikes in the plant. This is also related to the absence of malnutrition in the plant (Seyed Hayat Gheyb et al., 2019). Research results demonstrated that the highest spikes/m^2 in barley belonged to 60 kg/ha treatment and the lowest level of traits belonged to non-zinc fertilizer treatment (Seyed Hayat Gheyb et al., 2019).

3.7. Biological yield

Results of analysis of variance (Table 2) indicated that in addition to the main effect of cultivar (probability level of 5%) and zinc fertilizer (probability level of 1%), their interaction was also significant on biological yield (probability level of 5%). Results of comparing the means showed that the biological yield is also increased with increasing zinc fertilizer levels, so that the highest biological yield was related to the concentration of 1% zinc fertilizer. Foliar application of 1% zinc sulfate in Mehr, Goharan, and Armaghan cultivars significantly increased the biological yield by 7.8%, 9.7% and 7.8%, respectively, compared to the control (no foliar application of zinc fertilizer) (Table 3). The lowest mean biological yield was also seen in the absence of fertilizer, so that there was no significant difference between cultivars at this level of fertilizer (Table 3).

Improving biological yield followed by foliar application of zinc sulfate can be attributed to increased yield components and significant and positive correlation of these characteristics with biological yield. Results

showed that there was a significant difference between barley genotypes in regard of biological yield, so that the highest biological yield belonged to the fourth line of salinity tolerant and the lowest belonged to Morocco (stress sensitivity) (Mahlooji, 2017). Researchers found that foliar application of 1% zinc sulfate increased the biological yield of wheat by 12.35% and 23% compared to 0.5% treatment and control treatment, respectively (Fallah, 2019). Positive effect of zinc application on biological yield can be attributed to the role of zinc in the biosynthesis of tryptophan amino acid, participation in structure of active enzymes in carbon metabolism, such as carbonic anhydrase, ribulose-1,5-bisphosphate, fructose-1,6-diphosphate, increased chlorophyll synthesis, followed by increased photosynthesis and thus improved plant growth and yield (Akay, 2011; Hafeez et al., 2013).

Results suggested that there was a positive and significant correlation between biological yield and grain yield at probability level of 1% (Table 4). In order to achieve a high yield, there is a need for proper chlorophyll growth and plants with suitable vegetative power. Proper vegetative growth increases weight, length, and yield of spike and thus increases grain yield (SeyedAghamiri et al., 2012).

Researchers found that the correlation between barley grain yield and biological yield was more than the correlation between grain yield and other traits, and this means that although traits, such as straw yield, spikes/m^2, and grain filling rate have been effective in increasing grain yield, the role of biological yield in increasing grain yield is more than all other traits, It seems that cultivars with higher biological yield could use photosynthetic sources in a more favorable way by producing more foliage and provide the conditions for increasing grain yield (Ahmadi et al., 2014).

3.8. Grain yield

Results of analysis of variance indicated that in addition to the main effects of zinc fertilizer and cultivar ($p \leq 0.01$), their interaction was also significant on grain yield at the probability level of 5% (Table 2). The highest grain yield of 6118.5 kg/ha belonged to Mehr cultivar in foliar application of 1% zinc sulfate, although as shown in Table 3, Mehr and Goharan cultivars are in a statistical group. It seems that greater grain yield in Mehr cultivar is due to higher grains/spike and more spikes and a significant and positive correlation between the aforementioned traits and grain yield. Results of the yield comparison tests in territories under salinity stress at stations in temperate regions of the country showed the superiority of Mehr cultivar over Khatam cultivar, so that this cultivar with mean grain yield of 4751 kg/ha and 655 kg/ha (16%) had an increased yield compared to the mean cultivar (Nikkhah et al., 2019). In studying the effect of irrigation water salinity and foliar application of zinc fertilizer on barley genotypes, the results showed that the highest grain yield was related to fourth line of salinity tolerant, which was increased by 100.5% compared to Morocco genotype (stress sensitivity). Research results showed that various wheat cultivars had different response to zinc fertilizer. Some cultivars were more responsive to zinc fertilizer application compared to other cultivars and grain yield in fertilizer treatments was significantly increased compared to the control. In contrast, some cultivars were less responsive to fertilizer application or fertilizer application did not significantly affect the grain yield compared to the control (Malian et al., 2014).

Lowest grain yield of 4530.5 kg/ha was found in Armaghan cultivar and in the absence of zinc sulfate fertilizer, which was significantly different from all combined treatments of fertilizer and cultivar. Foliar application of 1% zinc sulfate in Mehr, Goharan, and Armaghan cultivars significantly increased the grain yield by 22.2%, 25.7% and 0.29%, respectively, compared to the absence of foliar application of zinc sulfate fertilizer (Table 3). Increasing yield with zinc sulfate fertilizer could be due to various reasons, including increased auxin biosynthesis in the presence of zinc, increased chlorophyll concentration, increased phosphoenolpyruvate carboxylase and ribulose bisphosphate carboxylase, reducing sodium accumulation in plant tissues and increasing efficiency of nitrogen and phosphorus uptake in the presence of the zinc element (Khan et al., 2003). Results of trait correlation showed that among the yield components, 1000-grain weight is negatively and significantly correlated with grain yield at the probability level of 1% (Table 4). It should be noted that there is a negative correlation between the yield components, and with increasing number of grains due to the increased reservoir capacity against a fixed content of storage substance, it is natural to store lower content of substance in each reservoir capacity. It is noteworthy that the essence of correlations between components is not merely genetic and varies from environment to environment, and hence different and contradictory results are seen in tests (Ahakpaz et al., 2020). Researchers said that 1000-grain weight was negatively and significantly correlated with barley yield. Given that the yield is derived from the cereal yield formula, it can be justified that with increasing 1000-grain weight, grains/spike is reduced as one of the yield formula components, which will be consequently effective in reducing yield (Baraty et al., 2014).

3.9. Harvest index

Results of analysis of variance (Table 2) showed that the main effect of cultivar at the probability level of 1%, main effect of zinc fertilizer, and interaction of fertilizer and cultivar at the probability level of 5% were significant on harvest index. Results of the interaction of the studied factors indicated that the highest harvest index belonged to Mehr cultivar in both levels of zinc sulfate fertilizer (0.5 and 1%), which were statistically in a significant group. In the absence of zinc fertilizer, Mehr cultivar had a higher harvest index by 5.2 and 10.7%, respectively, compared to Gohran and Armaghan cultivars (Table 3). In this regard, in investigating the effect of irrigation water salinity and foliar application of zinc fertilizer on barley genotypes, the results suggested that the difference was significant between genotypes in terms of harvest index, so that the highest harvest index (30.6%) belonged to the fourth line

of salinity tolerant and the lowest harvest index belonged to Morocco genotype (stress sensitivity) (Mahlooji, 2017).

According to the results of comparing the means, foliar application of 1% zinc sulfate in Mehr, Gohran and Armaghan cultivars significantly increased the harvest index by 13.4%, 14.8% and 19.8%, respectively, compared to the absence of foliar application of zinc sulfate fertilizer (Table 3). In a research conducted to investigate the effect of zinc sulfate on wheat cultivars, the results demonstrated that the highest harvest index belonged to 60 kg/ha fertilizer level and the lowest index belonged to 0 kg/ha zinc sulfate (Mirtalebi et al., 2012). In studying the effect of irrigation water salinity and foliar application of nano-fertilizers and zinc plots on barley genotypes, the results indicated that the highest harvest index belonged to zinc nano oxide (30.5%) and the lowest index (25.6%) belonged to the absence of foliar application (Mahlooji, 2017). Results of trait correlation showed that harvest index had the highest positive and significant correlation (0.93**) with grain yield (Table 4). In this regard, research results showed that cumin grain yield had a positive and significant correlation with harvest index and biological yield (Nasiri Dehsorkhi et al., 2018). In the absence of stress, grain yield had a positive and significant correlation with biological yield (r = 0.777**) and harvest index (r = 0.698**) (Nikkhah et al., 2015).

4. Conclusion

Results of the present research demonstrated that the interaction of zinc sulfate fertilizer and barley cultivars was significant on traits such as chlorophyll a, grains/spike, spikes/m^2, biological yield, grain yield, and harvest index. The highest growth rate, photosynthetic pigments, yield, and yield components were observed with foliar application of 1% zinc sulfate in Mehr cultivar. This could be attributed to superiority of Mehr cultivar under salinity conditions as well as the positive role of zinc element in improving plant growth. Therefore, this level of zinc sulfate fertilizer in this cultivar is appropriate and suggested for barley production in similar conditions to the present research. Generally, given the positive effect of zinc fertilizer on improving barley yield and also with respect to the lack of this element in most territories where barley is grown, this micronutrient should be particularly considered in plant nutrition programs.

References

Abbasi, A., & Shekari, F. (2016). Effect of zinc sulfate on growth and yield of wheat under soil zinc deficiency and drought stress. *Cereal research, 6(2),* 145-158. **doi: 10.22067/gsc.v16i3.67795**

Ahakpaz, F., Bernosi, I., Abdollahi, B., Golkari, S., Jafarzadeh, J., & Udupa, S. (2020). Evaluation of barley genotypes based on morphological traits and drought tolerance indices under rainfed and supplementary irrigation conditions. *Iranian Journal of Dryland* Agriculture, *8(2),* 153-176. **doi: org/10.22092/idaj.2019.126360.257**

Ahmadi, M., Astaraee, A., Keshavarz, P., & Nasiri Mahalati, M. (2006). Effect of irrigation water salinity and zinc application on yield and chemical compositions of wheat. *Desert, 11(1),* 129-141. [In Persian].

Ahmadi, A., Hosseinpour, T., & Soltani, M. (2014). The effect of plant density on yield and its components in three rain fed barley cultivars. *Agronomy Journal (Pajouhesh & Sazandegi*), 27(102), 131-140. **doi: 10.22092/aj.2014.100939**

Akay, A., (2011). Effect of zinc fertilizer applications on yield and element contents of some registered chickpeas varieties. *African Journal of Biotechnology, 10(60),* 12890-12896. **doi: 10.5897/ajb10.1834**

Arnon D. I. (1949). Copper enzymes in isolated chloroplasts; polyphenol-oxidase in Beta vulgaris. *Plant Physiology, 24,* 1-15.

Askary, M., Amini, F., & Hosseinpour, L. (2016). Study of variability in growth, antioxidant defense system and protein content by zinc element application in periwinkle (*Catharanthus roseus* (L.) G. Don.) under salinity stress. *Iranian Journal of Medicinal and Aromatic Plants, 32(1),* 35-46. **doi: org/10.22092/ijmapr.2016.106135**

Bagci, S. A., Ekiz, H., Yilmaz, A., & Cakmak, I. (2007). Effect of zinc deficiency and drought on grain yield of field-grown wheat cultivars in Central Anatolia. *Journal of Agronomy and Crop Science, 193(3),* 198-206. **doi: 10.1111/j.1439-037x.2007.00256.x**

Baligar, V. C., Fageria, N. K., & He, Z. L. (2001). Nutrient use efficiency in plants. *Communications in oil science and plant analysis, 32,* 921-950. **doi: 10.1081/css-100104098**

Baraty, M., Amiri, R., Ebrahimi, M., Naghavi, M. R., & Nikkhah, H. R. (2014). Study of genetic diversity in some agronomic traits of barley using recombinant inbred lines. *Agronomy Journal (Pajouhesh & Sazandegi), 27(102),* 61-70. [In Persian].

Bates, L. S. (1973). Rapid determination of free proline for water- stress studies. *Plant and Soil, 39,* 205- 207.

Brennan, R. F. (2007). Effectiveness of zinc sulfate and zinc chelate as foliar sprays in alleviating zinc deficiency of wheat grown on zinc deficient soils in Western Australia. *Australian Journal of Experimental Agriculture, 31,* 831-834. **doi: 10.1071/ea9910831**

Cakmak, I. (2000). Possible roles of zinc in protecting plant cells from damage by reactive oxygen species. *New Phytologist, 146,* 185-205. **doi: org/10.1046/j.1469-8137.2000.00630.x**

Dadashi, M. R., Noorinia, A., Askar, M., & Azizi, Sh. (2010). Evaluation of correlation between physiological and morphological traits with yield in hull- less barley lines. *Journal of Crop Ecophysiology, 4(15),* 29-40. [In Persian].

Erenoglu, B., Nikolic, M., Romheld, V., & Cakmak, I. (2002). Uptake and transport of foliar applied zinc (65Zn) in bread and durum wheat cultivars differing in zinc efficiency. *Plant and Soil, 241,* 251-257. **doi: 10.1023/a:1016148925918**

Fallah, A. (2019). Effect of drought stress and zinc sulfate spraying on growth, yield and photosynthetic pigments

in wheat cultivar Alvand. *Plant Ecophysiology, 11(39),* 217-228. [In Persian].

Hafeez, B., Khanif, Y. M., & Saleem, M. (2013). Role of zinc in plant nutrition-a review. *American Journal of Experimental Agriculture, 3,* 374-391. **doi: 10.9734/ajea/2013/2746**

Hellubust, J. A., & Caraigie, J. S. (1978). Handbook of physiological methods. Physiological and biochemical methods. Cambridge University Press.

Hemantaranjan, A., & Grag, O. K. (1988). Iron and zinc fertilization with reference to the grain quality of wheat (*Triticum aestivum* L.). *Journal of Plant Nutrition, 11,* 1439-1450. **doi: org/10.1080/01904168809363900**

Hoseini Ebrahimi, M., Azari, A., Tabatabaei, S. A., & Madah Hoseini, Sh. (2016). Effect of salt stress on yield quality and quantity of promising lines of barley. *Environmental Stresses in Crop Sciences, 8(2),* 285-295. **doi: org/10.22077/escs.2016.239**

Jamshidi, P., Baradaran Firoozabadi, M., Oloumi, H., & Naghavi, H. (2017). Evaluation of foliar spraying of zinc and calcium fertilizers on yield and physiological traits of safflower under lead stress. *Iranian Journal of Field Crops Research, 15(2),* 368-379. **doi: 10.22067/gsc.v15i2.51279**

Kannan, S., (2010). Foliar fertilization for sustainable crop production. *Genetic Engineering, Biofertilisation, Soil Quality and Organic Farming, 23(4),* 371-402. **doi: 10.1007/978-90-481-8741-6_13**

Karimian, N., & Moafpouryan, G. R. (1999). Zinc adsorption characteristics of selected calcareous soils of Iran and their relationship with soil properties. *Communication Soil Science and Plant Analyses, 30,* 1721-1731.

Karmollachaab, A., & Gharineh, M. H. (2013). Effect of zinc element on growth, yield components and some physiological characteristics of maize under NaCl salinity stress. *Iranian Journal of Field Crops Research, 11(3),* 446-453. **doi: 10.22067/gsc.v11i3.29744**

Kaya, C., & Higgs, D. (2002). Response of tomato (*Lycopersicom esculentum* L.) cultivars to foliar application of zinc when grown in sand culture at low zinc. *Scientia Horticulturae, 93,* 53-64. **doi: 10.1016/s0304-4238(01)00310-7**

Khan, H. R., McDonald, G. K., & Rengel, Z. (2003). Zn fertilization improves water use efficiency, grain yield and seed Zn content in chickpea. *International Journal of Plant and Soil Science, 241,* 389-400. **doi: 10.1023/a:1022808323744**

Kumar Parida, A., & Bandhu Das, A. (2005). Salt tolerance and salinity effects on plants: a review. *Ecotoxicology and Environmental Safety, 60,* 324-349. **doi: 10.1016/j.ecoenv.2004.06.010**

Mahlooji, M. (2017). Effects of salinity of irrigation water and nano zinc oxide foliar application on morphophysiological characterstics of barley (*Hordeum vulgare* L.) genotypes. PhD Thesis in Agronomy Crop Physiology, University of Mohaghegh Ardabili. [In Persian].

Makarian, H., Shojaei, H., Damavandi, A., Nasiri Dehsorkhi, A., & Akhyani, A. (2017). The effect of foliar application of Zinc oxide in common and nanoparticles forms on some growth and quality traits of Mungbean (*Vigna radiata* L.) under drought stress conditions. *Iranian Journal of Pulses Research, 8(2),* 166-180. **doi:10.22067/ijpr.v8i2.51644**

Malian, M., Khoshgoftarmanesh, A. H., Shariati, H., Majidi, M., Sharifi, H. R., & Sanaee, A. (2014). The effect of zinc fertilizer application on grain yield of different zinc-efficient spring and winter wheat cultivars. *Journal of Crop Production and Processing, 4(12),* 157-169. **doi: 20.1001.1.22518517.1393.4.12.14.0**

Mamnoei, E., & Seyed Sharifi, R. (2010). Study the effects of water deficit on chlorophyll fluorescence indices and the amount of proline in six barley genotypes and its relation with canopy temperature and yield. *Journal of Plant Biology, 2(5),* 51-62. **doi: 20.1001.1.20088264.1389.2.5.6.1**

Mirtalebi, S. H., Hosseini, S. M., Khajehpour, M. R., & Soleymani, A. (2012). Effects of zinc sulfate on yield, yield components, zinc and protein content of three winter wheat cultivars in the Eghlid of Fars province. *Water and Soil Conservation, 19(3),* 185-199. [In Persian].

Moradi Telavat, M. R., Roshan, F., & Siadat, S. A. (2015). Effect of foliar application of zinc sulfate on minerals contenet, seed and oil yields of two safflower cultivars (*Carthamus tinctorius* L.). *Iranian Journal of Crop Sciences, 17(2),* 153-164. **doi: 20.1001.1.15625540.1394.17.2.6.0**

Mosavi, S. R., Galavi, M., & Ahmadvand, G. (2007). Effect of zinc and manganese foliar application on yield, quality and enrichment on potato (*Solanum tuberosum* L.). *Asian Journal of Plant Sciences, 6,* 1256-1260. **doi: 10.3923/ajps.2007.1256.1260**

Nasiri Dehsorkhi, A., Makarian, H., Varnaseri Ghandali, V., & Salari, N. (2018). Investigation of effect of humic acid and vermicompost application on yield and yield components of cumin (*Cuminum cyminum* L.). *Applied Research in Field Crops, 31(1),* 93-113. [In Persian].

Nasiri Dehsorkhi, A., Varnaseri Ghandali, V., Makarian, H., Ramezan, D., & Estekhdami, P. (2020). The effect of poultry manure and zinc sulfate on growth and yield of cantaloupe (*Cucumis melo* L.) in competition with weeds. *Horticultural Plants Nutrition, 2(2),* 46-69. [In Persian].

Nikbakht, M., Solouki, M., & Aran, M. (2021). Effects of foliar application of zinc nano-chelate and zinc sulfate fertilizers on some quantitative and qualitative properties of bitter apple (*Citrullus colocynthis* L.). *Iranian Journal of Medicinal and Aromatic Plants Research, 36(6),* 898-911. **doi: org/10.22092/ijmapr.2021.342937.2789**

Nikkhah, H. R., Mohammadi, V. A., Naghavi, M. R., & Soltanloo, H. (2015). The effect of salinity stress on morphological and physiological traits of recombinant inbred lines population of barley derived a cross between Arigashar×Igri. *Iranian Journal of Field Crop*

Science, 46(2), 181-192 . **doi: 10.22059/ijfcs.2015.54866**

Nikkhah, H. R., Tabatabaee, S. A., Yousefi, A., Ghazvini, H., Saberi, H., Tajali, H., Mahlooji, M., Binabaji, M. H., Aghnoum, R., Dehghan, M. A., Zakeri, A., & Safavi, S. A. (2019). Mehr, Barley cultivar tolerant to salt stress for cultivation in the temperate climate of the country. *Research Achievements for Field and Horticulture Crops, 7(2),* 235-249. [In Persian].

Sadeghzadeh, B. (2013). A review of zinc nutrition and plant breeding. *Journal of Soil Science and Plant Nutrition, 13(4),* 905-927. **doi: 10.4067/s0718-95162013005000072**

Sadeghzadeh, B., & Rengel, Z. (2011). Zinc in Soils and Crop Nutrition. In: Malcolm J. Hawkesford and Peter Barraclough (eds.). The Molecular and Physiological Basis of Nutrient Use Efficiency in Crops, Chapter 16. pp: 335-375.

SeyedAghamiri, S. M. M., Mostafavi, Kh., & Mohammadi, A. (2012). Investigation of the relationship between grain yield and yield components in barley varieties and new hybrids using multivariate statistical methods. *Iranian Journal of Field Crops Research, 10(2),* 421-427. [In Persian].

Seyed Hayat Gheyb, B., Mojaddam, M., & Derogar, N. (2019). Studying zinc sulphate effects on quantitative and qualitative characteristics of barley (*Hordeum vulgare* L.) under different irrigation regimes. *Environmental Stresses in Crop Sciences, 12(1),* 75-84. **doi: org/10.22077/escs.2018.1173.1239**

Seyed Sharifi, R., Kamari, H., & Nagafi, Gh. (2015). Effects of salinity stress and foliar application of nano-zinc oxide on yield per plant and some morphophysiological traits of barley (*Hordeum vulgare* L.). *Iranian Journal of Field Crops Research, 13(2),* 399-410. **doi: 10.22067/jcesc.2024.87923.1323**

Soleimani, A., Valizadeh, M., Darvishzadeh, R., Aharizad, S., & Alipour, H. (2017). Evaluation of yield and yield component of spring barely genotypes under late season drought stress. *Journal of Crop Breeding, 9(23),* 105-116. **doi: 10.29252/jcb.9.23.105**

Sun, J., Gu, J., Zeng, J., Han, Sh., Song, A., Chen, F., Fang, W., Jiang, J., & Chen, S. (2013). Changes in leaf morphology, antioxidant activity and photosynthesis capacity in two different drought tolerant cultivars of chrysanthemum during and after water stress. *Scientia Horticulturae, 161,* 249-258. **doi: 10.1016/j.scienta.2013.07.015**

Tester, M., & Davenport, R. (2003). Na^+ tolerance and Na^+ transport in higher plants. *Annual Botany, 91(5),* 503-527. **doi: org/10.1093/aob/mcg058**

Tigre, W., Worku, W., & Haile, W. (2014). Effects of nitrogen and phosphorus fertilizer levels on growth and development of barley (*Hordeum vulgare* L.) at Bore District, Southern Oromia. *American Journal of Life Sciences, 2(5),* 260-266. **doi: 10.11648/j.ajls.20140205.12**

Varnaseri Ghandali, V., Ramroudi, M., & Nasiri Dehsorkhi, A. (2020). The study foliar spraying of micronutrients (iron, zinc and manganese) on yield and yield components of Red Bean (*Phaseolus vulgaris* L.) under cutting irrigation conditions. *Applied Research in Field Crops, 33(1),* 105-124. **doi: 10.22092/aj.2019.121993.1303**

Vatankhah, A., Mohammadkhani, A., Hooshmand, S., & Kiani, Sh. (2016). Study the effect of humic acid and zinc on the quantity and quality of fruit, photosynthetic pigments and mineral concentrations of grapevine cv. 'Asgari'. *Journal of Crops Improvement, 18(2),* 303-318. **doi: org/10.22059/jci.2016.56570**

Vojodi Mehrabani, L., Hassanpouraghdam, M. B., & Valizadeh Kamran, R. (2018). Effect of NaCl salinity and $ZnSO_4$ foliar application on yield and some physiological traits of *Tagetes erecta* L. *Water and Soil Science, 28(3),* 105-115. [In Persian].

Weisany, W., Sohrabi, Y., Heidari, G., Siosemardeh, A., & Ghassemi-Glezani, K. (2012). Changes in antioxidant enzymes activity and plant performance by salinity stress and zinc application in soybean (*Glycine max* L.). *Plant Omics Journal, 5(2),* 60-67.

Whitty, E. N., & Chambliss, C. G., (2005). Fertilization of Field and Forage Crops. Nevada State University Pub., 21 pp.

Winch, T. (2009). Agronomy (General and Special). Translated by Fallah, S. Shahrekord University Press. 334 pp. [In Persian].

Guide for Authors

Preface

The Journal of *Agriculture, Environment and Society (AES)* welcomes articles in various areas of agriculture from all over the world. Contributions must be original and have not previously been published elsewhere. Please be ensure that there are no conflicts between the authors before submitting. Before being published, manuscripts submitted to *Agriculture, Environment and Society (AES)* are critically reviewed. The purpose of the review is to reassure readers that the papers have been approved by competent and unbiased professionals. The manuscript should be submitted only via the *Agriculture, Environment and Society (AES)* Editorial System (https://aes.uoz.ac.ir/). All papers are available free of charge at the Journal's webpage.

Types of article

The following types of contribution are published in Agriculture, Environment and Society (AES):

Original research article: It should describe novel and well validated findings, and experimental techniques should be described in sufficient detail to allow the study to be verified. Research papers of 6000-8000 words in length, with tables, illustrations and references, in which hypotheses are tested and results reported.

Review article: Review and perspective on current issues are accepted and encouraged. The format and length of review papers are more flexible than for a full paper. Typical reviews are less than 12000 words including references.

Short Communications: It is appropriate for recording the results of small-scale research or providing information on novel models or hypotheses, innovative methodologies, procedures, or apparatus. Research papers of 2500-3500 words in length, with tables, illustrations and references.

Structure of Articles

Text should be written in a succinct and cohesive manner, with an emphasis on significant points, conclusions, breakthroughs, or discoveries, as well as their broader relevance. All running text should be saved as a Word document. All writings should be written using Times New Roman font. Both American and British English format are accepted, but not their mixture. The font size for title is 14 point and for the main text is 12 point. The subtitles should be written in Bold and font size of 12 point. Figures and tables can be put within the text or at the bottom. Figures should have a high enough resolution to allow for refereeing.

The original research articles should contain the following sections:

Title

The title should be clear, intelligible to experts in different disciplines, and represent the substance of the article. There may be no abbreviations in the title. The title, authors, and affiliations should all be included on a title page as the first page of the manuscript file.

Name(s) of the author (s) not visible in the manuscript (Double Blind Reviews).

Abstract

The title's information does not need to be duplicated in the abstract. The abstract should not be more than 350 words long. It must include the study's goal, methods, findings, and conclusions. Abbreviations should be used sparingly and explained when first used. The abstract is presented separately from the article in a single paragraph after the title page in the manuscript file.

Keywords

Provide a maximum of six keywords appear immediately after the abstract with alphabetical order. Keywords should cover the most precise phrases in the article and should not be the same as the terms used in the title.

Introduction

The introduction should provide background that puts the manuscript into context and allows readers outside the field to understand the purpose and significance of the study. It should define the problem addressed and why it is important, with a brief review of the key literature and conclude with a brief statement of the overall aim of the work.

Material and methods
Provide sufficient details to allow the work to be reproduced by an independent researcher. Methods that are already published should be summarized, and indicated by a reference. If quoting directly from a previously published method, use quotation marks and also cite the source. Any modifications to existing methods should also be described.

Results
Results should be clear and concise.

Discussion
This should explore the significance of the results of the work, not repeat them. A combined Results and Discussion section is often appropriate. Together, these sections should describe the results of the experiments, the interpretation of these results, and the conclusions that can be drawn. Authors should explain how the results relate to the hypothesis presented as the basis of the study and provide a succinct explanation of the implications of the findings, particularly in relation to previous related studies and potential future directions for research.

Conclusions
The main conclusions of the study may be presented in a short Conclusions section, which may stand alone or form a subsection of a Discussion or Results and Discussion section.

Appendices
If there is more than one appendix, they should be identified as A, B, etc. Formulae and equations in appendices should be given separate numbering: Eq. (A.1), Eq. (A.2), etc.; in a subsequent appendix, Eq. (B.1) and so on. Similarly for tables and figures: Table A.1; Fig. A.1, etc.

Acknowledgements
Acknowledgements of persons, grants, money, and so forth should be included before the reference list in a distinct section.

References
Please ensure that every reference cited in the text is also present in the reference list (and vice versa). In the text, papers with more than two authors should be cited by the last name of the first author, followed by et al., space, and the year of publication (example: Jones et al., 2020). If the cited manuscript has two authors, the citation should include both last names, space, and the publication year (example: Smith and Ebrahim, 2018).

In the Reference section, a maximum of ten authors of the cited paper may be given. All references cited in the text must be listed in the Reference section alphabetically by the last names of the author(s) and then chronologically.

Format for Journal paper
Author, A. A., Author, B. B., & Author, C. C., (Year of publication). Title of article. *Name of Journal*, *Volume number*(issue number), pages. **doi: 10.0000**

Example:

Golshani, F., Asgharipour, M. R., Ghanbari, A., & Seyedabadi, E. (2023). Environmental accounting for croplands, livestock husbandry, and integrated systems based on emergetic indicators. *Energy, Ecology and Environment*, *8*(1), 28-49. **doi: 10.1007/s40974-022-00262-5**

Format for Books
Author, A. A., (Year of publication). Title of work: Capital letter also for subtitle. Location: Publisher.

Strunk Jr., W., & White, E. B., (2000). The Elements of Style, fourth ed. Longman, New York.

Chapter in an Edited Book
Author, A. A., & Author, B. B., (Year of publication). Title of chapter, in: Title of book (Eds.). Publisher, Location, pages of chapter.

Mettam, G. R., Adams, L. B., (2009). How to prepare an electronic version of your article, in: Jones, B. S., Smith, R. Z. (Eds.), Introduction to the Electronic Age. E-Publishing Inc., New York, pp. 281–304.

Note: To ensure accurate and efficient referencing, it is recommended to use reference management software such as EndNote for in-text citations and reference lists. The appropriate style (JELSA style) for EndNote can be downloaded from journal website.

Tables and Figures
Please submit tables and figures as editable text and not as images. All figures and tables should be embedded while correctly positioned.

Tables
Please avoid using vertical lines in tables. Please use "Table" in both text and captions. Number tables consecutively in accordance with their appearance in the text. Place footnotes to tables below the table body and indicate them with superscript lowercase letters. Avoid vertical rules. Be sparing in the use of tables and ensure that the data presented in tables do not duplicate results described elsewhere in the article. The table caption appears above the table using Times New Roman font with font size of 10 points in bold. Use no border for the tables. Footnotes to tables should appear beneath the tables and should be designated by a lower-case superscript letter, †, or z, y, x, etc.

Figures
Ensure that each illustration has a caption. Supply captions separately, not attached to the figure. A caption should comprise a brief title (not on the figure itself) and a description of the illustration. Keep text in the illustrations themselves to a minimum but explain all symbols and abbreviations used (preferably in the caption). The caption should allow the reader to understand the main elements of what is being shown without needing to refer to then main text. The figure caption appears below the figure and written using Times New Roman font with font size of 10 points in bold. Use no border for the figures. The font size within the figure should not smaller than 8 point and bigger than 10 point. Try to present the figures in gray scale instead of color illustration. Use (Figure) at the end of the sentence and captions and use Figure in text.

Math formulae
Present simple formulae in the line of normal text where possible. In principle, variables are to be presented in italics. Number consecutively any equations that have to be displayed separately from the text in the right margin (if referred to explicitly in the text).

Suggest Reviewers
With the manuscript, the author should include a list of three qualified, independent, prospective reviewers who could perform quality peer reviews of your document. Be sure to include their complete names, affiliations, and current e-mail addresses.

AES

University of Zabol

Agriculture, Environment & Society

Faculty of Agriculture, University of Zabol, Zabol, Iran
P.O. Box 538-98615, Tel: +98-54-31232102
Website: http://aes.uoz.ac.ir
Email: aes@uoz.ac.ir